Spectroscopic Investigation of Stability, Unfolding and Refolding of Outer Membrane Protein Porin from *Paracoccus denitrificans*

Dissertation

zur Erlangung des Doktorgrades

der Physik

vorgelegt beim Fachbereich Physik

der Johann Wolfgang Goethe-Universität

in Frankfurt am Main

Von

Suja Sukumaran

aus Thiruvanantapuram, Indien

Frankfurt am Main, 2004
(DF1)

Vom Fachbereich Physik der Johann Wolfgang Goethe-Universität als Dissertation angenommen.

Dekan : Prof. Dr. W. Assmus

Gutachter : Prof. Dr. W. Mäntele
Prof. Dr. B. Ludwig

Datum der Disputation :

Dedicated to my Daddy and Mummy

List of contents

1. Introduction 1

1.1 General Overview 1

1.1.1. Protein Folding 2

1.2 Membrane protein folding, stability and unfolding 4

1.2.1 Determinants of membrane protein stability 4

1.2.2 How does an integral membrane protein reach the bilayer 5

1.2.3 α-helical proteins 6

1.2.4 β-sheet proteins 7

1.2.4.1 Folding of β-barrels into lipid bilayer *in vitro* 8

1.3 Porin as an ideal Candidate 9

1.3.1 Stability of porins 11

1.3.2 Porin from *Paracoccus denitrificans* 12

1.4 Techniques available to study protein folding, unfolding and stability 14

1.5 Goal of this study 18

2. Materials and Methods 19

2.1 Materials 19

2.1.1 Chemicals 19

2.1.2 Biochemicals 19

2.1.3 Kits 19

2.1.4 Plasmid 20

2.1.5 PDB structure 20

2.1.6 Culture medium 20

2.1.7 Buffers 20

2.1.8 Cells 21

2.1.9 Primer Design 22

2.1.10 Antibiotics 22

2.2 Methods 23

2.2.1 Genetic techniques 23

2.2.1.1 Competent cell preparation 23

2.2.1.2 Plasmid purification 23

2.2.1.3 PCR conditions 23

2.2.1.4 Agarose Gel Electrophoresis 25

2.2.1.5 Site-directed mutagenesis 25

2.2.1.6 Deletion mutagenesis 25

2.2.1.7 Transformation of *E. coli* cells 25

2.2.1.8 Restriction digestion 26

2.2.1.9 DNA Sequencing 26

2.2.2 Protein Biochemistry Techniques 26

2.2.2.1 Protein expression in *E. coli* BL21(DE3) 26

2.2.2.2 Protein Purification 27

2.2.2.3 Protein Quantification 27

2.2.2.4 Protein quality detection by SDS-PAGE 28

2.2.2.5 Reconstitution into liposomes 28

2.2.3 Protein Refolding methods 29

2.2.4 Spectroscopic techniques 30

2.2.4.1 IR Spectroscopy 30

2.2.4.1.1 FTIR transmission 31

2.2.4.1.2 ATR-FTIR 32

2.2.4.2 CD Spectroscopy 34

2.2.4.3 Fluorescence Spectroscopy 36

2.2.5 Lipid Bilayer Activity Measurements 38

2.2.5.1 Single channel measurements 39

2.2.5.2 Activity profiling 39

3. Results and Discussion 41

3.1 Mutant Construction 41

3.1.1 Selection criteria 41

3.1.2 Site-directed mutants 46

3.2 Protein Purification 47

3.3 Secondary Structure analysis 49

3.3.1 IR spectroscopy of protein in detergent micelles and liposomes 49

3.3.2 CD spectroscopy of protein in detergent micelles 56

3.4 Functional Characterisation 59

3.4.1 Single channel conductance 59

3.4.2 Activity profiling 63

3.4.3 Structural and functional correlation 65

3.5 Thermal Stability and unfolding 66

3.5.1 Thermal unfolding in detergent micelles 66

3.5.1.1 Wild type porin 66

3.5.1.2 Mutant porins 71

3.5.1.3 Thermal stability analysis in SDS-PAGE 73

3.5.2 Thermal unfolding in liposomes 74

3.5.2.1 Wild type and mutant porins 74

3.5.2.2 SDS-PAGE analysis 77

3.5.3 Tyrosine side chain modes 78

3.5.4 Structural and functional correlation 84

3.5.4.1 Single channel conductance 84

3.5.4.2 Activity profiling 86

3.6 pH dependent stability and unfolding 87

3.6.1 Unfolding 89

3.6.1.1 Disaggregation of aggregated porin 89

3.6.1.2 Unfolding of native porin at high pH 92

3.6.1.3 Analysis of pH dependent thermal stability 94

3.6.1.4 A basic mechanism of ‘opening up’ 99

3.6.2 Refolding 101

3.6.2.1 Refolding of protein unfolded from an aggregate 101

3.6.2.2 Refolding of native protein unfolded at high pH 103

3.6.3 Thermal Stability of refolded protein 104

3.6.3.1 Refolded protein unfolded from an aggregate 104

3.6.3.2 Refolded protein native protein unfolded at high pH 105

3.6.4 Residues involved in the unfolding mechanism 108

3.7 Chemical denaturation 111

3.7.1 Unfolding studied by CD spectroscopy 111

3.7.1.1 GuHCl- induced unfolding 111

3.7.1.2 Urea-induced unfolding 113

3.7.2 Unfolding studied by flourescence spectroscopy 115

3.7.2.1 GuHCl-induced unfolding 115

3.7.2.2 Urea-induced unfolding 116

3.7.2.3 Change in tryptophan environment 117

3.7.3 Unfolding studied by SDS-PAGE 118

3.7.4 Unfolding mechanism of urea and GuHCl 119

3.8 Refolding 121

3.8.1 Refolding of porin into detergent micelles 121

3.8.2 Refolding of porin into liposomes 123

3.8.3 Thermal stability of refolded protein 125

4 Conclusions 128

5 Zusammenfassung 133

6 References 138

7 Abbreviations 147

8 Appendix 148

9 Acknowledgement 153

10 Curriculum vitae 155

Introduction

1.1 General overview

Proteins are one of the most abundant molecules in humans besides water. A human body contains more than 100,000 different types of protein and their role covers structure, communication, transport and catalysis. In general 20 different amino acids build up the protein. It is fascinating to recognize that the permutation combination of these 20 amino acids leads to the formation of different proteins assigned with different function. The properties of these proteins are not typical of random sequences, but have been selected through evolutionary pressure to have specific ability to fold to a unique structure and hence to generate enormous selectivity and diversity in their function (Dobson, 2004). Understanding the protein stability and folding, is the first step on the path to solve one of the most important questions that can be addressed by modern science.

Alzheimer's disease, cystic fibrosis, mad cow disease, inherited form of emphysema and many forms of cancer are all a result of protein misfolding. Apart from clinical importance, knowing the basic rules of protein folding is important for all researchers doing various structural and functional studies. From the evolutionary point of view it is quite appealing to understand how a nascent polypeptide formed in nature folded into such complex structures. It can answer questions like whether a protein folded itself to catalyze reactions or active sites of proteins are results of protein folded correctly based on evolutionary code. Biological systems are believed to have evolved en route from simple to complex, from small to large, guided by a multitude of laws of nature. Protein and DNA are polymers and they obey the laws of polymer physics. It is this search for the physical principles that various theories on protein folding have come up (Trifonov *et al*., 2003, Urversky *et al*., 2003). Protein folding studies should help researchers to make a quantitative prediction about the effects of various factors like amino acid sequence, chain topology, pH, salt concentration and temperature on the kinetics and thermodynamics of the folding process (Dobson, 1999).

1.1.1 Protein folding

The importance of protein folding was recognized almost half century ago in the pioneering work of Linus Pauling. In the 1970s, Christian Anfinsen in his marvelous experiments with Rnase, proved that proteins can fold back into native state after having been unfolded by a denaturant.

Proteins are classified broadly as cytoplasmic (soluble) and membrane protein based on the location they are found. A very general overview of protein stability and folding is presented in the next section followed by an introduction to membrane protein stability and folding. Pioneering work of various groups have chalked various basic principles underlying the folding of soluble proteins, especially the general thermodynamic principles (Ferguson *et al*., 2003).

When a protein folds or unfolds it passes through many intermediates. The folding landscape, shaped like a funnel, is a rough terrain, which contains numerous minima and multiple pathways that link them as explained for lysozyme (Figure 1.1.1). As folding progresses towards the native structure, it is likely that the intermediate states and the barriers between them will be better and better defined and associated with specific features recognizable in, and relevant to, the final structure (this is the narrowing of the “funnel”). It is reasonable to say that this landscape and the trajectory taken over it during the last stages of folding, coincides to some extent with the first stages of unfolding. Hence for a comprehensive study of the folding of a protein it is always a good strategy to include description of the unfolding process along with the folding pathways. As in any case, the methods developed to follow one will be suitable for the other, as are the conceptual and calculational tools. (Galzitskaya *et al*., 2001)

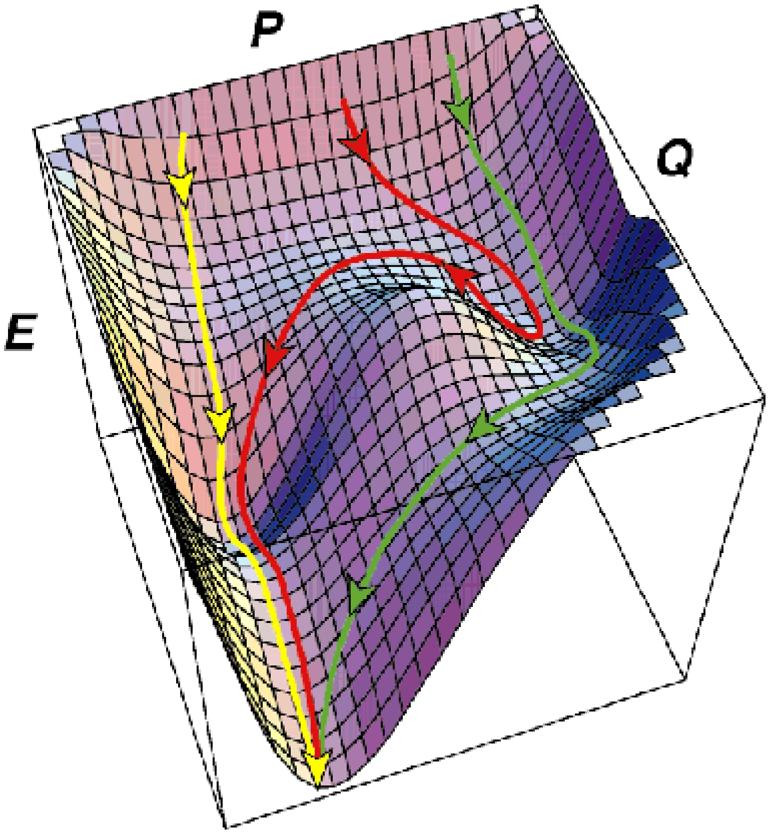

Figure 1.1.1 The energy surface of a folding funnel from experimental data for the folding of lysozyme. The axes are defined as follows: E represents the energy of the system, Q is defined as the proportion of native contacts formed, and P is a measure of the available conformational space. Three pathways are shown corresponding to (yellow) fast folding, (green) slow folding pathway that crosses the high energy barrier, and (red) slow folding pathway which returns to a less folded state before following the pathway for fast folding (reproduced from Dobson et al., 2004)

1.2 Membrane protein folding, stability and unfolding.

Integral membrane proteins (IMP) constitute as much as one third of the proteins encoded in the human genome and they facilitate various crucial cellular processes (Liu *et al.*, 2001). Membrane proteins (MP) can be broadly divided into two groups: outer membrane proteins which are predominantly β-sheet structures and inner membrane proteins which are mostly α-helical. These proteins depend on the lipid bilayer for their structural integrity (Schulz, 2000). Much attention is paid to their structure and function, as they are found responsible for various inherited diseases. It is becoming increasingly clear, however, that many, if not most mutations of membrane proteins that result in pathogenic do not affect the active catalytic or ligand binding sites but their folding into a correct 3-dimensional structure in the endoplasmic reticulum. This may be why deleterious single amino acid replacements are often distributed over the entire structure rather than cluster near functional regions (Garriga *et al.,* 2002). Similar to incorrectly folded soluble proteins, misfolded membrane proteins may be trapped in inactive or unstable conformations or in aberrant conformations that generate disease. Understanding the rules of the folding of membrane proteins is therefore of some urgency in understanding the causes of disease (White *et al.*, 1999).

1.2.1 Determinants of membrane protein stability

The two key factors that determine membrane protein stability are: (1) The chemical nature of the bilayer itself which is composed of two distinct regions: the hydrophobic core and the interface. Interfacial structure and chemistry may be important as the specificity of protein signaling and targeting by the membrane-binding domain could not otherwise exist. (2) The high energetic costs of dehydrating the peptide bond, as when transferring it to a non-polar phase, cause it to dominate structure formation. (Liu *et al.,* 1995) The only permissible structural motifs of transmembrane (TM) membrane proteins are α-helices and β-barrels, because internal hydrogen bonding amends this cost (White, 2003).

1.2.2 How does an integral membrane protein reach the bilayer?

Whether it is a cytoplasmic protein or a membrane protein, they are synthesized in the cytoplasmic compartment of the cell using a similar protein synthesis machinery. Exactly how a protein reaches its target is an ongoing research topic, still at its infancy. Current understanding in this field suggest that in the endoplasmic reticulum, the nascent polypeptide chains of integral membrane proteins are inserted into the translocon that spans the lipid bilayer, where they are prepared for insertion and formation of their secondary and tertiary structures. Hence to study the complete folding of a protein molecule into the bilayer one has to look at various stages: (1) The translocation of the molecule to the membrane, the factors which play a crucial role in stabilizing protein at this stage, modifications that may occur to the protein during this transport. (2) Once the protein reaches the periplasm, the sequential steps that happen till the insertion and forming of a mature protein. The details of how the translocon accomplishes these stages are not yet clear. The details known about the second step are discussed in two parts relating to α-helices and β-sheets separately. It is generally agreed in the case of α-helices that the folding takes advantage of the propensity of polypeptides to spontaneously assume a helical conformation in low dielectric environments like the bilayer. Accordingly, much effort has been expended on studying the insertion of the peptide bond and the various side-chains into the complex lipid matrix, the geometry and energetics of residue-residue and helix-helix interactions inside the membrane, and the pathways by which the helices form, traverse the membrane, and assemble into the bundles that constitute the functional membrane proteins (White, 2003).

1.2.3 α-helical proteins

The principles of how this kind of folding occurs into the membrane have been established from studies of bacteriorhodopsin, as well as from model peptides (White *et al*., 1999). According to the latest three-stage model postulated by Engelman and co-workers, it can be considered that the α-helices will form from random coils because intermolecular hydrogen bonds are favored by the anhydrous environment of the interfacial layer, and if the number and distribution of non-polar side-chains allow, the helical rods enter the core of the bilayer. Once inserted into the membrane, the helices in this "prefolded state" (Popot *et al*., 1987; Popot *et al*., 2000) interact (Zhou *et al.,* 2000) and rearrange into the native conformation. In the simplest case, the helices will form a bundle that spans the bilayer, with the hydrophilic side-chains facing inward while the hydrophobic side-chains face toward the lipids. The interhelical association is related to sequence motifs in which serine, threonine or glycine residues are arranged in alternating patterns with other, less specific residues (Fleming *et al*., 2001; Dawson *et al*., 2002). The active site then assembles in the protein interior, suggesting that the prosthetic group associates after the formation of the helix bundle (Engelman *et al*., 2003). This simple and plausible picture is consistent with a large number of observations in which the overall helical content, the polarity of tryptophan residues, and in some cases the proximity of fluorescent labels were followed during *in vitro* folding of various membrane proteins.

Much is known about the stability and unfolding of α-helices, and not too much data exist on β-barrel proteins. In the next sections the current knowledge on β-sheet folding and stability is summarized.

1.2.4 β-sheet structures

β-sheet structures are also assumed to undergo spontaneous insertion into the outer membrane. According to (Tamm *et al.,* 2001), outer membrane proteins (Omp) are synthesized with a signal sequence and are transported through the inner membrane by the SecA/Y/E/G export machinery in an unfolded form and in a reaction that requires energy in the form of ATP. Once the protein has arrived in the periplasmic space the signal sequence is removed by a signal peptidase. Insertion of β-barrel structures are rather spontaneous process as there is no signal recognized yet for the insertion. It is rather the conformation of the mature protein that determines its insertion into the outer membrane. Nevertheless various catalysts are known to exist in the periplamic space of gram-negative bacteria. Among them are protein disulphide isomerases, namely dsb gene products and peptidyl prolyl isomerases. Probably the Dsb proteins do not have a crucial role to play, as most of the Omps are devoid of a disulphide bond. The peptidyl isomerases found are SurA and RotA. SurA has been implicated in the folding of OmpA, OmpF, LamB, but there is no *in vitro* evidence yet. Sur A is known to play a role in preventing misfolding and aggregation, too (Chen *et al.,* 1996). Skp is postulated to function as a chaperone of Omps in periplasm (Kleinschmidt *et al*., 2004).

Even though these chaperones are present in the periplasm, the current evidences suggest that the membrane insertion is a spontaneous thermodynamically-driven process and it may not require any accessory proteins.

1.2.4.1 Folding of β-barrels into lipid bilayer *in vitro*

Most studies have been carried out using the outer membrane porins OmpA, OmpX and OmpF. Detailed kinetic experiments on the refolding and insertion of OmpA into a lipid bilayer led to the distinguishable folding intermediates and consequently to a quite detailed folding mechanism. Several different kinetic phases were recognized by fluorescence and kinetic gel shift experiments, indicating the existence of several intermediates on the folding pathway of OmpA. Protein folding and insertion into membranes is very slow, taking 20-30 minutes to go to completion at 37 °C (Kleinschmidt *et al*., 1996).

Using various techniques like kinetic gel shift assays, fluorescence spectroscopy , and TDFQ (time-resolved distance determination by fluorescence quenching) Kleinschmidt and Tamm have proposed a three-stage model of folding and membrane insertion. Stage (I) is a largely unstructured complex, (II) a molten disc and (III) an inside out molten globule intermediate. Figure 1.2.1 describes the stages for OmpA.

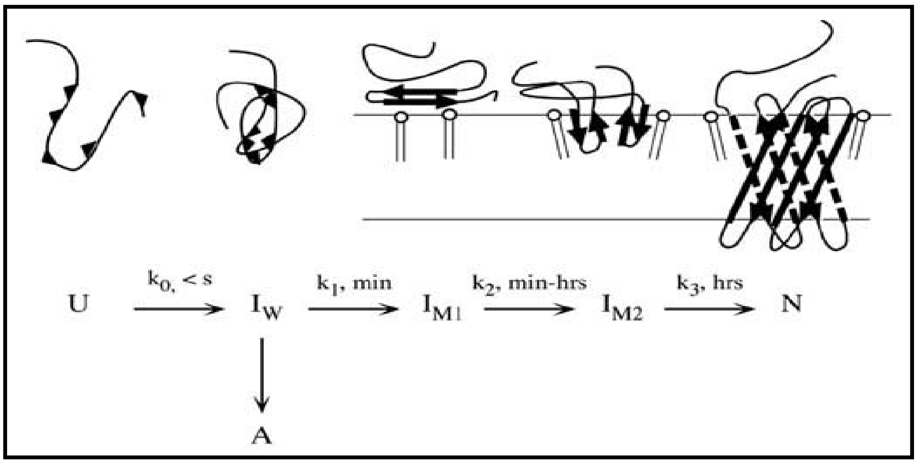

Figure 1.2.1 Tentative scheme for OmpA folding and insertion. Unfolded OmpA (U) first hydrophobically collapses in a kinetically unresolved step to a water-soluble intermediate (I_W) which then adsorbs to the lipid bilayer surface (intermediate I_{M1}) while a minor fraction of protein can aggregate (A). The membrane-adsorbed intermediate progress to a second membrane bound intermediate (I_{M2}) before it is converted to the inserted native state (N) (reproduced from Kleinschmidt *et al.*, 1996).

1.3 Porin as an ideal candidate

Porins are β-barrel proteins which are found in the outer membrane of bacteria, mitochondria and chloroplasts. The known sizes range from 8-22 stranded β barrels existing as monomers and oligomers. Their functions are as diverse as active ion transport, passive nutrient intake, membrane anchors, membrane bound enzymes and defense against attack proteins. Figure 1.3.1 depicts the structure of OmpA, the most commonly studied monomeric porin from *E. coli*.

Initial suggestion for a transmembrane β-barrel came from electron microscope data of a porin. Infrared dichroism studies indicated a 45 ° angle between the strands and the membrane. (Rosenbusch *et al.*, 1980; Schulz, 2000)

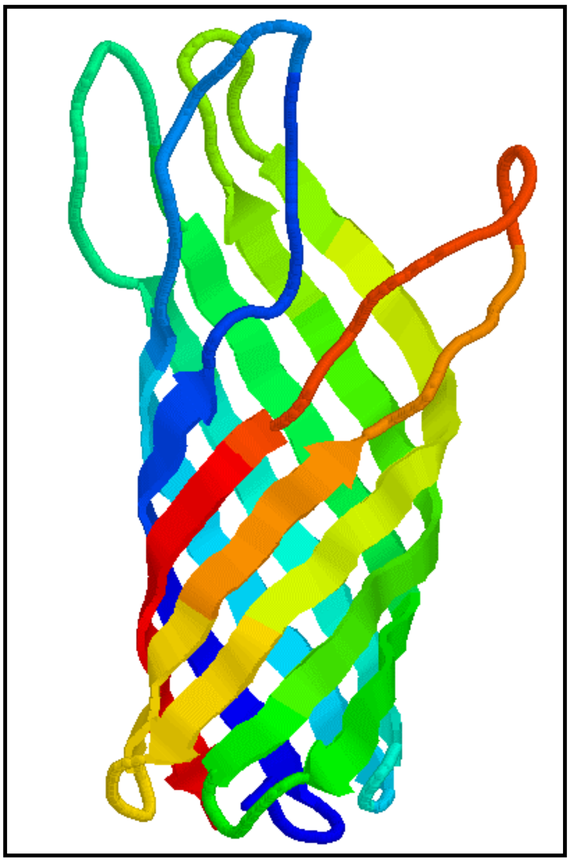

Figure 1.3.1 Outer membrane protein OmpA (Pautsch *et al.*, 2000).

The 10 construction rules of a barrel structure according to Schulz are as follows

1. The number of β strands is even and the N and C termini are at the periplasmic barrel end.
2. The β-strand tilt is always around 45 ° and corresponds to the common β-sheet twist.
3. The shear number of an n-stranded barrel is positive and around (n+2), in agreement with the observed tilt.
4. All β strands are antiparallel and connected locally to their next neighbor along the chain, resulting in a maximum neighborhood correlation.

5. The strand connections at the periplasmic barrel end are short turns composed of few residues and the turns are named T1, T2 and so on.
6. At the external barrel and the strand connections are usually long loops named L1, L2, and so on.
7. The β-barrel surface contacting the nonpolar membrane interior consists of aliphatic side chains forming a nonpolar ribbon with a width of about 22 Å.
8. The aliphatic ribbon is lined by two girdles of aromatic side chains, which have intermediate polarity and contact the two nonpolar-polar interface layers of the membrane.
9. The sequence variability of all parts of the β barrel during evolution is high when compared with soluble proteins.
10. The external loops show exceptionally high sequence variability and they are usually mobile (Schulz, 2000).

All known porins are oligomers of 3 β barrels each of which contains a single polypeptide chain. Besides trimers there exist monomers as Omp A and OmpX and iron transporters Fhu A and Fep A and octamers as Msp (Schulz *et al.*, 2004).

1.3.1 Stability of porins

There are various factors which contribute to the extreme stability of porins. In porins every second residue in the membrane spanning β-strand faces the lipid and is hydrophobic. The rest of the residues is hydrophobic and hydrophilic. The membrane-buried part of porin is solely composed of non-polar β-sheet surface with aromatic residues, forming two aromatic girdles (Seshadri *et al.*, 1998). In these aromatic zones phenylalanines are located toward the lipid core while tyrosine hydroxyl groups and tryptophans point toward the lipid headgroups. The charged external parts (loops) of the protein are stabilized by polar interactions with the lipopolysaccharides, present in the outer leaflet of the outer membrane. The hydrophobic core of the porin trimer is the monomer interface region, which involves one third of each monomer. In *E. coli* porins aromatic and small residues form complementary surfaces that pack optimally against each other at the interface. In addition to this the salt bridges termini of each of the monomer are located in the interface region. The porin trimer is highly stable in the presence of SDS, which is explained by the fact that SDS mimics the physiological action of lipopolysaccharides. Porins are resistant to many proteases too.

1.3.2 Porin from *Paracoccus denitrificans*

Paracoccus denitrificans is a Gram negative bacteria belonging to the order Rhodobacterales. The details from X-ray crystal structure data show that *Paracoccus* porin is a 16-stranded anti-parallel β-barrel structure (Hirsch *et al*.,1997). The length of the residues ranges from 7-16 residues and they have a tilt from the membrane which is between 35 and 55°. The height of the barrel wall is 27 Å at the intermonomeric contact surface and 33 Å at the membrane interface. Each trimer forms 3 independent pores through the membrane. The loops between the strands are shorter at the periplasmic face (2-4 residues) than at the extracellular face (4-50 residues). The longest extracellular loop is L3 between the strands 5 and 6, folded into the interior of the barrel and constricts the pore. Two girdles of aromatic residues run across the outer face of the barrel, with a vertical separation of 20-25 Å. The aromatic girdles appear to mark the boundaries of the barrel surface interacting with the hydrophobic core of the membrane. This structural feature is very similar to that reported for other porins as described in the section 1.3.

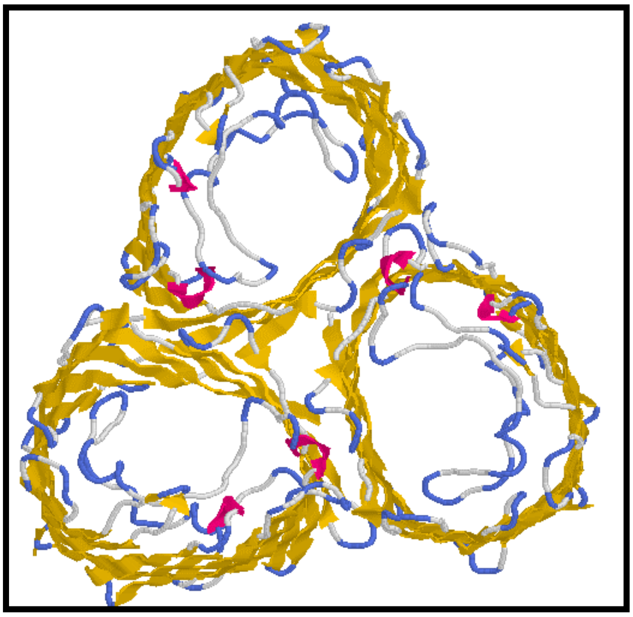

Figure 1.3.2 Trimer structure *of P. denitrificans* porin.
(personal communication Prof. Dr. W. Welte)

Paracoccus porin is very similar in structure to other non specific porins, having the same overall fold, disposition of loop 3 and aromatic girdles. The pore size is similar to that of the other non specific porins as is the unit conductance in 1M KCl (3.2nS). The main difference between *Paracoccu*s porin and other non specific porins is in the distribution of charges at the pore constriction site. In most non-specific porins of known structure, negative charges dominate and the porins are cation selective except for PhoE (Phospho porin) where positive charges dominate and are anion selective. In *Paracoccus* the positive and negative charge is almost balanced making *Paracoccus* porin non-selective.

1.4 Techniques available to study protein folding, unfolding and stability

Protein folding and stability is studied using various approaches ranging from genetic modifications, to labeling proteins, to the vast array of biophysical methods. (Myers *et al*., 2002; Arora *et al*., 2001; Brockwell *et al*., 2000). Investigations in the field of folding has expanded in recent years with the help of improved and time resolved biophysical methods available. Table 1.4.1 summarizes the main techniques used to study *in vitro* and *in vivo* protein folding. The time range represented is the maximum possible as far as the method is concerned and not indicative of the examples given. In some cases optical triggering can be used to induce folding by a photochemical process. The advantage is that it can provide kinetic data below nanosecond time range, but applicability is limited. An attractive technique is to add an artificial dye specifically to switch the protein; this however is still in the infancy.

Temperature jump (T-jump) analysis can be used to rapidly heat the protein for unfolding using a pulsed laser. These experiments can provide kinetic data in the nanosecond time range. Unfolding rates of peptides and staphylococcal protein A have been determined using this technique (Xu *et al.,* 2003; Vu *et al*., 2004). Other techniques like pressure jump and ultrafast mixing can provide data in the microsecond to millisecond time range.

Of the various methods described in Table 1.4.1, fluorescence spectroscopy and circular dichroic spectroscopy (CD) spectroscopy are most commonly used techniques. CD is the most preferred choice as it provides easy handling of samples, it requires lower concentrations, it is extremely useful when chemical denaturants are used and when combined with stopped flow technique ms kinetics can be obtained. Measurements are hampered by light scattering, and absorption in lower UV wavelengths due to presence of high concentration of salts, detergents and some other buffer materials. However, many successful experiments were reported using this technique (Kleinschmidt *et al*., 2003; Engelman *et al*., 2003). Most of data reported on folding of bacteriorhodopsin and porins used CD. The use of other methods like NMR is right now restricted to only a few proteins as NMR cannot be used very easily for studying the membrane proteins of sizes above 30 kDa. FTIR has been used very successfully in case of various soluble proteins but not too many reports are known with respect to membrane proteins. In this report FTIR, CD and fluorescence spectroscopy are combined with genetic manipulations to study the stability, unfolding and refolding of the integral membrane protein porin from *Paracoccus denitrificans*.

Table 1.4.1 Techniques used to study protein folding and stability*

Technique	**Time range**	**Comments/ Information obtained**	**Examples of Proteins studied**
Stopped flow CD			
Far UV	10^{-3} s	Secondary structure changes.	OmpA, OmpF (Kleinschmidt *et al*., 1996)
Near UV	10^{-3} s	Detects aromatic side chain and formation of fixed tertiary structures	
Stopped Flow Fluorescence			
Intrinsic tryptophan	10^{-3} s	Tryptophan environment	OmpA (Surrey et al., 1996)
ANS binding	10^{-3} s	Transient binding to hydrophobic patches	SecA (Song et al., 1997)
Fluorescence Anisotropy	10^{-3} s	Correlation time	p53 (Butler et al., 2003)
FRET (Forster Resonance energy transfer)	10^{-3} s	Distance measurements within protein	Chymotrypsin inhibitor 2 (Weiss, 2000)
Real time NMR	10^{0} s	Chemical shifts and NOE gives information on environment of protein side chains.	Staphylococcal nuclease (Gillespie *et al,* 1997)
Dynamic NMR	10^{-6} s	Line shape analysis. Used in transition region.	Omp A (Arora *et al.,* 2001)
Pulsed Hydrogen Exchange NMR	10^{-3} s	Residue specific information on rate of formation of backbone hydrogen bonds.	Interleukin-1β (Varley *et al.,* 1993)
Pulsed Hydrogen exchange ESI MS	10^{-3} s	Measures the rate of protection of hydrogen in folding populations.	Myoglobin (Simmons *et al.,* 2002)
Atomic Force Microscopy	10^{0}s	Folding and unfolding rates as well as force required to induce unfolding	Bacteriorhodopsin (Muller *et al*, 2002) Porin (Muller *et al*., 1999) Fibronectin (Rief *et al*., 1998)

Small Angle X-ray scattering	10^{-3} s	Dimensions and shape of polypeptide chain.	Cytochrome c (Pollack *et al,* 1999)
Acoustic absorption	10^{-9} s	Usable ultrasonic frequencies range from 0.1-100 MHz. Provides a technique faster than most folding reactions.	Helix-coil kinetics in polypeptides and DNA. (Myers et al., 2001)
EPR	10^{-6} s	Efficient method to detect exact distance between labelled residues in folded, partially folded and unfolded states.	K^+ channel (Peruzo *et al.,* 1999) Iso-1-cytochrome c (De Weerd et al, 2001) Ferredoxin (Mitou *et al*., 2003)
Raman Spectroscopy	10^{-6} s	Secondary structure determination and fast dynamic studies.	Alpha-synuclein (Maiti *et al.,* 2004) Photoactive yellow protein (Takeshita et al., 2002)
IR Spectroscopy	10^{-6} s	Change in secondary structure, lipid protein interactions and ligand binding	Rhodopsin (Vogel *et al*., 2003) Rnase (Fabian *et al*.,1996) K^+ channel (Tatulian, 2003)

* Modified from Brockwell *et al*., 2000.

1.5 Goal of this work

It is obvious from the previous sections that membrane protein stability and unfolding is still at its infancy. The major goal of this work is to investigate the stability, unfolding, refolding of outer membrane protein porin from *P. denitrificans* using genetic manipulations and various spectroscopic methods to develop a sequential pathway for unfolding and refolding.

Various aims of this work are as follows:

- To generate porin mutants and characterize them structurally and functionally.
- To study the thermal stability and unfolding of porin.
- To study the pH dependent stability and unfolding.
- To study unfolding in presence of urea and guanidinium hydrochloride.
- To refold the unfolded proteins back to native structure.
- To correlate stability and function.

2.0 Materials and Methods

2.1 Materials

2.1.1 Chemicals

All the chemical used for this work was obtained from Roth Germany, Merck Germany, Serva Germany, Fluka Germany and Sigma Germany.

2.1.2 Biochemicals

Restriction Enzymes	MBI Fermentas, NEB
Taq DNA polymerase	MBI Fermentas
DNA Ligase	MBI Fermentas, NEB
Pfu Turbo^{TM} DNA Polymerase	Stratagene
IPTG	Peqlab, MBI Fermentas
Benzonase	Novagen
Trypsin	NEB, Novagen
Biobeads SM-2	Bio-rad
Ethidium bromide	Bio-rad
Q Sepharose fast flow	Amersham Pharmacia

2.1.3 Kits

Plasmid DNA extraction Kit	Peqlab
*Qiaquic*k PCR Purification Kit	QIAGEN
Quick change^{TM} Site-directed Mutagenesis Kit	Stratagene

2.1.4 Plasmid

The plasmid pJC40 with the recombinant PorG gene of *P. denitrificans* was provided by Prof. Dr. Bernd Ludwig and Dr. Krishna Saxena, Institut für Biochemie I, Frankfurt am Main, Germany.

2.1.5 PDB Structure

The PDB structure of *P. denitrificans* porin was kindly given by Prof. Dr. W. Welte, Universität Konstanz, Konstanz, Germany.

2.1.6 Culture medium

LB medium

For 1000 mL of media

10 g Tryptone

5 g Yeast extract

10 g NaCl

2.1.7 Buffers

TEN

Tris 100 mM

EDTA 50 mM

NaCl 100mM

TCM solution

10 mM Tris HCl

100 mM $CaCl_2$

10 mM $MgCl_2$ pH adjusted to 7.0

TBE Buffer

For 1000 mL

Tris 12.1 g

Boric acid 6 g

EDTA 10mM

2.1.8 Cells

E. coli

Cell	Genetic marker	Reference
DH5α	*sup*E44, lacU169 (φ80lacZΔM15), *hsd*R17, *rec*A1, *end*A1, *gyr*A96, *thi*-1,*rel*A1	Hanahan, 1983 Bethesda, 1986
BL21 (DE3)	ompT hsd(rB$^-$ mB$^-$) dcm+Tetr *gal(*DE3) *endA* Hte	Stratagene
BL21 (DE3_pLysS)	ompT hsd(rB$^-$ mB$^-$) dcm+Tetr *gal(*DE3) *endA* Hte [pLysSCm^R]a	Stratagene

The list of cell stocks produced during this study is provided in the appendix.

2. 1.9 Primer Design

All primers were designed so that they contain the following features:

1. Both the primers contained the desired mutation and both the sequences were complementary to each other so that they could anneal to opposite strands of the plasmid.
2. The primer length was adjusted between 25-35 bases in length and the melting temperature (T_m) was greater than or equal to 78 °C.
3. The desired mutation was positioned in the middle of the primers and wherever possible a restriction site was incorporated for easy screening of clones.
4. The primers had a minimum GC content of 40 % and were made to terminate with one or more C or G bases.

All primers used in this study were synthesized by MWG Biotech. The list of primers is provided in the appendix.

2.1.10 Antibiotics

Ampicillin was prepared at a concentration of 100mg/mL in H_2O, filter sterilized and stored at –20 °C. It was used at 50-100 μg/mL final concentration

2.2 METHODS

2.2.1 Genetic Techniques

All genetic manipulation of the PorG gene was carried out following the rules and regulations of S1/R1 genetic engineering laws (Gentechnikgesetz (Gen TG)).

2.2.1.1 Competent cell preparation

Competent cells of *E. coli* DH5α and BL21(DE3) were prepared according to a protocol available in the laboratory. 5 mL of LB was inoculated with a single colony and grown overnight. 0.5% innoculum was used to seed 100 mL of LB medium. Cells were grown till OD_{546} of 0.3-0.4. The cells were centrifuged at 6000 RPM for 10 minutes at 4 °C. The pelleted cells were resuspended in 50 mL TCM medium. The mixture was incubated on ice for 30 minutes and further pelleted by centrifuging at 6000 RPM for 10 minutes at 4 °C. The cells were finally resuspended into 10 mL of TCM- glycerol (20% glycerol and 80 %TCM), 100 μl aliquots were frozen in liquid N_2 and stored at –80 °C.

2.2.1.2 Plasmid Purification

Plasmid DNA was purified using plasmid purification kit from Peqlab Germany. 5 mL overnight grown cells were centrifuged (Biofuge *pico*, Heraeus). The pellets were resuspended in 300 μL of buffer I and vortexed thoroughly. 300 μL of buffer II was added and mixed gently, followed by 400 μL of buffer III. The solutions were mixed by inverting the tubes. The mixture was centrifuged for 15 minutes at 13000 RPM. The supernatant was loaded to the special binding column and centrifuged for 1 minute at 13000 RPM. 500 μL of buffer HB (High Binding) was added and centrifuged for 1 min at 13000 RPM (High Binding). Columns were further washed with 500 μL washing buffer twice and centrifuged at 13000 RPM for 1 minute. The empty column was centrifuged to remove the last traces of washing buffer and transferred to a sterile eppendorf tube. Plasmid DNA was eluted out with 30 μL of sterile distilled water.

2.2.1.3 PCR conditions

PCR conditions were optimized so as to give approximately 100% positive clones. For further details on PCR and cloning optimization please see section 7.1 appendix.

The reaction mixture was always kept to 50 μl. The volumes of constituents are given below :

10X PCR buffer	5 μL
dNTPs (2 mM)	5 μL
Primer 1 (10 pM)	2 μL
Primer 2 (10 pM)	2 μL
Template	5 ng
Polymerase	0.5 μL
H_2O	to make 50 μL

PCR was carried out in a thermocycler from Peqlab (Cyclone 25). Standard PCR conditions used for all the reaction were initial denaturation at 95 °C for 3 minutes followed by cycles 20-35 of denaturation at 94 °C for 45 seconds, annealing 55 °C for 60 seconds, extension at 68 °C for 240 seconds, with a final extension of 72 °C for 10 minutes. Small changes in annealing temperature were done whenever required.

2.2.1.4 Agarose Gel Electrophoresis

Agarose gel electrophoresis was carried out in a Bio-rad wide submerged gel electrophoresis unit. 0.7 to 1% agarose gel in TBE buffer was used. Ethidium bromide was added while preparing the gel. Bromophenol blue was used as the tracking dye. To estimate the quantity and size of the DNA 100 bp DNA ladder, and λ/ Hind III ladder (MBI Fermentas) were used.

2.2.1.5 Site-directed Mutagenesis

Site-directed mutagenesis was carried out using Quick change^{TM} Site-directed mutagenesis kit. PCR based mutations were carried out. The details of Primer design and the list of primers used are given in detail in section above. The required mutation was made in the primer and PCR reaction was optimized accordingly. PCR product was subjected to digestion with Dpn I. The resulting mixture was used directly for transformation of *E. coli* DH5α cells.

2.2.1.6 Deletion Mutagenesis

Deletion mutations in the N-termini was also designed based on PCR amplification strategy. PCR primers with ATG in a cleavable Nco I site was designed and the PCR product was ligated to *Nco* I/ *Bam*H I site of vector pJC 40 digested with *Nco* I/*Bam*HI.

2.2.1.7 Transformation of *E. coli* cells

Chemical competent *E. coli* cells were thawed for 5 minutes on ice. 2 μL of plasmid DNA was added, mixed very gently and incubated on ice for 30 minutes.

The cells were heat-shocked for 45 seconds at 42 °C and incubated further on ice for 5 minutes. 1000 μL of LB medium were added and incubated at 37 °C with mild shaking for 45-60 minutes. 100 μL of the mix was plated into LB plates with ampicillin.

2.2.1.8 Restriction Digestion

Restriction digestion of various clones for screening was carried out according to the directions given by the restriction enzyme supplier.

2.2.1.9 DNA Sequencing

Automated DNA sequencing was carried out by Mrs. Elizabeth Uloth at Max Planck Institute for Biophysics, Frankfurt Main, Germany

2.2.2 Protein Biochemistry Techniques

To maximize the expression of the protein the constructs were expressed in *E. coli* BL21(DE3) cells. The proteins were expressed in form of inclusion bodies which was solubilized and refolded. Subsequent headings explains each step briefly.

2.2.2.1 Protein expression in *E. coli* BL21(DE3)

Plasmid DNA having the required construct was transformed in *E. coli* Bl21(DE3) cells. A Single colony was used to prepare a pre-innocula, with required LB medium supplemented with ampicillin. It was grown overnight at 37 °C. 10 mL of the preculture were used to seed 1 L of LB medium with ampicillin. The culture was grown for 4-5 hours till OD_{600} of 0.6-0.7. The cells were induced with 0.5 mM IPTG. The cells were allowed to grow further for 4-5 hours and centrifuged (Sorvall

GS3, 5000 RPM, 30 minutes). The cells were resuspended in buffer TEN and stored at –80 °C .

2.2.2.2 Protein Purification

Purification of protein was carried out according to Saxena *et al*. *E. coli* BL21(DE3) cells (from 1 liter culture) were incubated with Benzonase for 1 hour and the cells were lysed by sonication (Branson sonifier 250, 4 minutes, 30 %, level 4). The suspension was centrifuged (Sorvall GS3, 5000 RPM, 60 minutes). The pellet obtained was resuspended in 30 mL TEN-2 % (w/v) Triton-buffer and incubated by shaking overnight at 37 °C. The solution was centrifuged (GS3, 5000 RPM, 30 minutes) to remove the Triton-buffer, the resulting pellet was further suspended in 30 mL of buffer TEN and incubated at 37 °C for 2 hours followed by centrifugation (GS3, 5000 RPM, 30 minutes). The pellet (inclusion bodies) was resuspended in 30 mL TEN-Urea buffer (8 M urea in buffer TEN) and incubated at 37 °C for 2 hours and centrifuged (Sorval ultra centrifuge, Ti 60, 35000 RPM, 30 minutes). The supernatant was mixed with equal volume of TEN-LDAO 10 buffer(10% (w/v) Lauryldimethyl aminoxide in TEN buffer). The solution was loaded into Q sepharose fast flow column which was equilibrated with 0.2% LDAO TEN buffer. After loading the protein, the column was washed with 0.2 % LDAO TEN buffer. Elution of protein was achieved by running a NaCl gradient of 0.1- 1 M NaCl in 0.2% LDAO TEN buffer. The porin protein eluted out at 0.7 M NaCl. The fractions were pooled and analyzed in SDS and quantified.

2.2.2.3 Protein Quantification

Protein was quantified by the Bio-rad *Dc* protein assay kit.

2.2.2.4 Protein Quality Detection by SDS-PAGE (Laemmli)

Proteins were analyzed for their purity in 12 % SDS-PAGE gels, which were made according to Laemmli. All purified proteins were analyzed for the presence of monomer and trimer by using heated (100 °C for 5 minutes) and unheated samples. For temperature dependent studies the samples were pre-incubated at the required temperatures in a dry heating block (a_1 biotech, Germany) uniformly for 5 minutes, then cooled to room temperature and mixed with equal volume of loading dye. For all experiments heating up of the gels due to high voltage was avoided. Staining of the gels was done with Coommasie brilliant blue solution. Destaining was achieved with destain solution (10 % Acetic Acid, and 40 % Methanol in H_2O)

2.2.2.5 Reconstitution into liposomes

Reconstitution of the protein into liposomes was carried out by a modified freeze thaw method. 2 mg of L α phosphatidyl choline was dissolved in chloroform and dried overnight. The dried lipids were resuspended in 2 mL of protein solution (0.5mg/ mL). The mixture was incubated at 37 °C for 30 minutes under agitation. Detergent was removed using Bio-rad bio-beads (pre-treated with methanol and water). This was followed by 4 freeze thaw cycles. After removing the last traces of bio-beads the lipid vesicles were collected by ultra-centrifugation at 35000 RPM for 3 hours. To remove the residual bio-beads the pellet was washed with buffer TEN followed by centrifugation at 35000 RPM for 20 minutes. The liposomes collected were directly used for IR spectroscopy.

2.2.3 Refolding Methodologies

(a) Chemically denatured protein

Protein denatured with 8 M urea and 7.5 M GmHCl was refolded either into micelles or into liposomes. For refolding into micelles, the denatured protein was diluted to a concentration of 0.5 M using buffer TEN and loaded to a Q-sepharose column and eluted using NaCl gradient. For refolding into liposomes, the denatured protein was diluted using a lipid emulsion in buffer TEN containing Bio-beads. Then the freeze thaw method described above was used.

(b) pH denatured protein

Denatured protein was loaded to a Amicon microcon YM -10 centrifugal column and diluted with buffer TEN pH 8, continuously, untill a complete buffer exchange was achieved which was verified by analyzing the pH of the elute. The protein was concentrated and then investigated with IR spectroscopy.

(c) Heat denatured protein

Protein denatured by heat (90 °C for 4 minutes) was refolded in a 2-step process. The white insoluble mass of denatured protein was incubated with buffer TEN pH 13, for 1 hour, and observed for the solubilization of the white insoluble mass into transparent soluble solution. The unfolded protein hence obtained was refolded as described above in section (b).

2.2.4 Spectroscopic Techniques

Fourier Transform infrared (FTIR), Circular dichroism (CD), and Fluorescence spectroscopy were used in this study.

2.2.4.1 IR spectroscopy

IR spectroscopy probes the vibrational modes of a molecule. In general a polyatomic nonlinear molecule with N atoms has 3N-6 distinct vibrations. Each vibration has an associated set of quantum states and in IR spectroscopy the IR radiation induces a transition from the ground level to the first excited quantum state. Thus, the vibrational transitions of a molecule result in an absorption band in the infrared region. However, not all molecules are infrared active; those bond groups which exhibit a change in electric dipole moment during the vibration can be characterized for their vibrations very precisely in the infrared region. Vibrational spectra are traditionally plotted against the inverse of the wavelength, which is termed as “wavenumber”. The IR spectrum is roughly divided into three regions: the near infrared (from 12990 cm^{-1} to 4000 cm^{-1} ≡ 700 nm to 2.5 μm), the mid-infrared (from 4000 cm^{-1} to 400 cm^{-1} ≡ 2.5 μm to 25 μm), the far infrared (400 cm^{-1} to 10 cm^{-1} ≡ 25 μm to 1000 μm). In this study only transitions in the mid infrared region are analyzed.

A basic infrared spectrometer consists of a light source emitting IR radition (Globar), a monochromator, a detector and a recorder.

Five decades ago the use of IR spectroscopy for elucidation of secondary structure was shown by Elliot and Ambrose. From then the technique has undergone many changes and today it is applied to study the structure, function, protein-ligand interaction and protein-protein interactions. Apart from that, IR spectroscopy has entered the field of biomedical spectroscopy for the analysis of body fluids.

The modern day spectrometers use Fourier transformation methods, hence called Fourier transform infrared (FTIR) spectroscopy. The basic difference between a dispersive IR and FTIR instrument is the replacement of the monochromator by a Michelson interferometer. In the FT spectrometer the spectrum of the sample is not measured directly. Instead an interferogram is produced, which is converted by means of Fourier transformation into a spectrum.

FTIR-transmission and Attenuated total reflection (ATR)-FTIR were used this study.

2.2.4.1.1 FTIR transmission Spectroscopy

The measurements are carried out in a transmission mode, where the protein sample is sandwiched between two calcium fluoride (CaF_2) windows with an optical pathlength of a few micrometers. The IR beam passes through the sample.

Sample Preparation

The protein sample (20 μL of 2mg/ mL) was dried in a gentle stream of N_2 and re-suspended in 3 μL D_2O. Approximately 1.5 μL of sample was loaded in the center of a demountable CaF_2 microcell with an optical path length of 7.4 µm (Fabian and Mäntele, 2002). The cuvette was sealed by coating the outer ring of one of the windows with a thin layer of an ethanol-oil-mixture, to prevent loss of sample by evaporation. The sample in the sample holder was mounted in a home built motor-driven sample shuttle which allows recording of the background immediately before recording of the sample spectrum without opening the spectrometer and thus without perturbing the dry atmosphere in the spectrometer. Thus, water vapor did not contribute to the spectra and no subtraction of vapor bands was necessary.

Temperature changes were achieved by heating the sample holder. Temperature was controlled by a thermocouple placed close to the sample which was connected to a Haake C25 water-bath. Temperature was controlled using the display in the monitor of the water-bath.

Measurement of IR spectra

IR spectra were recorded with a Bruker VECTOR 22 FTIR spectrometer equipped with a DTGS (deuterated triglycine sulfate) detector. For each spectrum 20 interferograms were averaged, apodized with a Blackman-Harris-4-term function, zero-filled and Fourier-transformed to yield a nominal spectral resolution of 2 cm^{-1} with an encoding interval of 1 cm^{-1}. The spectra were processed and visualized using windows OPUS version 3.1 software. The built-in program for calculating second derivatives of the spectra in the OPUS software was used to identify the minute changes in smaller peaks

2.2.4.1.2 ATR-FTIR Spectroscopy

Figure 2.2.1 depicts the schematic representation of an ATR cell. It is based on the basic principle of total internal reflection by lightguide. A diamond crystal is fixed on top of the ZnSe reflection element. The IR radiation is focussed on to the end of the ZnSe, which in turn is reflected through the diamond crystal several times before reaching the detector. The IR radiation actually penetrates into the sample deposited on the diamond crystal surface as a film. The penetration depth is in the range of 1μm.

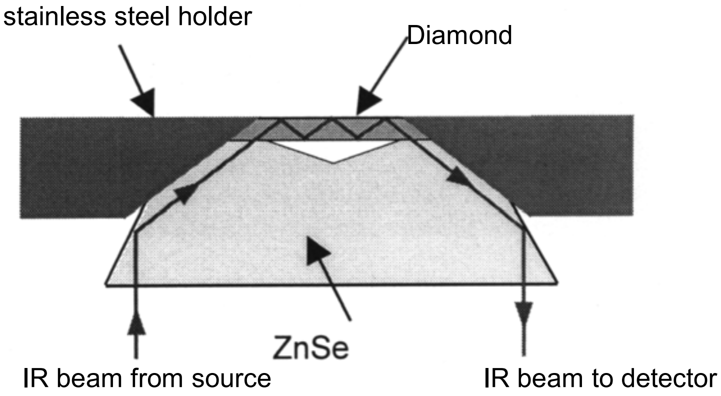

Figure 2.2.1 Schematic representation of the ATR cell used in this study. (reproduced from Prof. Dr. W. Mäntele (personal communication))

Sample preparation

A 5 μL protein sample in H_2O was deposited on the surface of the diamond crystal and it was allowed to dry in the continuous stream of air in the closed chamber. For H/D exchange experiments 2 μL of D_2O were added to the dried sample and the sample chamber was sealed with parafilm to prevent drying under the continuous flow of dry air.

Measurement of IR spectra

Spectra were measured with a Bruker VECTOR 22 FTIR spectrometer equipped with a MCT detector (Mercury Cadmium Telluride). The detector was cooled using liquid N_2 . The background spectra recorded was air (no protein on the diamond). The protein was then spread on the crystal and was allowed to dry for few a minutes before measuring the spectrum. 50 interferograms were averaged, apodized with a Blackman-Harris-4-term function, zero-filled and Fourier-transformed to yield a nominal spectral resolution of 2 cm^{-1} with an encoding interval of 1 cm^{-1}. The spectra were processed and visualized using windows OPUS version 3.1 software.

2.2.4.2 CD Spectroscopy

Light is a transverse electromagnetic wave, but natural light is generally unpolarized, all planes of propagation being equally probable. Light in the form of a plane wave in space is said to be linearly polarized. Circularly polarized light consists of two perpendicular electromagnetic plane waves of equal amplitude and 90° difference in phase. Elliptically polarized light consists of two perpendicular waves of unequal amplitude which differ in phase by 90°. Figure 2.2.2 explains the three kinds of polarized light.

When a plane polarized light passes through an optically active sample, two effects are observed. (1) After passing through the sample, the plane of polarization is rotated with respect to the plane before entering the sample; this is termed optical rotatory dispersion. (b) In certain regions the light that emerges from the sample is no longer linearly polarized but elliptically polarized. This is called “ellipticity”. It is caused by the difference in absorbance of right and left circularly polarized light, which in known as circular dichroism (CD).

For practical reasons, an acousto-optical or electro-optical modulator is used to modulate the polarization of the light at high frequency (typically 50-100kHz). A synchronous detection allows demodulation of the difference in signal between absorption of left and right circularly polarized light. The absorbance difference (A_L-A_R) is typically very small with respect to the overall absorbance (10^{-3} – 10^{-4}).

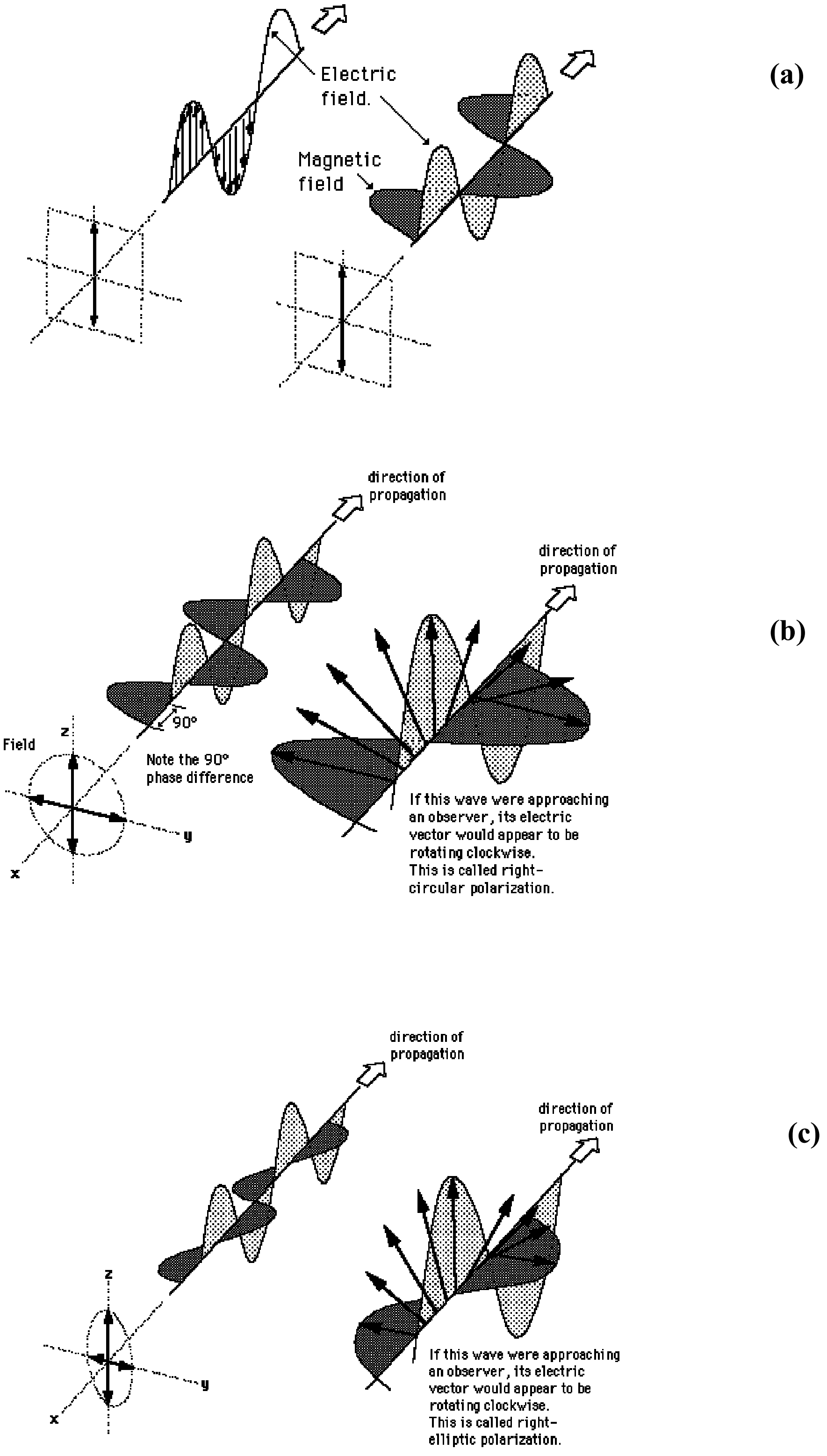
Electric field.
Magnetic field
(a)
direction of propagation
direction of propagation
(b)
Field
z
y
x
90°
Note the 90° phase difference
If this wave were approaching an observer, its electric vector would appear to be rotating clockwise. This is called right-circular polarization.
direction of propagation
direction of propagation
(c)
z
y
x
If this wave were approaching an observer, its electric vector would appear to be rotating clockwise. This is called right-elliptic polarization.

Figure 2.2.2 (a) Linearly polarized light
(b) Circularly polarized light
(c) Elliptically polarized light (copied from www.hyperphysics.phy-astr.gsu.edu/)

Sample preparation for CD spectra

All samples were diluted to approximately 1mg/mL concentration in buffer TEN with LDAO.

Spectra recording

A JASCO J 720 spectropolarimeter was used to record the CD spectra in range of 195-260 nm. The spectral band width used was 1 nm, response time of 1 sec with standard sensitivity. A quartz sample cell of path length 0.01 cm was filled with 20 μL of sample, closed with the stoppers and carefully placed in the sample holder located in the sample chamber. Before the measurement of the sample spectra, the spectra of air and buffer was also recorded. Each spectrum was recorded by accumulating 4 scans with a speed of 50nm per minute. All data were analyzed using a spectrum analysis program of the instruments software and were converted into text files, which was used by PSI-Plot version 6.5 to generate the output spectra shown in results.

2.2.4.3 Fluorescence Spectroscopy

Fluorescence is the emission of light from a molecule that has been excited by the absorption of light. The intrinsic fluorescence of proteins arises from the amino acids tryptophan (Trp), tyrosine (Tyr) and phenylalanine (Phe). The emission of Phe is weaker than that of Tyr and Trp. Tyrosine emission is insensitive to the polarity of the solvent. Trp emission is very sensitive to the polarity of the solvent. In this study the change of intrinsic fluorescence of Trp was observed upon the change of environment. Figure 2.2.3 depicts a Jablonski scheme for Trp. The first and second electronically excited state are very close together. They are called ^1L_a and ^1L_b ; depending on the environment either ^1L_a or ^1L_b has the lower energy. The

${}^1L_a$ state has higher energy in apolar environment than ${}^1L_b$ but lower energy in polar environment. In most cases ${}^1L_a$ has lower energy and fluorescence emission takes place from this state.

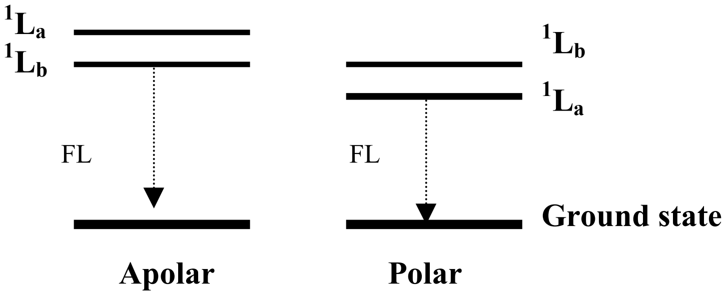

Figure 2.2.3 Jablonski Scheme for Trp. (reproduced from Cantor and Schimmel, 1980)

Sample preparation for fluorescence spectroscopy

The samples were diluted in buffer TEN. A concentration of 0.01mg/mL was used for each measurement. 1500 μL of sample volume was used for all the measurements.

Recording of Fluorescence spectra

A Perkin Elmer Luminescence spectrometer LS 50 was used for all measurements. A quartz cuvette was used to hold the sample. Emission spectra were recorded in the wavelength range from 300-400 nm, with a excitation wavelength of 290 nm. The slit width was adjusted to 5 nm. A scan speed of 50nm per minute was used. The data were analyzed using the software of the instrument. All the data was converted into ASCII format and further analyzed using Origin 5.0.

2.2.5 Lipid Bilayer Activity Measurements

All measurements were carried out in the laboratory of Prof. Dr. R. Benz, Biozentrum, Universität Würzburg.

The basic set up of the instrument is shown in Figure 2.2.4. The bilayer chamber (cuvette) (Benz *et al.*, 1978) is made of teflon separated with a partition having a septum with a circular hole. The chambers are filled with electrolyte, in this study it was 1 M KCL. The lipid bilayer is painted on the septum using a loop. 5µL of lipid is added on the tip of a loop and dipped into the electrolyte and stroked over the septum hole, the formation of the bilayer is described by Benz *et al.*, 1973. The membrane area formed is approximately 2×10^{-2} cm^2. The potential is applied through the Ag/AgCl electrodes immersed in the electrolyte. The signal is amplified using the amplifier. The output is recorded using a chart recorder at variable sensitivity. The small magnetic strirrers help to mix the solution in the chambers constantly.

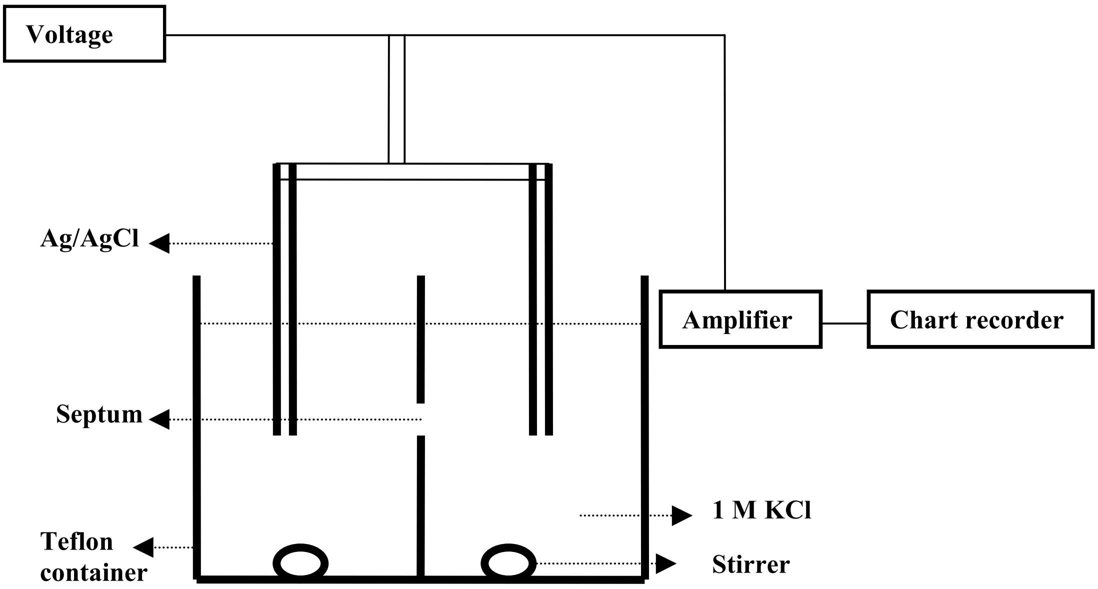

Figure 2.2.4 Schematic representation of the lipid bilayer setup.

Single channel recordings

Sample preparation

Protein sample was diluted to 0.3 mg/ mL using 1% genapol, a non ionic detergent. 5 µL of the sample was added to both sides of the cuvette containing 5 mL of 1M KCl.

Channel recording

Single channel measurements were carried out in the set up shown above. The cuvettes were cleaned with ethanol and double distilled water and dried throughly. To prepare the pore in the cuvette to hold the membrane, the pore was filled with 5 µL of 1% Diphytanoyl phosphatidylcholine (DPC) in chloroform and allowed to dry for a few minutes and then filled with the electrolyte 1M KCL. The cuvette was then mounted to the thermo jacketed cuvette holder and the Ag/AgCl electrodes were immersed into each sides. The membrane was painted using a loop with 5 µL of 1% solution of DPC in n-decane. A fixed membrane potential of 20mV was applied through the Ag/AgCL electrode. The current through the membrane was boosted by a current amplifier . The printer setting was set to 500mV full scale with a speed of 3 cm/min. The membranes were broken by tapping the cuvette when too many pores were inserted and the recording becomes noisy. Each measurement was carried out until approximately 100 pores were recorded.

Activity Profiling

Sample Preparation

The protein sample was diluted to final concentration of 3 µg /mL in 1% Genapol.

Activity recording

The cuvettes were thoroughly washed with ethanol and water and dried before each new measurement. The preparation of the membrane holding pore in the cuvette was done as described for single channel recording. After the membrane is formed a background measurement was recorded for 3 minutes. 5 μL of the sample was added to both sided of the cuvette containing 1M KCl and was stirred continuously throughout the measurement. All activity measurements were performed at minimum 3 times and the results shown are the average of 3 recordings. All measurements with single stable membrane for 30 minutes were used to calculate the activity.

.

3.0 Results and Discussion

The main aim of this study was to characterise the stability and unfolding of *Paracoccus denitrificans* porin in the presence of various denaturants like heat, pH, urea and GmHCl. Hence it was crucial to study the effects of denaturants on wild type and a few structural variants generated by mutations.

3.1 Mutant Construction

To study the effect of single and multiple mutations on the stability of the protein, site-directed and deletion mutants were constructed. The mutants were strategically designed by studying the available structures and previous results with other porins. (Saxena *et al.*, 1999; Gokce *et al.*, 1997; Phale *et al.*, 2001; Bainbridge *et al.,* 1998)

3.1.1 Selection criteria

The selection of mutants was based on the comparison of protein sequences of *Rhodopseudomonas blastica*, *Rhodobacter capsulatus, Paracoccus denitrificans.* porin. Figure 3.1.1 shows the result of a multiple sequence alignment, which was generated using the Clustal X programme (www-igbmc.u-strasbg.fr/BioInfo). The numbering in the ruler has 20 amino acid less than the original protein sequence, as the comparison is carried out for the sequence after the signal peptide, as that is the part expressed in the studies here, but the mutants are named according to the original sequence (P95467). Most of the porins that are expressed in *E. coli* are expressed in a similar way, as it allows porin to be hyper expressed without causing toxicity to the host. The alignment shows that there is not much sequence similarity between the 3 organisms; only 45 residues are conserved, but they share a good amount of similarity as far as the arrangement of residues and hence the fold similarity is concerned.

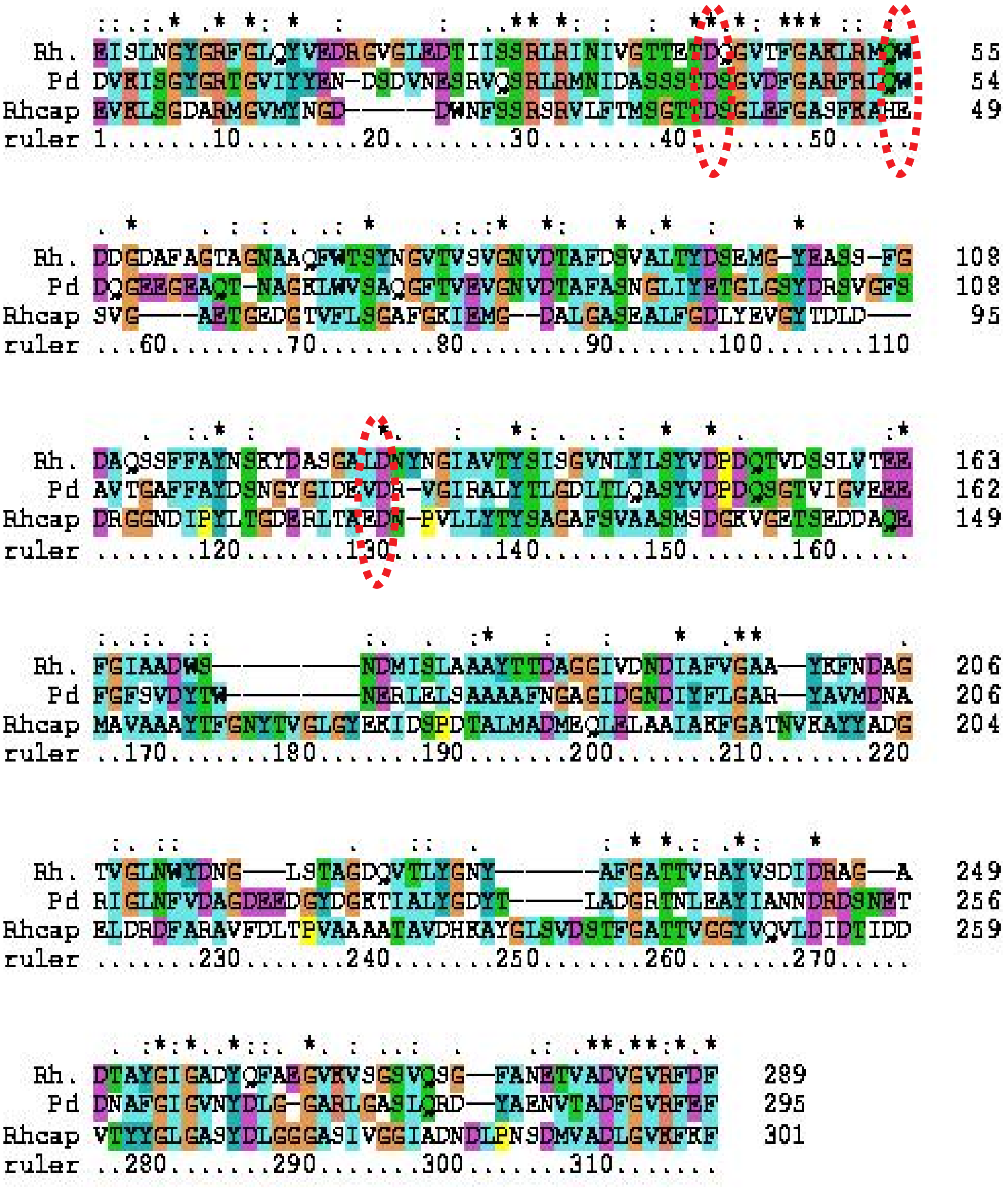

```
      ::.:.* .* *: *  :      :  ..** *: :  :  **.*: *** :: :
  Rh. EISLNGYGRFGLQYVEDRGVGLEDTIISSRLRINIVGTTETDQGVTFGARLRMQW    55
   Pd DVKISGYGRTGVIYYEN-DSDVNESRVQSRLRMNIDASSSTDSGVDFGARFRIQW    54
Rhcap EVKLSGDARMGVMYNGD------DWNFSSRSRVLFTMSGTTDSGLEFGASFKAHE    49
ruler 1.......10........20........30........40........50.....

      . *    . : : . .: *    .:.:*  *:   * .*  :     *
  Rh. DDGDAFAGTAGNAAQFWTSYNGVTVSVGNVDTAFDSVALTYDSEMG-YEASS-FG   108
   Pd DQGEEGEAQT-NAGKLWVSAQGFTVEVGNVDTAFASNGLIYETGLGSYDRSVGFS   108
Rhcap SVG----AETGEDGTVFLSGAFGKIEMG--DALGASEALFGDLYEVGYTDLD---    95
ruler ...60........70........80........90.......100.......110

         .  :.* :        *.   :   *: . ..:  *  * .         :*
  Rh. DAQSSFFAYNSKYDASGALDNYNGIAVTYSISGVNLYLSYVDPDQTVDSSLVTEE   163
   Pd AVTGAFFAYDSNGYGIDEVDR-VGIRALYTLGDLTLQASYVDPDQSGTVIGVEEE   162
Rhcap DRGGNDIPYLTGDERLTAEDN-PVLLYTYSAGAFSVAASMSDGKVGETSEDDAQE   149
ruler .......120.......130.......140.......150.......160.....

      :..:. ::          :.  .  :*   :   :    *  .**         .
  Rh. FGIAADWS----------NDMISLAAAYTTDAGGIVDNDIAFVGAA--YKFNDAG   206
   Pd FGFSVDYTW---------NERLELSAAAAFNGAGIDGNDIYFLGAR--YAVMDNA   206
Rhcap MAVAAAYTFGNYTVGLGYEKIDSPDTALMADMEQLELAAIAKFGATNVKAYYADG   204
ruler ..170.......180.......190.......200.......210.......220

       :. ::           .   ::  .        : * *.: .*:   *
  Rh. TVGLNWYDNG---LSTAGDQVTLYGNY-------AFGATTVRAYVSDIDRAG--A   249
   Pd RIGLNFVDAGDEEDGYDGKTIALYGDYT-----LADGRTNLEAYIANNDRDSNET   256
Rhcap ELDRDFARAVFDLTPVAAAATAVDHKAYGLSVDSTFGATTVGGYVQVLDIDTIDD   259
ruler .......230.......240.......250.......260.......270.....

       . :*:*..*::. *. : ..:  .    .: .**.**:*.*
  Rh. DTAYGIGADYQFAEGVKVSGSVQSG--FANETVADVGVRFDF   289
   Pd DNAFGIGVNYDLG-GARLGASLQRD--YAENVTADFGVRFEF   295
Rhcap VTYYGLGASYDLGGGASIVGGIADNDLPNSDMVADLGVKFKF   301
ruler ..280.......290.......300.......310.......
```

3.1.1 Multiple sequence alignment. Rh (*Rhodopseudomonas blastica*) Pd (*Paracoccus denitrificans*), Rhcap (*Rhodobacter capsulatus*). The residues selected for mutations are marked in red circles.

Residues D61, W74 and D148 common to all compared proteins were selected for mutation. Residue 61 lies in a small loop in the periplasmic side see Figure 3.1.2 and the residue 148 is positioned in the small helix region. Aspartic acid residues at position 61 and 148 were selected to be changed into Asparagine so that the size of the residue is not altered heavily as only OH is replaced by NH_2 , but at the same time the charge could be removed. Tryptophan residue at position 74 was altered to cysteine, as *Paracoccus* porin did not contain any cysteines, and the residue 74 was positioned at the monomer interface, making it more probable to formation of disulfide bridges. Another interesting characteristics was to use cysteine as labelling site.

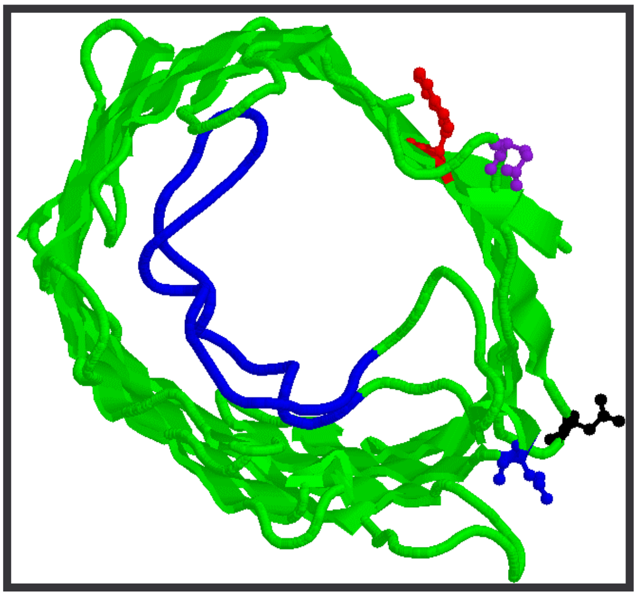

Figure 3.1.2 The porin monomer with the mutated residues. D61 (black), W74C (red), E81 (purple), D148 (blue) and the highlighted loop (blue) region shows the deletion (Δ116-136).

Mutant E81Q was based on the study by Phale *et al.* with Omp F porin where the substitution of similarly positioned E71 resulted in a drastic reduction of the transition temperature (T_M) from 76 ℃ to 48 ℃ which was explained by the prevention of salt bridge and hydrogen bond formation between E71 and R100 and R132 of the adjacent monomer (Figure 3.1.3).

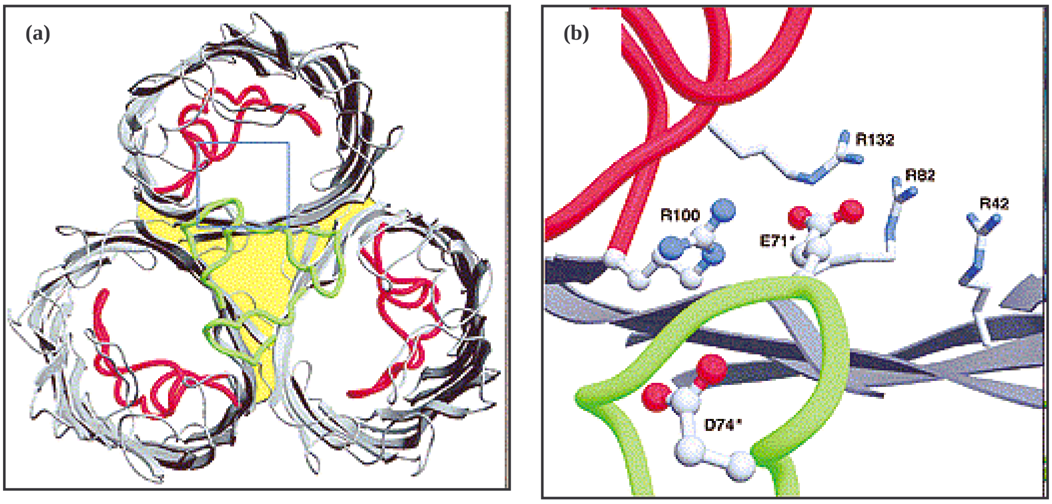

Figure 3.1.3 (a) OmpF trimer. The latching loop is depicted in green.
(b) Residues E71, R132 and R100 are highlighted
(reproduced from Phale *et al*., 1998).

Deletion mutants were selected based on the structural details available according to which the large loop L3 should have a very major role in the stability (Figure 3.1. 2). The mutation was designed on the β-sheet structure to study the effect of deletion on stability of the entire porin. Figure 3.1.4 (a) and (b) depicts the deleted segment of the porin mutant (Δ 21-25) in comparison with the wild type monomer. The model was generated using first approach mode of SWISS MODEL software (www.expasy.org/swissmod/SWISS-MODEL). Even though the regions selected for mutation were quite large, earlier reports had shown successful construction and purification of small deleted regions from other porins. (Srikumar *et al.*, 1997 Saint *et al.,* 1996*).*

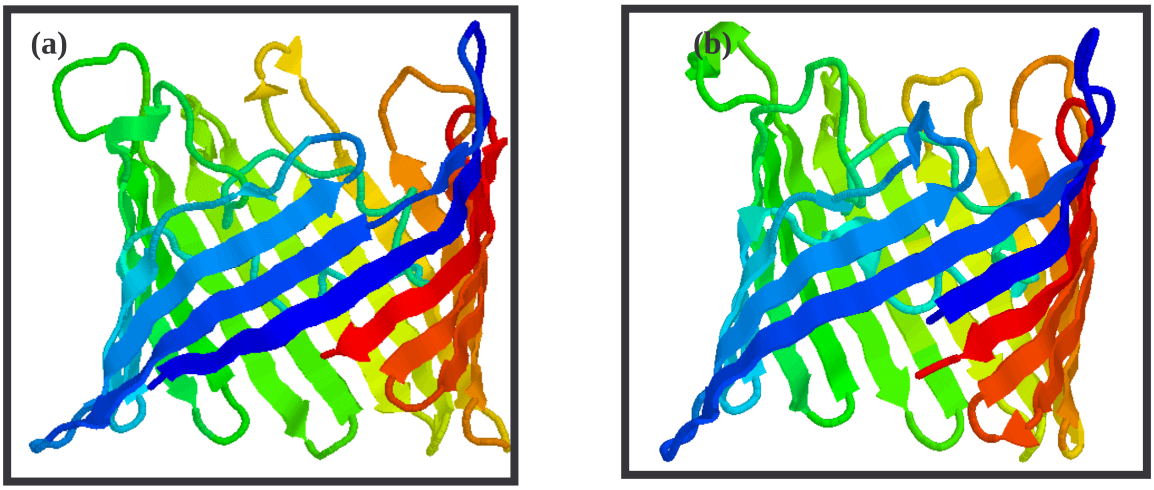

Figure 3.1.4 (a) Side view of wild type monomer. (b) Deletion mutant (∆21-25).

3.1.2 Site-directed mutants

Plasmid pJC40 with recombinant por G gene cloned into NcoI/ BamH I site was used as the template for the construction of single mutants (Saxena *et al.*, 1997, 1999). A PCR based mutation strategy was used and the cloning efficiency was optimised so as to attain approximately 100 % positive clones. The details of the PCR optimisation and results from screening are explained in detail in section 8.2 The result of restriction analysis and sequencing are summarised in Table 3.1.1. Single mutants E81Q, W74C, D61N and D148N were further used as templates for constructing the double and triple mutants. All plasmids with mutated porin gene were transformed into *E. coli* DH5α. Plasmid purification was also carried out using the DH5α construct. The sequenced DNA was used to transform *E. coli* BL21(DE3) and BL21(DE3)pLysS cells. The constructs in *E. coli* BL21DE3 were used for all expression studies.

Table 3.1.1 Summary of the cloning trials

Name of the clone	**Restriction analysis**	**Sequencing Results**
Wild	positive	positive
E81Q	positive	positive
W74C	positive	positive
D61N	positive	positive
D148N	positive	positive
E81Q/D148N (ED)	positive	positive
W74C/D148N (WD)	positive	positive
E81Q/D148N/W74C (EDW)	positive	positive
Del I (Δ 106-126)	positive	positive
Del II (Δ 21-25)	positive	positive

3.2 Protein Purification

Wild type and the mutants E81Q, W74C, E81Q/D148N, W74C/D148N, E81Q/W74C/D148N, Del I and Del II were retransformed into *E. coli* BL21(DE3). Attempts were made to produce protein from all of them, but it was found that only the site-directed mutants produced protein as inclusion bodies.Table 3.2.1 gives a brief summary of the expression attempts in *E. coli* Bl21DE3. Some control experiments were also conducted to analyze if any *E. coli* proteins contaminate the purification and it was found that the purified fraction contained only *Paracoccus* porin in detectable amount. Even though all of the single mutants expressed well, when the same went to form double mutants or triple mutant, refolding of the protein from inclusion bodies was not very successful. Figure 3.2.1 shows the SDS-PAGE gel profile of wild type and mutants E81Q, W74C, E81Q/D148N which were refolded and used for various spectroscopic studies. The major bands are in the trimer region when the protein is not heated before loading. Under similar expression and purification conditions W74C/D148N and E81Q/W74C/D148N produced protein, which on refolding formed denatured or aggregated proteins, hence it was not used for all spectroscopic studies but only to determine the structure and function.

Del I and Del II did not produce protein in detectable amount in small scale expression studies, so no large scale purification was attempted. The reason for deletion mutants not expressing can be due to large deletion in the protein, perhaps the polypeptide formed gets degraded on formation itself. The possibility of incorporating a wrong reading frame during gene manipulations cannot be ruled out, even though none was seen in the sequenced results. Hence for most spectroscopic analysis wild type and three mutants were used.

Table 3.2.1 Summary of protein expressions attempts

Clone used	Small scale expression	Quantity of protein obtained
Wild type	Positive	2 mg/mL
E81Q	Positive	1.54 mg/mL
W74C	Positive	1.7 mg/mL
E81Q/D148N	Positive	1.9 mg/mL
W74C/D148N	Positive	1 mg/mL
E81Q/W74C/ D148N	Positive	1.8 mg/mL
Del I	Negative	-
Del II	Negative	-

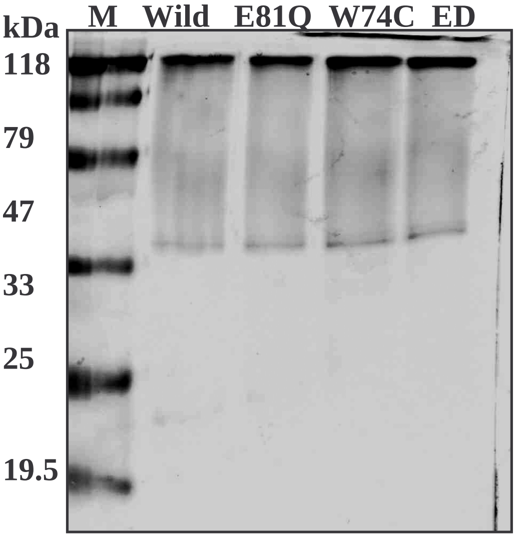

Figure 3.2.1 SDS-PAGE gel analysis of purified protein from wild type and mutants E81Q, W74C, E81Q/D148N.

3.3 Secondary structure analysis

All purified proteins were subjected to spectroscopic characterisation of their secondary structures. ATR-FTIR, FTIR transmission and CD spectroscopy was carried out to analyze the wild type and the mutants. The goal of the experiments was to examine the secondary structure critically with 2 methods and to establish the advantages and disadvantages of each spectroscopic technique for the analysis of porins. Towards the end of this section a detailed explanation of the advantages and disadvantages is explained with respect to one of the mutants E81Q/D148N/W74C.

3.3.1 Wild type characterisation in detergent micelles and liposomes

(i) IR Spectroscopy

It was first shown by Elliot *et al.*, in 1950 that the secondary structure of protein can be analysed by IR spectroscopy. The infrared spectrum of polypeptides is made up of bands designated as amide bands. A typical polypeptide spectrum contains 9 amide bands called amide A, B, I, II, III, IV-VII from the polypetide backbone as well as contributions from amino acid side chains. The amide bands in particular amide I, II and III are modes characteristic for secondary structure of the proteins. The details from amino acid side chain absorption are crucial in the study of ionisation states, dynamics, and functional studies of proteins.

The Amide I and II modes are the most important in the study of secondary structure. The Amide I is found in the region between 1700 cm^{-1} and 1600 cm^{-1}; the exact frequency of the band depends on the geometry of the protein and its back bone hydrogen bonding. This mode is associated with C=O stretching vibration: ν(C=O) accounts for 70-85 %, ν(C-N) contributes 10-20% of the potential energy. Amide I also contains in plane N-H bending, which is mainly responsible for the downshifts of amide I frequency on N-deuteration. The exact analysis of the amides I mode with mathematical procedures like Fourier self deconvolution, second derivatives and others can lead to the separation of overlapping absorption bands which forms the basis for quantitative analysis of the secondary structure of proteins. The position of various secondary structure elements referred in this study is summarised in table 3.3.1. (Jackson *et al*., 1995; Barth, 2000)

Secondary structure	**In H_2O (cm^{-1})**	**In D_2O (cm^{-1})**
α-helix	1648-1657	1642-1660
β-sheet (high frequency component)	1623-1641 1674-1695	1615-1638 1672-1694
Random	1642-1657	1639-1654
Coils	1662-1686	1653-1691

Table 3.3.1 Position of secondary structure elements

It is reported by Jackson *et al.* (1950) that the dihedral angles of a polypeptide chain determine the chain geometry, which in turn dictates the length and direction of hydrogen bonds involving amide C=O and N-H groups. Variation in the length and direction of hydrogen bonds results in variation in the strength of the hydrogen bond for different secondary structures, which in turn produce characteristic electron densities in the amide C=O group and the lower the amide I absorption appears.

The Amide II mode derives from the in-plane N-H bending (40-60%), ν(C-N) (18-40%) and ν(C-C)(10%). Upon H/D exchange the in-plane N-D bending appears in the 940-1040 cm^{-1} region mixing with other modes and the ν(C-N) moves in the

1450-1490 cm^{-1} region where it mixes with other modes to yield a large band called amide II', which is used for analysing the degree of H/D exchange of the protein.

In this study amide I is used to analyse the secondary structure and the changes occurring in secondary structure in presence of denaturants.

The structure of the wild type protein is explained in detail together with that of the mutant protein. Figure 3.3.1 shows the FTIR transmission spectra (a) and the ATR-FTIR (b) of the amide I region of the porin wild type. With both spectra it can be established that the porin contains predominantly β structures, characterised by the peaks at 1629 $cm^{-1}$and 1694 cm^{-1}. This clearly indicates that the protein has anti-parallel β-sheet structure. According to Moore *et al*, 1975 the explanations for these bands are that if the protein contains anti parallel β-sheet structures, then one of the absorption is closer to 1630 $cm^{-1}$and another absorption above 1670 cm^{-1}, which is assigned to a high frequency β-sheet component that arises from transition dipole coupling . Generally the position of this absorption is found to be 50-70 cm^{-1} above the main β-sheet component, for *Paracoccus* porin it is always 65 cm^{-1} higher. There is a remarkable difference in the spectral shapes in in Figure 3.3.1 (a) and (b), which arises from different water content. In Figure 3.3.1(a) where the protein was dried and resuspended in D_2O, there are some contributions from water in the 1680 cm^{-1}–1635 cm^{-1} region, masking the minor details in that region. In the ATR spectrum (Figure 3.3.1(b)) the β-sheet components are sharper and all the minor features in region between 1600 and 1700 are clearly seen as the protein was dried on the surface of the ATR crystal as a film. The second derivative spectra (Figure 3.3.2) show small peaks at 1650 $cm^{-1}$and 1670 cm^{-1} which represents the helix and loop regions. The spectra also indicates that the spectral details obtained for mutant porin E81Q, W74C, and E81Q/D148N are similar to that of the wild type. W74C/D148N and E81Q/W74C/D148N did not produce the native-like spectral features (data not shown). The probable reasons for incorrect spectra were mis-folded proteins, the protein would be highly unstable and not able to fold correctly. These two proteins showed strange SDS-PAGE pattern after purification: Instead of 2 bands a multitude of bands was observed indicating that the protein was not pure or it has aggregated, the former argument can be ruled out as all the other mutants were also purified using same procedure.

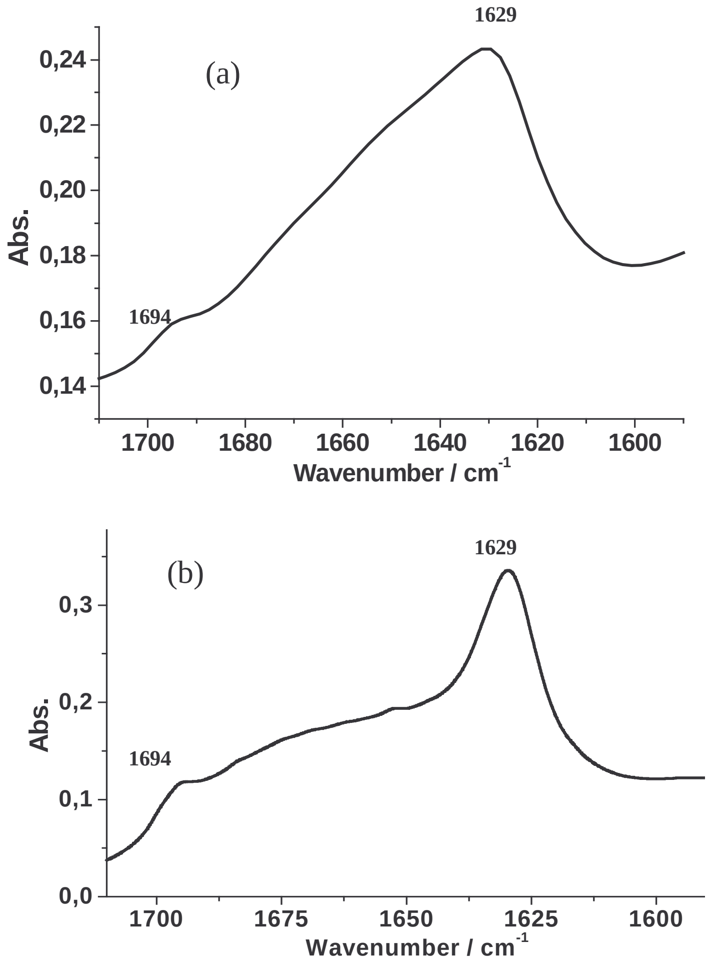

Figure 3.3.1 (a) FTIR transmission spectra of wild type porin in detergent micelles.
(b) ATR-FTIR spectra of wild type protein in detergent micelles.

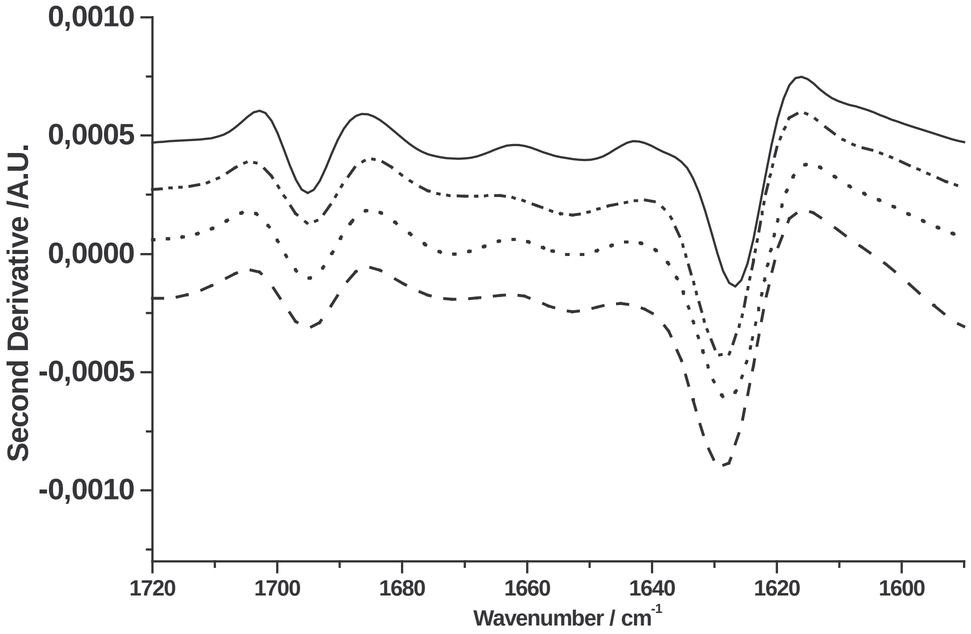

Figure 3.3.2 Second derivative spectra of protein in detergent micelles measured in the FTIR transmission mode. Spectra are shifted on the absorbance axis for easier comparison. From top to bottom (solid line) wild type, (dash dotted line) E81Q, (dotted line) W74C, (dashed line) E81Q/D148N.

Structure of porin reconstituted into liposomes

The protein was reconstituted into L α phosphatidyl choline. It was known from previous studies with *E. coli* OmpF that porin shows a high affinity for phosphatidyl choline (Lee, 2003). Figure 3.3.3 depicts the IR spectra of the wild type and mutants in the spectral region between 1600 cm^{-1} and 1700 cm^{-1} of the protein reconstituted in liposomes. The characteristic peaks at 1630 cm^{-1} and 1695 cm^{-1} point out that the secondary structure of the wild type is predominantly composed of β-sheet, which is in line with the structural information available from the X-ray crystal structure data (Hirsch *et al.*, 1997) The mutants E81Q, W74C and E81Q/D148N had similar IR spectra as the wild type; this allows to conclude that the mutant exhibit the same secondary structure. The minor differences seen in spectral region between 1700 cm^{-1} and 1600 cm^{-1} are due to different protein-to-lipid ratio in each of the sample. Hence the content of H_2O also varied in each sample measured. The spectral features of protein reconstituted into liposomes and the protein in detergent micelles studied by FTIR transmission mode are rather similar . The FTIR results obtained here for *Paracoccus* also compare well to the results obtained for *E. coli* OmpF porin. (Nabedryk *et al.,* 1988; Kleffel *et al*., 1985)

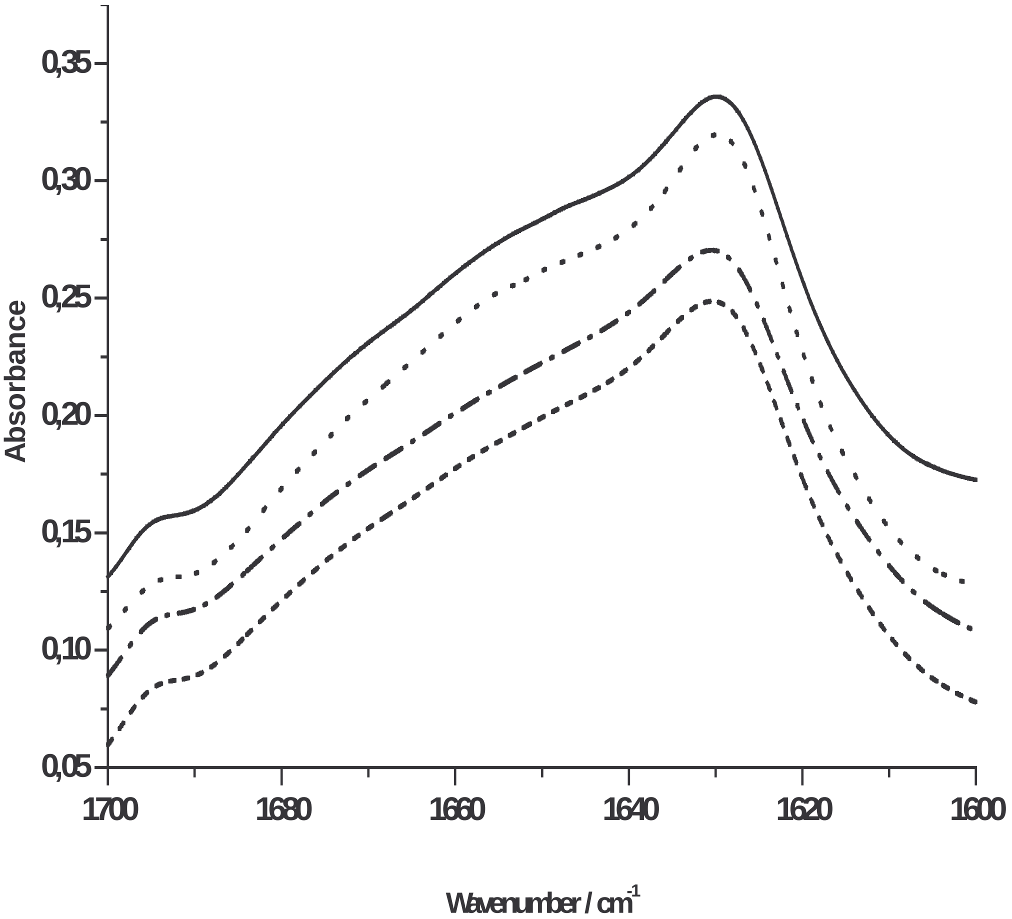

Figure 3.3.3 FTIR transmission spectra of protein reconstituted into phosphatidyl choline vesicles. Spectra are shifted on the absorbance scale for easier comparison. From top to bottom (solid line) wild, (dotted line)E81Q, (dashed dotted line) W74C, (dotted line) E81Q/D148N.

(ii) CD Spectroscopy

Circular dichroism is very sensitive to the secondary structure of polypeptides and proteins. It has been reported by (Chou *et al.*, 1974; Greenfield *et al.*, 1969; Kelly *et al.,* 2000) that CD spectra between 260 and approximately 180 nm can be analyzed for the different secondary structural types: alpha helix, parallel and anti-parallel beta sheets, turns, and others.

The simplest method of extracting secondary structure content from CD data is to assume that a spectrum is a linear combination of CD spectra of each contributing secondary structure type (e.g., "pure" alpha helix, "pure" beta strand etc.) weighted by its abundance in the polypeptide conformation. The major drawback of this approach is that there are no standard reference CD spectra for "pure" secondary structures.

So various groups have developed different methods to correctly analyse the experimental CD spectra using a database of reference protein CD spectra containing known amounts of secondary structure. These methods are in general more accurate and reliable (Greenfield *et al.*, 1969; Sreerama *et al*., 2004). Similar multivariate analysis of multi-component spectra developed by Klein *et al*. (personal communication), which has been applied successfully in the analysis of multicomponent spectra are found to be 99 % accurate in predicting each components. A similar approach can be applied for membrane protein spectra, with development of a database exclusively for membrane proteins with measurements in range of 260-180 nm. However the success of such an approach will always depend on the vastness of the database and completeness of the range measured as in case of membrane proteins the major hindrance is to get measurements up to the wavelength 180 nm because of light scattering.

The CD spectra were generally recorded for the 260-195nm range in this study. The spectra (Figure 3.3.4 (a) to (e)) shows typical negative peaks at 217 nm and positive values from 207nm. It was concluded from analysing the spectra that the protein is predominantly β- structure. As the spectra showed only one minimum at 217 and no minima at 222 nm and 204nm, it was concluded that the protein does not contain any significant amount of α-helix structure. The spectra obtained are very similar to those obtained for other porins (Wolf *et al.*, 1996; Conlan *et al.,* 2000). But the spectral features of the mutant E81Q/D148N/W74C (e) is not very similar to others, it shows a broader region and there is negative value close to 195 nm, which is unusual for β- structure. Attempts were made to quantify the secondary structure elements present in the protein using the programmes Dicroprot 2000 (Deléage *et al*., 1993) and CDNN version 2.1(www.bioinformatik.biochemtech.uni-halle.de/cdnn) but unfortunately all the methods provided different ratios of secondary structures. It is not surprising to see such results as various other groups have reported similar problems with analysing CD data of β- structure proteins. (Conlan *et al*., 2000; Manavalan *et al*., 1987). Another aspect for not obtaining a constant secondary structure ratio is absence of data at wavelengths below 195 nm, as most of the methods are based on database of proteins measured at wavelength down to 180nm, which was not possible with porins due to presence of high concentration of detergents.

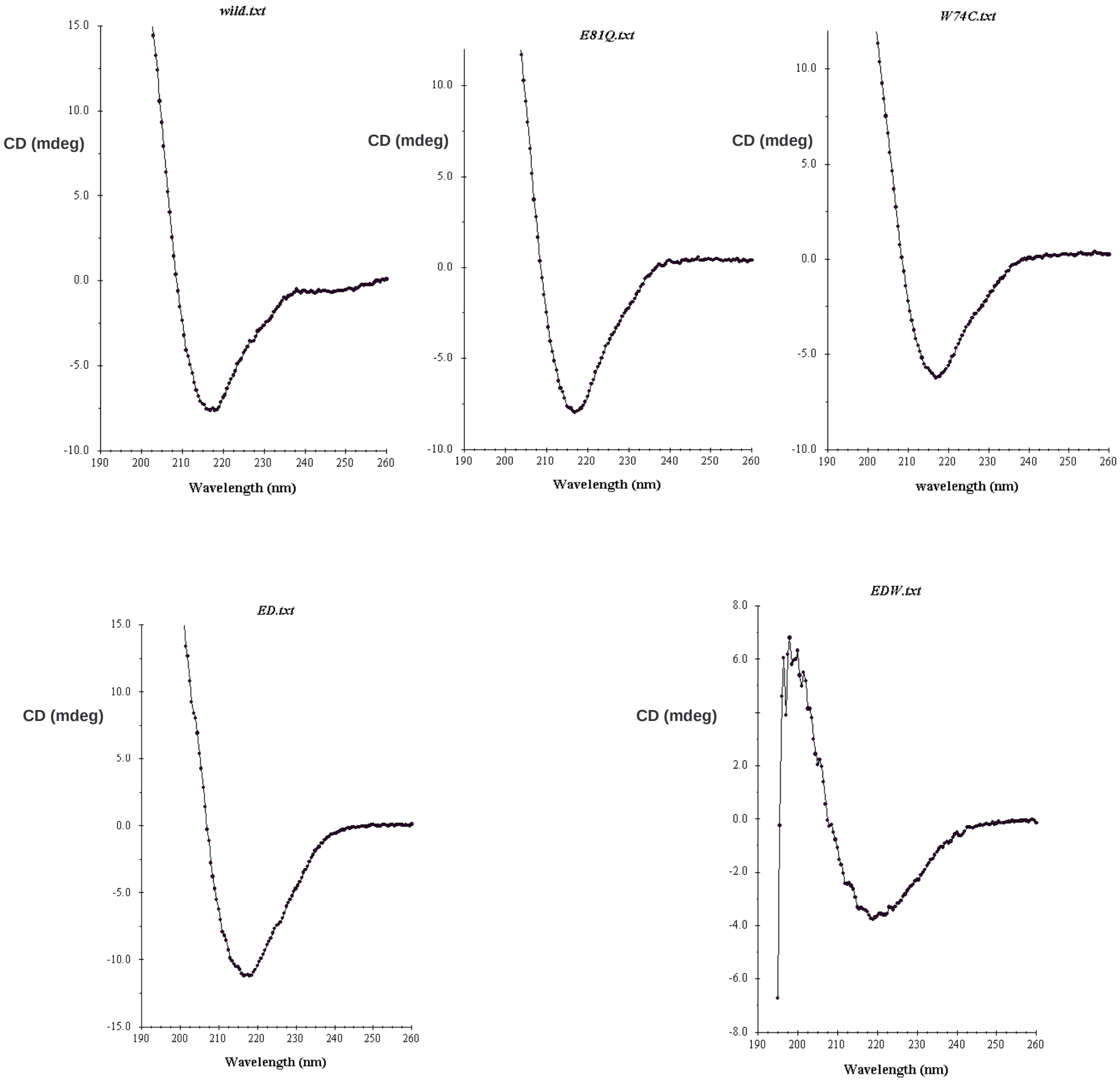

Figure 3.3.4 CD spectra of (a) wild type (b) E81Q (c) W74C (d) E81Q/D148N (e) E81Q/D148N/W74C

3.4 Functional Characterisation

3.4.1 Single channel conductance

In order to analyze the single channel conductance and activity of the protein, functional studies using black lipid bilayer measurements were carried out. As explained in the section 2.2.7 protein was added to both sides of the chamber after the appearance of a black lipid membrane to the incident light. The stepwise insertion of pores into the membrane is depicted in graph (Figure 3.4.1). Measurement were made up to the insertion of approximately 100 pores.

The single channel conductance was calculated for the x-t plot traces, taking into account the amplifier gain (10^9 V/A), the plotter sensitivities, and the applied voltage between the chamber compartments. In the plot shown here (Figure 3.4.1), one division corresponds to a conductivity of 0.25 nS.

The plot here (Figure 3.4.1) represents steps of various sizes, which are counted manually and tabulated into a frequency table, which is then represented as a frequency versus conductance graph. Figures 3.4.2 (a) to (e) represents the frequency of pores at various conductance. Figure 3.4.2 (a) depicts the frequency distribution for wild type, it has to be noted that the frequency of the pores with 3.25 nS conductance is 29 %, and there seems to be some pores distribution with a mean conductance of 1.75 nS. Similar pore distribution pattern was obtained for wild type porin and recombinant wild type porin reported earlier (Saxena *et al*., 1997, 1999). It can be clearly established from the data that the channel conductance of *Paracoccus* wild type porin is 3.25 nS. The same is true for W74C and ED. The mutant E81Q (Figure 3.4.2(d)) gives a predominant conductance at 1.25 nS along with 3.25 nS and there is a broad distribution for each of the conductance. In wild type, W74C and ED also there is some pores of conductance of 1.75 and 2 nS, which may be arising due to some monomer or dimer species. The unusual conductance for the mutant E81Q may be arising because of highly unstable trimers. From the Figure 3.4.2 (a) it can be analysed that the frequency of pores with 3.25 nS, which indicate trimer conductance is 29% in wild type. The distribution of the pores with lower conductance is not very broad. In the mutants it is observed that frequency of trimer conductance is less than 20% and there is a broad distribution of the conductance, clearly indicating the presence of various species which insert into the bilayer.

EDW was also checked for any functionally active pores. It showed the presence of very few pores, at high protein concentration. The pores formed were noisy and flickering. Hence showing that, at a very low concentration of protein has a secondary structure similar to β-sheet structure, some of them having capability to form functional pores.

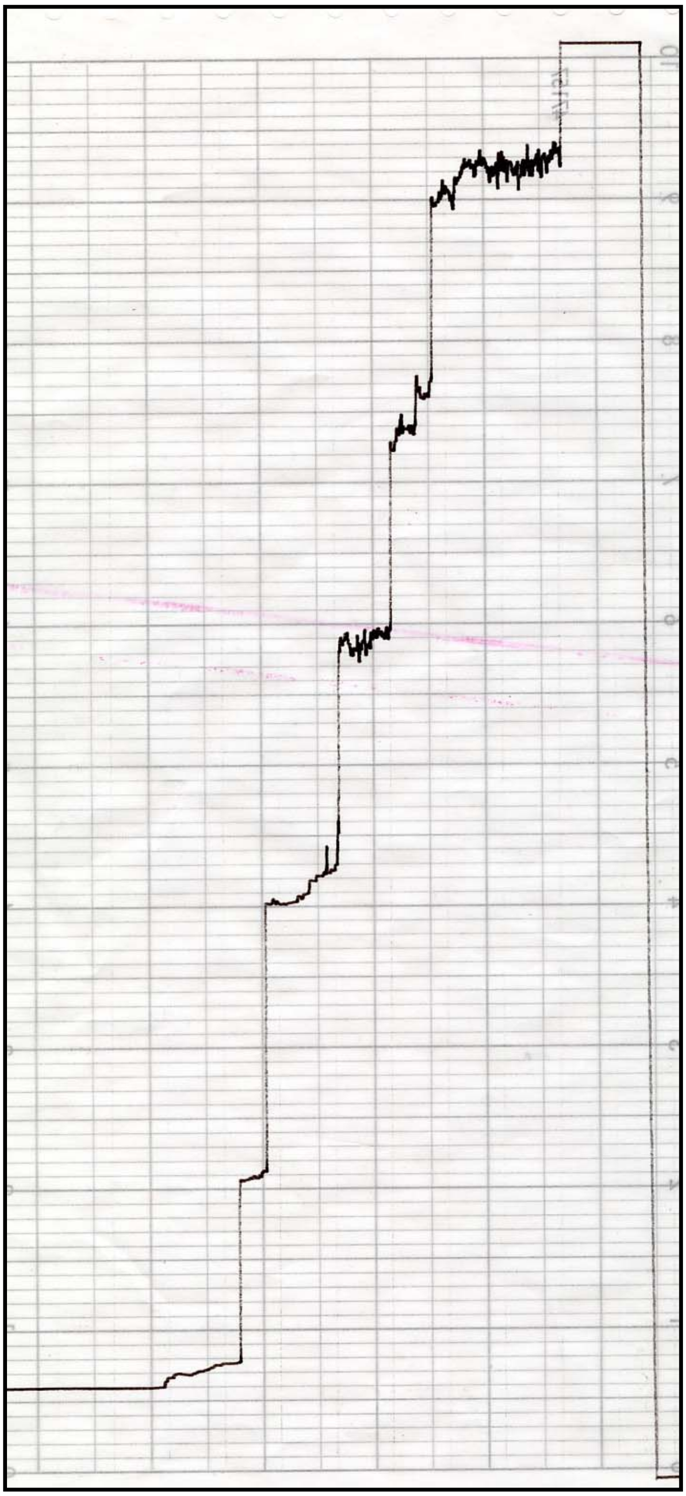

Figure 3.4.1 Stepwise increase of membrane current after addition of protein.

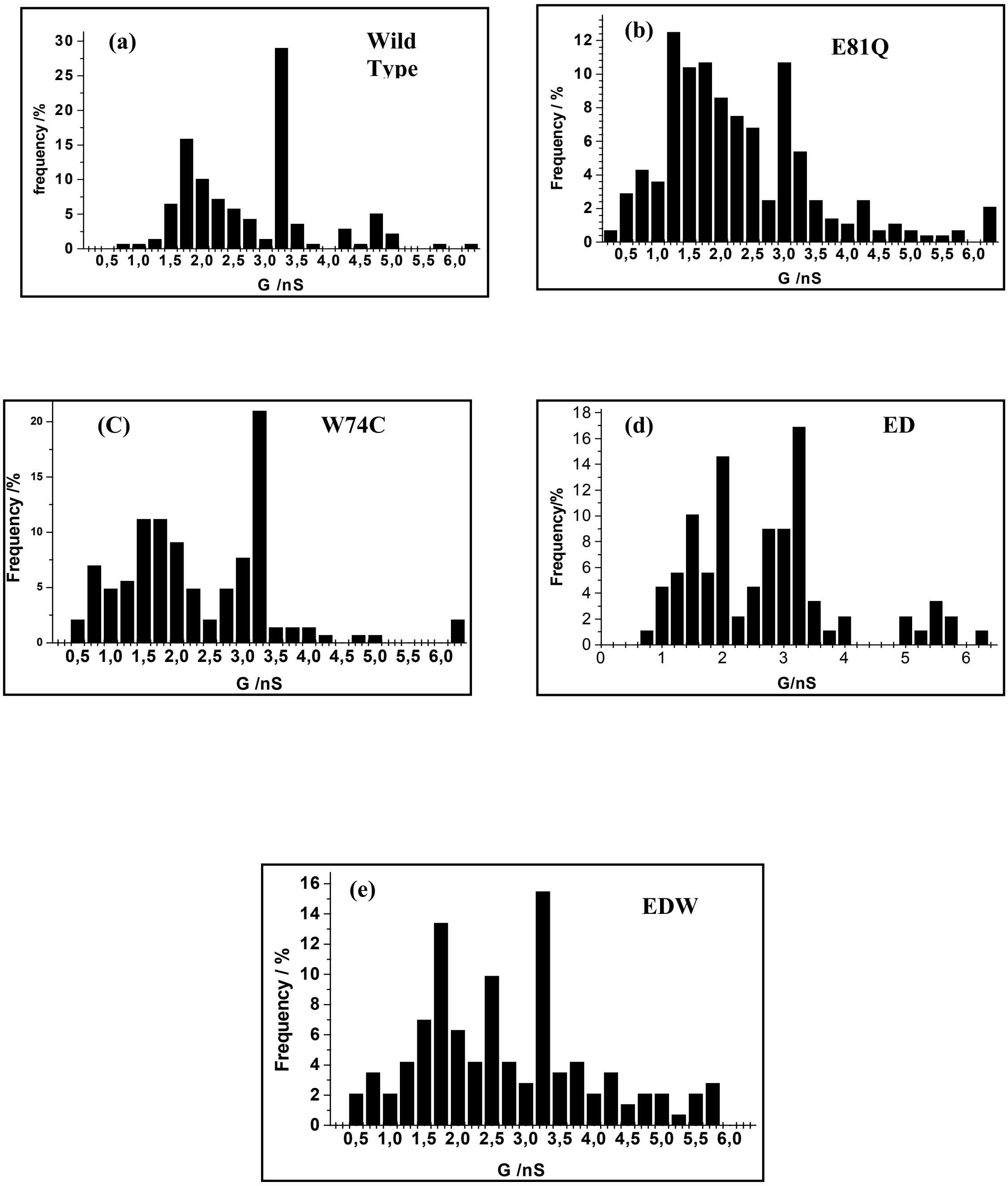

Figure 3.4.2 (a) to (e) Frequency histogram of wild type and mutants

3.4.2 Activity profiling

The maximum conductance attained through single membrane was measured for 30 minutes. Figure 3.4.3 depicts the saturation activity measured for wild type porin. The maximum conductance was averaged from 3 individual measurements under the same conditions and continuous mixing. The conductance obtained for wild type was the highest when compared to mutants. The amount of protein used varied in each measurement, for mutants a higher concentration of protein had to be used hence a relative activity was calculated using the amount of protein used and maximum conductance attained. The activity of wild type protein was considered 100 %.

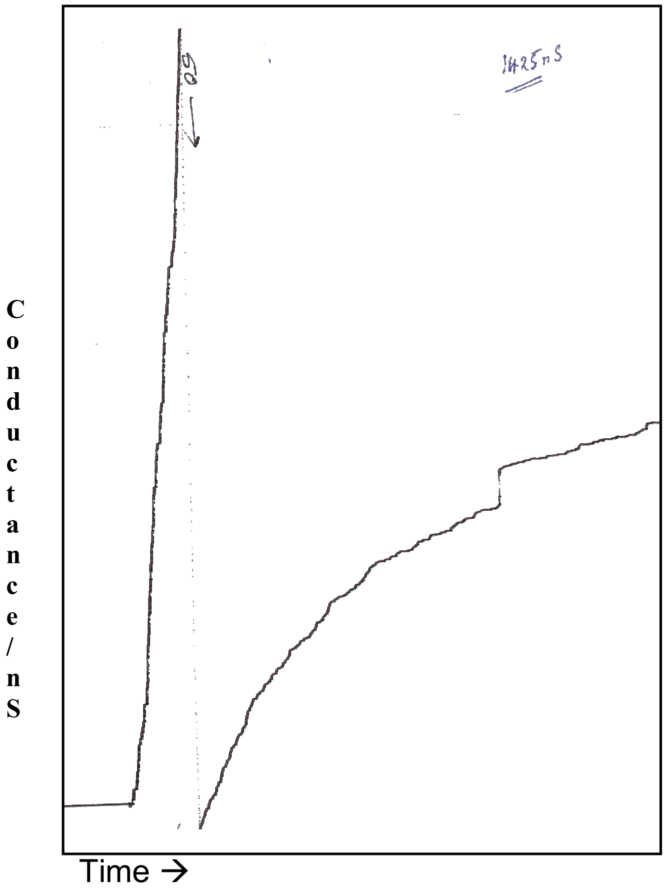

Figure 3.4.3 The activity profile of wild type porin.

Figure 3.4.4 depicts the relative activity of the mutants in comparison to the wild type. It is surprising to see that even though W74C and E81Q and ED had shown good channel conductance with the same amount of protein as the wild type their relative activity seems to have reduced to a large extent. It can be explained by analysing the single channel conductance graphs (Figure 3.4.1(a) to (e)) where it is quite clear that even though the mutants form pores of similar conductance as the wild type, the frequency distribution is entirely different. The wild type porin has maximum frequency of pores with 3.25nS conductance (29 %) wheras in mutants this seems to fall below 20 %. In mutants it is observed that the frequency distribution of pores is very broad compared to the wild type which indicates that the wild type protein has more stable trimers compared to the mutants. This result is surprising because all the proteins showed similar secondary structure by spectroscopy. It has to be noted that the concentration of protein used in activity studies is far less compared to the spectroscopic studies. The ratio of trimers, dimers and monomers which cannot be distinguised spectroscopically in case of porins, causes a major effect in the functionality of the protein.

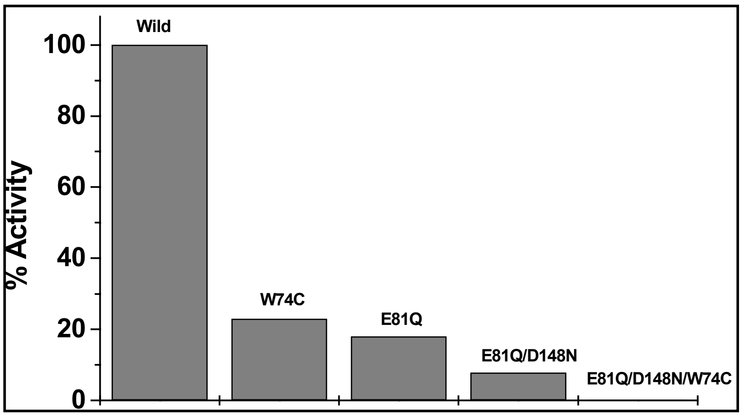

Figure 3.4.4 Relative activity of wild type porin and mutants

3.4.3 Structural and functional correlation

It can be concluded from this section that structurally *Paracoccus* porin has a β-sheet structure. The mutants E81Q, W74C, ED are structurally very similar to the wild type but differ functionally. All the mutants are active and they made pores of size reported in earlier studies (Saxena *et al.*, 1999). Hence it can be said that single and double mutations do bring about minor changes in structure, which could not be identified spectroscopically, but are evident from the conductivity measurements. Another important factor to be concluded is that mutations brings about changes in the refolding pattern of the protein from inclusion bodies, which is evident with the kind of protein quality obtained from WD and EDW.

EDW which as explained in the previous sections, is misfolded to a large extend that it does not produce a characteristic β-sheet spectrum in FTIR or CD signal compared to other porin mutants. In addition, it does not show any significant amount of activity, even though it produces a few pores with conductance of 3.25 nS.

3.5 Thermal stability, unfolding and activity profiling

Thermal stability was analyzed for wild type and mutant proteins E81Q, W74C and E81Q/D148N in micelles and for protein reconstituted in liposomes. The results from wild type are explained in detail and the results from mutants are discussed in comparison to the wild type.

3.5.1 Thermal unfolding in detergent micelles

3.5.1.1 Wild type porin

The thermal unfolding and denaturation of the protein was analyzed using IR spectra which were measured for a temperature series from room temperature up to 95°C. The three-dimensional representation of the changes in the amide I absorption with respect to temperature is shown in Figure 3.5.1 (a) and (b). The development of the amide I spectra between 25 and 95°C is depicted in Figure 3.5.2 in the absorbance spectra (a) and the second derivative (b), in the region between 1580 cm^{-1} and 1710 cm^{-1}. It is clearly evident from the spectra that there is a shift of 10 cm^{-1} at the amide I region from 1630 cm^{-1} to 1620 cm^{-1} and from 1695 cm^{-1} to 1685 cm^{-1} upon heating. In Figure 3.5.2(b) it can be clearly observed that some smaller minima at 1675 cm^{-1} and 1650 cm^{-1} (previously assigned to turns and helices) disappear and instead a minimum at 1649 cm^{-1} appears, which indicates that some part of the protein unfolds into random structure. The band at 1620 cm^{-1} indicates that the protein is aggregated at high temperature. The shift in the band position can be explained on the basis of reports from Jackson *et al.,* 1995.

In denatured β-sheet proteins, where the most common form of unfolding and denaturation is forming an aggregate, forming an aggregate may not be always involved with the concentrations used, but can be a proteins intrinsic property. Intramolecular hydrogen bonds may not be possible in such extended β-polypeptide but due to the close proximity and alignment of the chains intermolecular hydrogen bonds are formed and the formation of these strong hydrogen bonds are expected to produce a correspondingly low amide I frequency. In the case of porins forming aggregate is probably the only way for the protein to prevent its hydrophobic residues from exposing to the solvent environment and hence in doing so it may be attaining a rather low energy level too. The downshift of the band indicates the formation of intramolecular hydrogen bonds, which stabilizes the aggregate. The appearance of a band at 1649 cm^{-1} reveals that a considerable fraction of the protein attained a random structure. Hence it can be assumed that certain parts probably the turns, coils and helix unfolds into a random structure, whereas the β-sheet structures participate in aggregate formation.

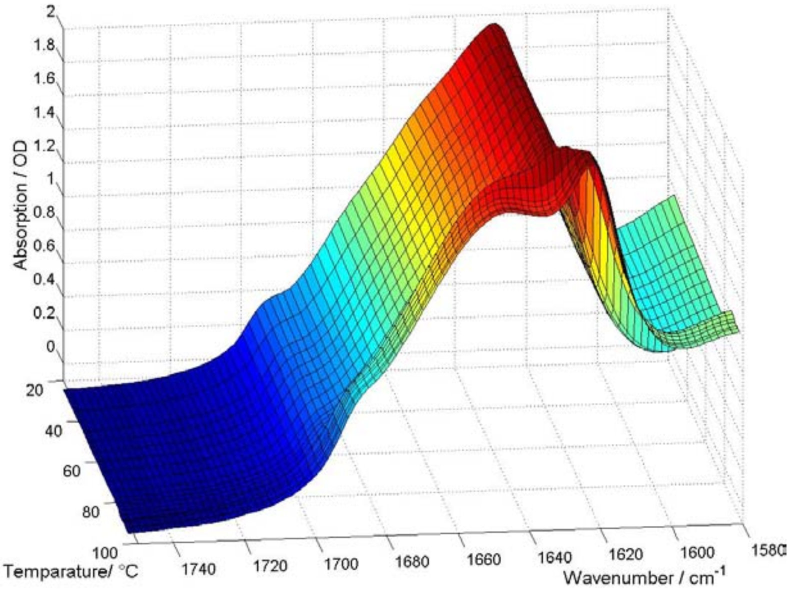

Figure 3.5.1 (a) Absorbance spectra of wild type porin as a function of temperature.

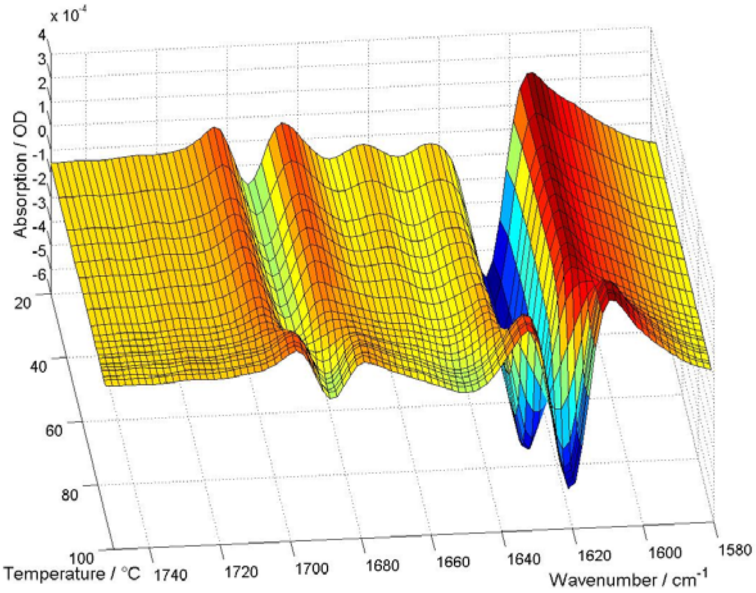

Figure 3.5.1 (b) Second derivative spectra of wild type porin as a function of temperature**.** The plot was generated using MATLAB version 5.3

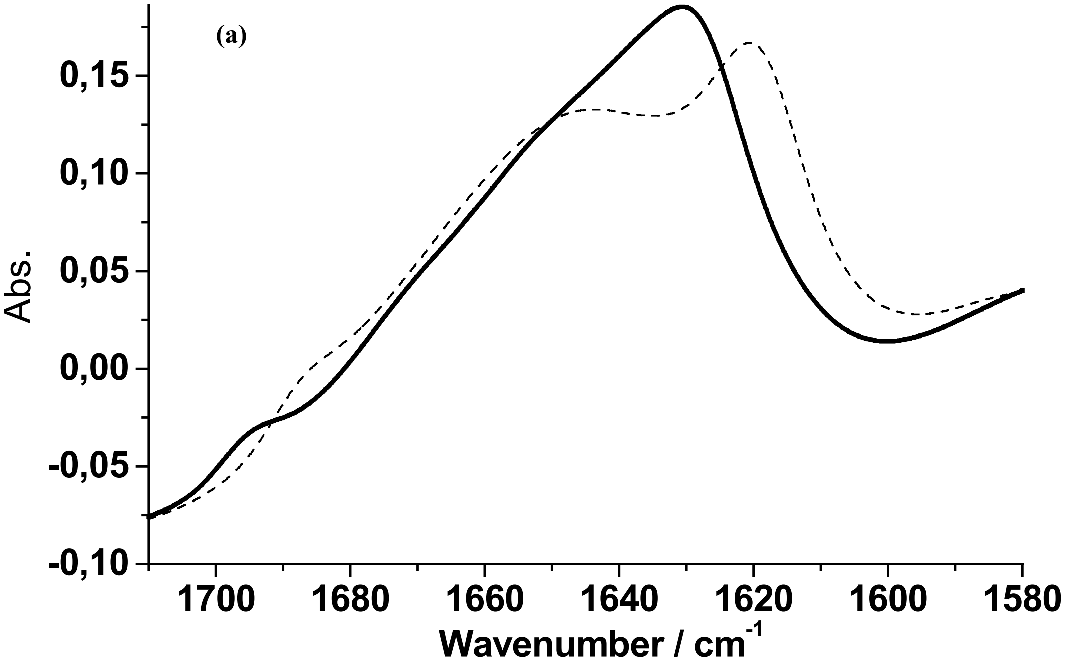

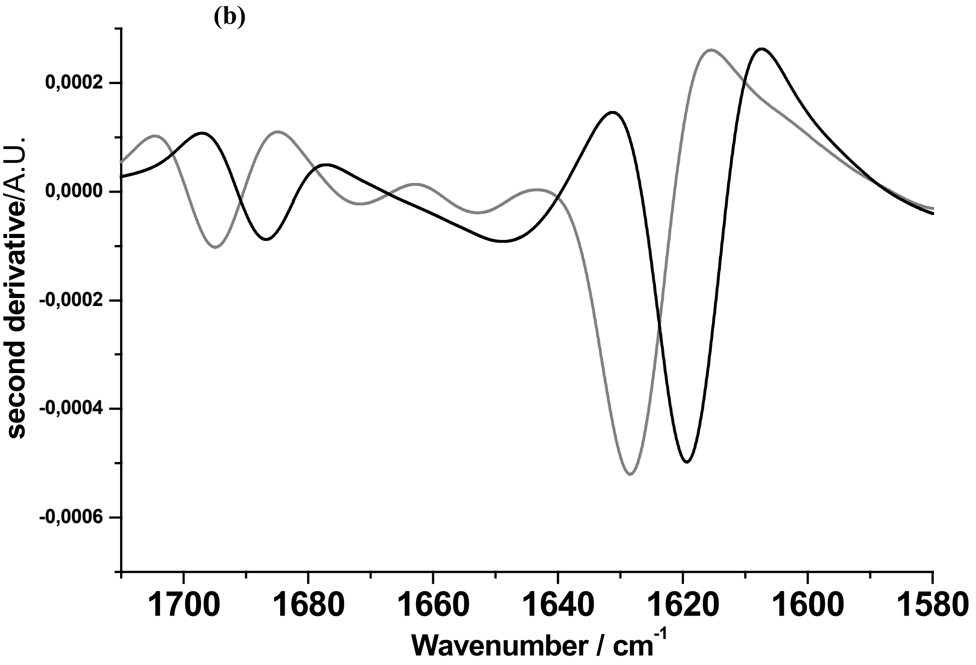

Figure 3.5.2 (a) Absorption spectra of wild type porin (black line) at 30 °C and (dotted line) 95 °C. (b) Second derivative spectra of wild type porin (grey line) at 30 °C and (black line) 95 °C.

The peak position of the amide I band at various temperatures was used to find the transition temperature (T_m) of the protein (Figure 3.5.3). The original unprocessed spectra were analyzed and band positions were determined by the standard peak picking function of the Bruker OPUS software. Since the output of this function is the wavenumber of the interpolated maximum, the band positions of a series of measurements with the same sample can be compared with a resolution much better than the nominal spectral resolution of 2 cm^{-1}. Peaks were plotted against the corresponding temperature using the software Origin 5.0.

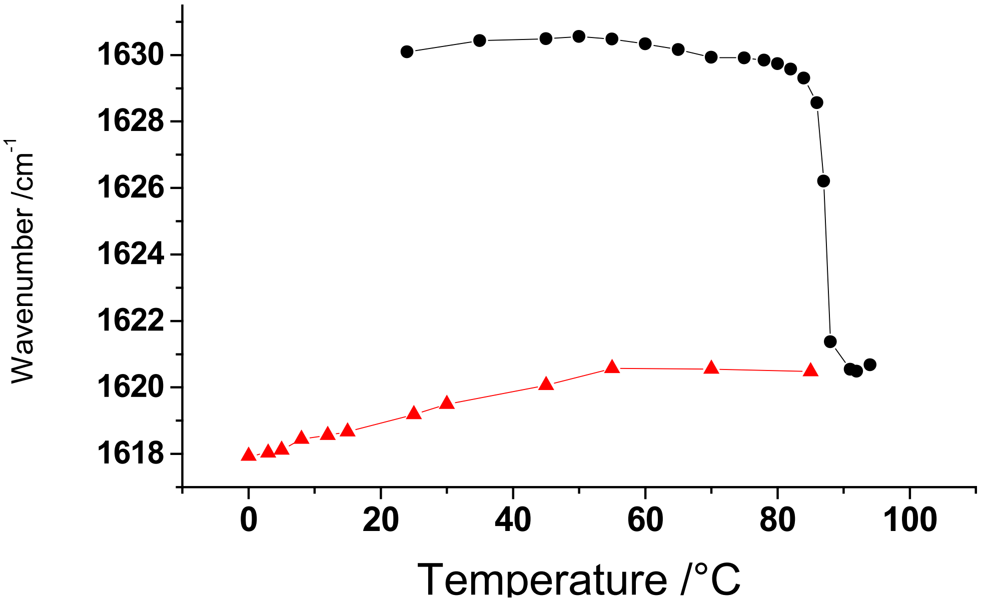

Figure 3.5.3 The amide I peak positions of wild type (•) heating, (▲) cooling.

The midpoint unfolding transition temperature T_m was calculated from the temperature dependent data using the following function.

$$f(\mathrm{T}) = \frac{(a_1\mathrm{T}+b_1)+(a_2\mathrm{T}+b_2)\cdot\exp(c\cdot(\mathrm{T}-\mathrm{T_m}))}{1+\exp(c\cdot(\mathrm{T}-\mathrm{T_m}))},$$

where the parameters a_1, a_2, b_1, and b_2 characterize the linear parts of the function at temperatures sufficiently below and above the transition temperature, respectively. The parameter c describes the steepness of the transition.

Figure 3.5.3 shows the position of amide I band on cooling also, which indicates that on reducing the temperature the band does not shift back to 1630 cm^{-1} indicating that the denaturation is irreversible The transition temperature for the wild type was calculated to be 86.2 °C.

3.5.1.2 Mutant Porins

Figure 3.5.4 depicts the amide I peak position at various temperature of the mutants E81Q, W74C and ED. Similar thermal analysis on mutant porins showed spectral results similar to wild type porin. Transition temperatures calculated for the mutants are summarized in table. 1.

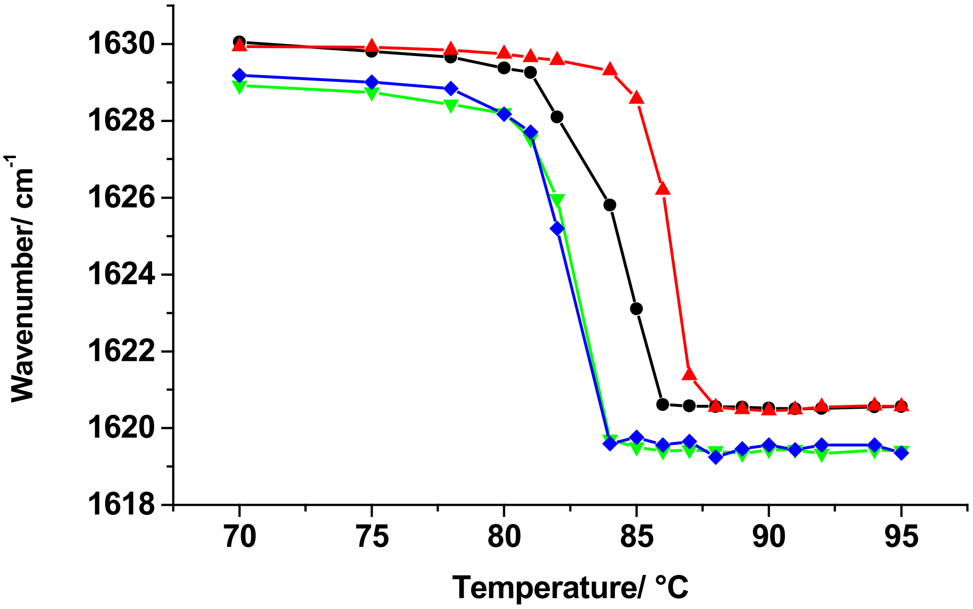

Figure. 3.5.4 Temperature dependent peak positions of the amide I mode
(▲) wild type in micelles,
(●) E81Q in micelles,
(◆) E81Q/D148N in micelles,
(▲) W74C in micelles.

Protein	**Transition Temperature (°C)**
Wild	86.2
E81Q	84.2
W74C	82.4
E81Q/D148N	82.3

Table 3.5.1 Transition temperatures of wild type and the mutant proteins.

The reduction of T_m for the E81Q mutant by only 2 °C demonstrates that the glutamic acid at position 81 in the porin of *P. denitrificans* does not play a crucial role for the stability of the protein. In the case of *E. coli* OmpF, the substitution of E71 resulted in a drastic reduction in the T_m from 72 to 48 °C which was explained by the prevention of salt bridge and hydrogen bond formation between E71 and R100 and R132 of adjacent monomer. The similarly positioned residue E81 of *P. denitrificans* either does not contribute to any salt bridge or it can easily be substituted by another residue. This is a key point in this study as it emphasizes on the dissimilarities in stability two structurally similar proteins.

Substitution of a bulky aromatic residue with a small nuleophilic residue, which is positioned at the trimer interface, brings about a reduction of T_m by 3.8 °C in the W74C mutant. In E81Q/D148N mutant, two acidic residues, replaced by two neutral residues of similar size also brings about a reduction of T_m by 3.9 °C. The mutants have a lower T_m in comparison with the wild type, suggesting that the substitution of the highly conserved amino acid residues (W74C, D148N) resulted in decrease in the thermal stability of the protein, but the instability caused by these single and double amino acid substitutions are not drastic enough to introduce severe disorder in the highly stable β-barrel structure as all the mutants had similar secondary structure as the wild type. However, there are small differences in the spectra pointing to subtle disarrangement in the structure. An impaired interaction with the micelle molecule must also be considered.

3.5.1.3 Thermal stability analysis in SDS-PAGE

SDS-PAGE analysis was carried out corresponding to the thermal analysis by IR spectroscopy to observe the changes in the quaternary structure of the protein (Figure 3.5.5). The results obtained from protein in detergent micelles point out that although monomerization starts at temperatures above 50 °C, complete monomerization of the trimer occurs at temperatures above 85 °C for the wild type. Similar results were observed for the mutants. The transition was from trimer to monomer with no dimer detected.

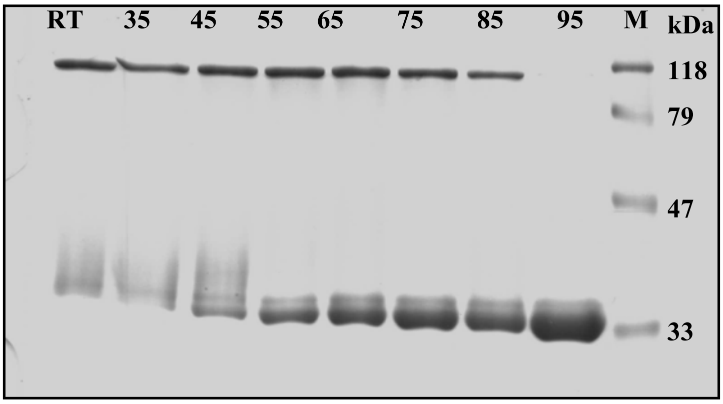

Figure 3.5.5 SDS-PAGE profile of wild type porin.
Lane 1-8 represents various temperatures.
M is the protein molecular weight Marker.
RT is room temperature

Hence the results from protein in detergent micelles indicate that *P. denitrificans* porin is a highly stable structure in detergent micelles undergoing denaturation at high temperature. This result is not surprising since other membrane proteins like bacteriorhodopsin and other porins are known to be highly thermostable as well. The explanation given for such high stability of membrane proteins is that the transmembrane part of the protein is remarkably thermostable but the extramembraneous regions are not. After unfolding of the hydrophobic part of a membrane protein, aggregation is very probable because the exposition of large hydrophobic parts to water is energetically unfavorable. However, the band at 1649 cm^{-1} proves that the protein contains also random structure

3.5.2 Thermal unfolding in liposomes

Purified protein was reconstituted into liposomes so as to analyze the thermal stability and unfolding in a native-like environment as in the outer membrane of bacteria which is composed of lipids and polysaccharides.

3.5.2.1 Wild type and mutant porin

Figure 3.5.6 shows the amide I spectral region for wild type porin. It is clearly evident from the spectral regions that there is no shift in the amide I position of the β-sheet structure. The change observed at high temperatures in the region between 1635 cm^{-1} and 1670 cm^{-1} is due to the loss of water associated with the lipid and proteins because the protein sample used was a paste in H_2O. The amide I band shape of protein heated to 95 °C is similar to the band shape of ATR-FTIR spectra of the protein in micelles after drying. Hence it can be said that the protein reconstituted into liposome vesicles maintains its secondary structure even after heating it up to a temperature of 95 °C.

Similar results were obtained for the mutants (data not shown), none of them showed any shift in amide I band position. Figure 3.5.7 shows the comparison of amide I position of protein in detergent micelles and in liposomes.

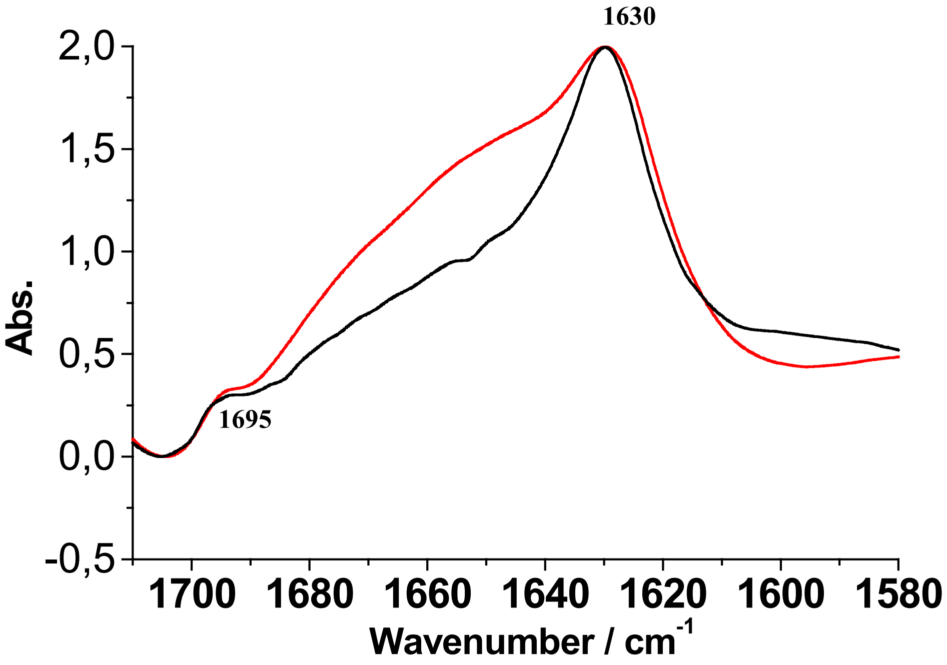

Figure 3.5.6 Amide I absorption spectra of wild type porin at 25 °C (black line) and 95 °C (red line).

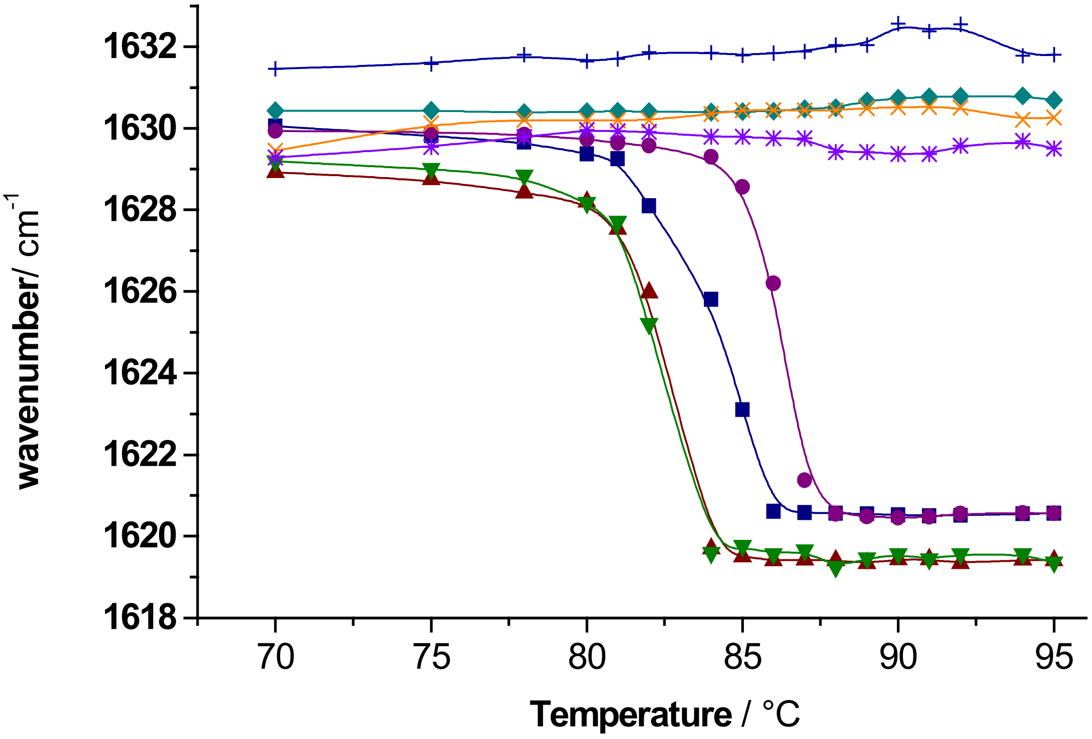

Figure 3.5.7 Temperature dependent peak positions of the amide I band.

(●) wild type in micelles	(✳) Wild type in liposomes
(■) E81Q in micelles	(◆) E81Q in liposomes
(▲) E81Q/D148N in micelles	(+) E81Q/D148N in liposomes
(▼) W74C in micelles	(X) W74C in liposomes

3.5.2.2 SDS-PAGE Analysis

In order to analyze the quaternary structure of the protein reconstituted into liposomes, thermal stability analysis was carried out using SDS-PAGE. Figure 3.5.8 shows the SDS-PAGE gel with native protein in liposomes heated to 100 °C and temperatures above that. It is clearly evident from the bands that the trimer band of the protein does not undergo a change into monomers at the thermal conditions. At very high temperature above 125 °C it monomerizes, and some change can be observed in the amide I region too. These high temperatures are not physiologically relevant so is not discussed here. Moreover at such high temperature the liposomes will be not be stable, due to loss of water molecules. The indicates that the protein is thermostable in liposomes and that a temperature of 100 °C is not high enough to dissociate the protein into monomers.

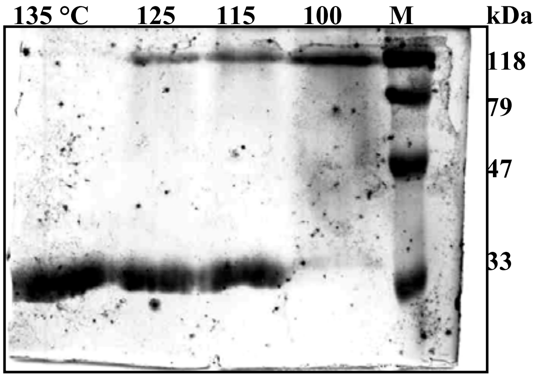

Figure 3.5.8 SDS-PAGE heating profile of protein reconstituted in liposomes.
M is protein molecular weight marker.
Temperature is in °C.

This report shows that among the trimeric porins, *Paracoccus* porin has the highest stability in a detergent and liposome environment. The stability of the protein is not the result of functional evolution but probably structural evolution, because *Paracoccus* survives at a temperature up to 30 °C, so having a membrane protein with such high thermal stability was no evolutionary advantage.

However, porin would have evolved to be thermostable when it got incorporated into lipids. The data support earlier findings with other porins that the porin trimer is a highly stable structure, tightly bound to lipopolysaccharides. This is indicated by a very recent report on Msp porin of Mycobacteria (Faller *et al.*, 2004) which is an octamer with a very peculiar arrangement of subunits. The Msp porin in a mixed micelle system has a very high stability with T_m above 100 °C (Heinz *et al.*, 2003). Various other groups have suggested that three structural factors appear to play a pivotal role in the stability of the porin trimer:

(i) the extensive hydrogen bonding in the β barrel

(ii) (ii) the rigid and structured loops on both sides of the membrane

(iii) (iii) the strong interaction between the monomers (Haltia *et al.*, 1995).

The incorporation of a protein into the lipid bilayer provides a means of achieving a remarkably thermostable structure in organisms which are not thermophiles like *P. denitrificans* investigated in this study.

3.5.3 Tyrosine side chain modes

There is some molecular evidence, which has come up as a result of this study which supports the reason for extreme stability for porins in liposomes. The second derivative spectra not only provide information about the minute secondary structure details but also appreciable amount of information about the amino acid side chains. Tyrosine side chain absorption is easily distinguishable as it does not lie in the amide I or II region.

Temperature induced unfolding of proteins leads does not only to the breakdown of various secondary and quaternary structural elements, but also involves the changes in the microenvironment of side chain groups. One such side chain vibration which can be distinguished very well in the spectra of proteins in ^2H_2O and H_2O is the C—C stretching vibration of the tyrosine aromatic ring at 1515 cm^{-1} (Chirgadze *et al.*, 1975; Barth, 2000). Since changes in the environment of the tyrosine residue may result from changes in both secondary and quaternary structure, it provides a reporter group to observe such changes. A porin monomer has 18 tyrosine residues, hence the strong and narrow band at 1515 cm^{-1}, clearly seen in the second derivative spectra, can be assigned to the tyrosine side chains.

In order to follow the unfolding process, the temperature dependence of the position of the tyrosine band has been studied (Figure 3.5.9 and 3.5.10). For the protein reconstituted into detergent micelles the frequency of this band gradually shifts by more than 1 cm^{-1} towards lower frequencies between room temperature and 95 °C. A linear dependence of the frequency on the temperature, but no full reversibility is observed. This explains that a change in the environment of one or more tyrosine residues upon denaturation.

Even though the shift seems to be very small, it is significant when compared to the variation of the values given for the tyrosine peak position of different proteins in the literature (1513 cm^{-1}-1517 cm^{-1}) (Barth, 2000). Analogous temperature dependent frequency shifts of the tyrosine C-C mode have been reported for RNase T1 (Fabian *et al.*, 1993 and 1994) and RNase (Fabian *et al.*, 1993). The observation in this study is similar to that reported for downshifts of the tyrosine bands of concanavalin A (Reinstädler *et al.*, 1996), myoglobin (Arrondo *et al.*, 1988) and tendamistat (Zscherp *et al.,* 2003), upon aggregation. Another recent report by (Nazarova *et al.*, 2003) shows an accuracy of ±0.2 cm^{-1} in peak positions determined by derivative spectra.

A linear temperature dependence was reported for a short, tyrosine containing peptide which does not undergo conformational changes in the temperature region studied (Fabian *et al.*, 1994) which can explain the slight change in tyrosine band position observed for protein reconstituted into liposomes (Figure 3.5.10). Compared to the protein in detergent the tyrosine band position remains stable upon heating. The major secondary structure seems not to change, however at high temperatures, the loss of water has to be taken into account as it brings about a change in the environment of the tyrosine, but this change is not able to influence the highly stable secondary structure, as no change was observed in the secondary or quaternary structure till 100 °C. Corresponding to the changes seen in the tyrosine band, some minor shifts are seen in the amide I spectra (Figure 3.5.7) after 80 °C, what can be confidently designated as changes happening due to change in water molecules. (Figure 3.5.6). The cooling data was not recorded for all the samples to similar values.

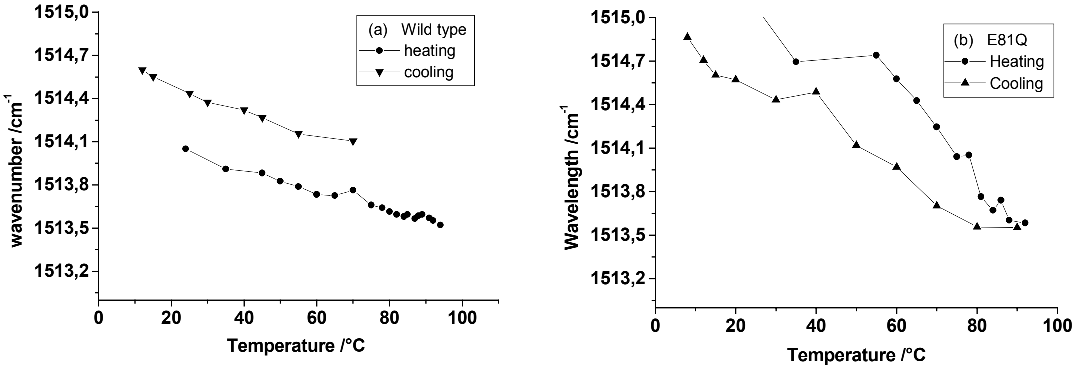

Figure 3.5.9 Change in tyrosine band position of protein in detergent micelle .
(a) WT
(b) E81Q

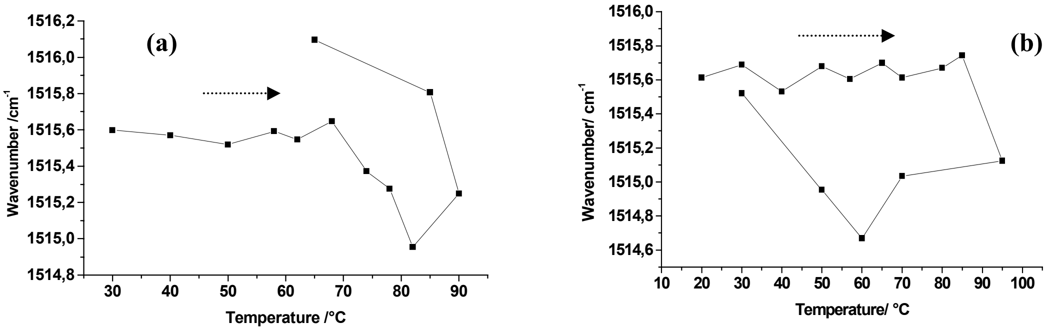

Figure 3.5.10 Change in tyrosine band position of protein reconstituted in liposomes .
The arrow represents the direction of heating followed by cooling.
(a) Wild type
(b) E81Q

It is evident from Figure 3.5.9 and 3.5.10 that the Tyr reacts entirely different to the increase in temperature. It should be noted that it was earlier suggested that the shift in the amide I band of porin occurs due to intramolecular hydrogen bonding Zscherp *et al.* (2003) state that the distance between the tyrosine oxygen and hydrogen is modulated by hydrogen bonding, which influences the electron density and thus the strength of the bonds between the carbons of the aromatic ring. The frequency of the corresponding C-C ring stretch vibration reflects the strength of the bonds. Therefore, as pointed out by Fabian and coworkers in the case of RNase T1, (Fabian *et al.*, 1993 and 1994) the downshift of the tyrosine band due to aggregation of the can be explained by stronger hydrogen bonds of the tyrosine O-H with acceptors in the protein aggregates.

Another line of evidence for porins to support the data comes from the peculiar β-barrels. It is known for the small β-barrel proteins OmpA and OmpX that they contain girdles of aromatic residues. For *Paracoccus* porin it is observed that there is a clear pattern of residue location, which is very similar to the distribution reported for other non specific porins (Hirsch *et al*., 1997). There is a central belt of non polar residues bordered at each edge by girdles of aromatic amino acids (Figure 3.5.11). The girdles are defined predominantly by Tyr residues with their hydroxyl groups pointing towards the aqueous phase. Various groups have concluded that the hydroxyl groups of the Tyr residues are located in the glycerol backbone of the bilayer, then the thickness of the hydrophobic core of the bilayer is 24-28 Å, comparable to the thickness that will be formed by L α phosphatidyl choline. Assuming the same case here, it can be concluded that when the protein is in phosphatidyl choline, the Tyr residues are embedded in the bilayer, hence up to the temperature of 70 °, there is no change in position of the Tyr band. At high temperatures (70 °C for wild type and 90 °C for E81Q/D148N mutant (Figure 3.5.10)) a decrease in frequency is observed what can be explained by the loss of water as mentioned previously. This results in the frequency down shift. However the frequency bands shift in cooling is different for the wild type (Figure 3.5.10 (a)) and the mutant (Figure 3.5.10 (b)). May be this is due to the inequality of water content.

Neutron diffraction studies have shown that in crystals grown from β-OG or LDAO the hydrophobic region of OmpF is covered by detergent, with the two girdles of aromatic residues coinciding with the boundary between the polar and non polar regions of the detergents. A location of the aromatic residues is also seen in molecular dynamic simulation of OmpF in bilayers of phophatidyl choline (C14:0). Detergents may cover the protein but there are no interactions. However in case of PC there may be interacting residues between the protein and PC causing the enormous increase in stability. Beyond the external girdle of aromatic residues, the external barrel surface contains a number of acidic residues, which could interact with lipopolysaccharides (LPS) molecules through divalent metal ion bridges. Hence it can be concluded that when the protein is in detergent micelles, its residues are in a less stable state in comparison to the protein in liposomes. Therefore a clear delineation exist in their stability and unfolding.

.

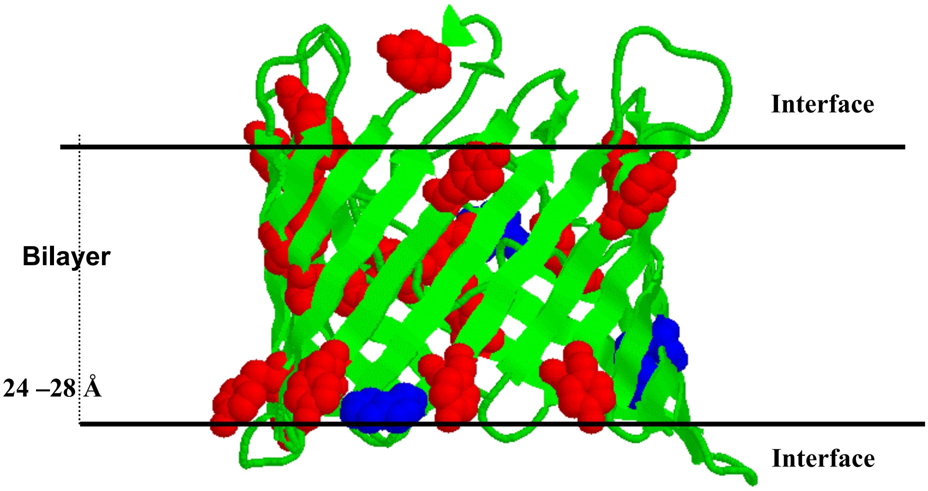

Figure 3.5.11 *Paracoccus* porin monomer.
Residues highlighted in red are tyrosines.
Residues in blue are tryptophans.

3.5.4 Structural and functional correlation

3.5.4.1 Single channel conductance

In order to correlate structural stability with function, black lipid bilayer measurements were performed with preheated protein samples. Protein heated at 50 °C and 100 °C is compared with the single channel activity of protein at room temperature. It is evident from (Figure 3.5.12) that porin tends to show single channel conductance at very high temperatures with very high concentration of protein. In comparison to room temperature (30 °C) the distribution of pores seems to change at 50 °C, the frequencies of pores with lower conductance are reduced drastically, indicating that probably those frequencies were produced by (a highly unstable) protein with monomers, dimers. At 100 °C the frequency distribution changes again; probably the appearance of the pores of lower conductance in large frequencies is due to disintegration of most of the stable trimers.

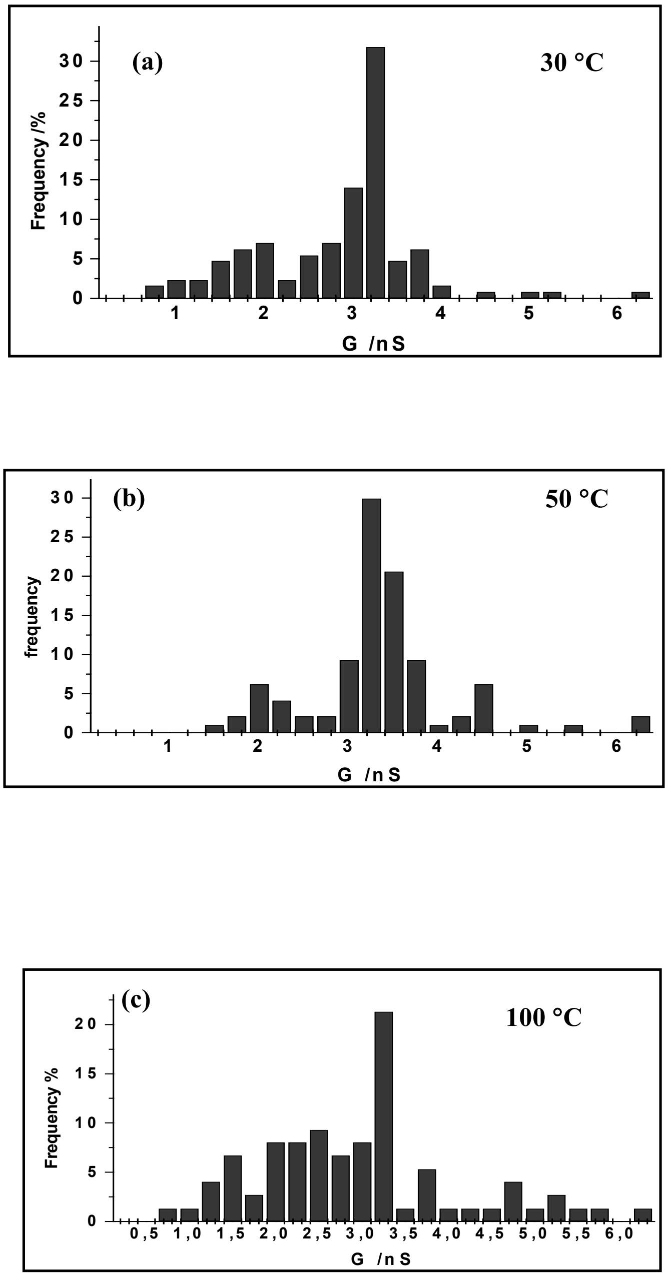

Figure 3.5.12 Single channel conductance of wild type porin at various temperatures.

3.5.4.2 Activity profiling

At equal concentration of the protein used, the protein tends to loose activity at 50 °C itself, which can be explained based on the results from SDS-PAGE and change in tyrosine side chain environment.

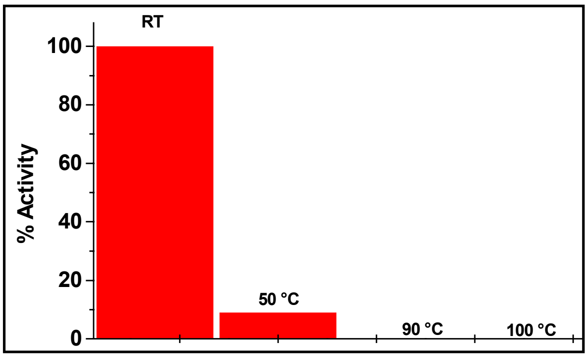

Figure 3.5.13 Activity profile of wild type protein heated to various temperatures.

The SDS-PAGE gel shows that the monomeric species seems to increase above a temperature of 50 °C, showing that the ratio of trimer to monomer is continuously changing and is completed by 90 °C.

Another factor to be considered is that the distribution of monomers, dimers and trimers are also changing continuously at different temperatures. The small changes happening in the loops may cause a problem for the protein to insert into the bilayer.

The change in Tyr band position is linear from the starting temperature (RT) showing that the changes in Tyr environment is occurring with small increase in temperature. Even though there is no apparent change in secondary structure, there are slight changes in the loop regions due to a change in Tyr environment, since these regions behave more like soluble protein fraction and they unfold.

3.6 pH dependent stability, unfolding and refolding

Proteins can be denatured by changes of various external parameters: temperature, pressure, chemical denaturants, and pH. For soluble proteins it is often seen that the protein precipitates at its pI value. The protein is inactive below that value, and the pH of activity range for most proteins closer to physiological pH of 7. This rule is not true for all proteins but for most of them. The pH of the solution is crucial for the proteins because their net charge depends not only on the amino acids constituting them but also on the acidity or basicity of the buffer environment. Thus in this study attempts were made to analyze the stability of porins at different pHs.

For porins the calculated pI value is 4.03. It has 17 % acidic residues and 7 % basic residues with a peculiar arrangement of these residues (Figure 3.6.1 (a) and (b)). All the basic residues are positioned inside the channel except two of them which are in the loops in each monomer. All the acidic residues are positioned in the loops except a few in the barrel wall, which are positioned inside the channel to neutralize the effect of the basic residues to maintain the pore non-specific (Hirsch *et al.*,1997).

It can be assumed from the above details that a thermodynamically stable protein will exist when the various charged residues are electrostatically neutralized. Another point to be noted is that any change in pH will first introduce changes in these acidic and basic residues, which are located in the solvent-accessible regions of the protein.

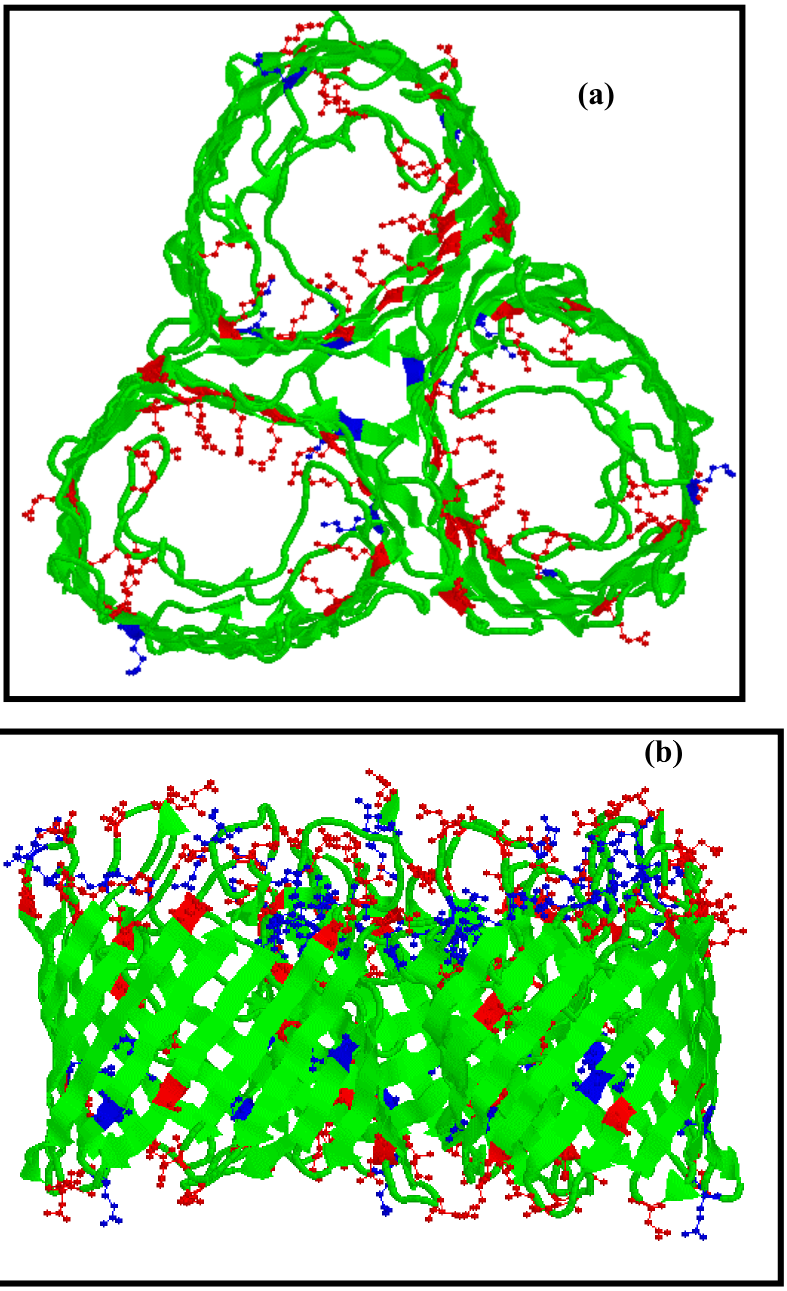

Figure 3.6.1 (a) *Paracoccus* porin trimer with arginine residues in red and lysine residues in blue. (b) *Paracoccus* porin trimer with aspartic acid residues in red and glutamic acid residues in blue.

3.6.1 Unfolding

Unfolding of porin was investigated in acidic and basic conditions. Changes in the aggregated and the native porin at high and low pH were studied by FTIR and CD spectroscopy. The changes in thermal stability of the protein at different pH values was investigated using FTIR spectroscopy.

3.6.1.1 Disaggregation of aggregated porin

Aggregation is the fate of most membrane proteins on heating to high temperatures (Goni *et al*., 1995). It was previously reported for Bacteriorhodopsin and for Bovine and *Paracoccus* Cytochrome *c* oxidases, that most of the intramembraneous secondary structure is maintained even above the denaturation temperatures (Arrondo *et al*., 1994; Haltia *et al*., 1994). Numerous other studies, too, have revealed that aggregated proteins still contain a majority of their secondary structures (Hsu *et al*., 1985; Fish *et al.,* 1985), hence suggesting that a far more minor structural alteration than the unfolding of the secondary structure is sufficient to cause aggregation. This minor structural alteration is also the primary cause of the aggregation *in vitro* conditions of protein purification. Aggregation is also facilitated by partial unfolding during thermal or oxidative stress and by alteration in primary structure caused by mutation, RNA modification or translational misincorporation. Protein aggregation can be defined as an inevitable consequence of cellular existence. Aggregates are oligomeric complexes of non-native conformers that arise from non-native interactions among structures of kinetically trapped intermediates in protein folding or assembly. (Wetzel,1994; Kopito, 2000)

It is evident from section 3.5 that porin in detergent micelles aggregates upon heating. It is quite likely, too, that in case of porin also most part of the secondary structure is maintained after denaturation. Aggregation was evident due to the downshift of the absorbance maxima of the β-sheet component and it was suggested that formation of intramolecular hydrogen bonds are responsible for the downshift. Some other interactions may also be involved in aggregation.

Aggregated protein possesses a large fraction of the secondary structure and most of the aggregated fractions are held together and stabilized by hydrogen bonds and electrostatic interactions. So to disaggregate an aggregated protein mass these electrostatic and hydrogen bond interactions thus have to be broken. It can be argued that the easiest way to break H-bond is by heating up. This cannot be applied here as aggregates are a consequence of heating and the protein has modified itself in a way that it has attained energy minimum. Heating it beyond its denaturation temperature would result in the destruction of the proteins chemical properties. Another approach to disaggregate a protein is to change its environment by perturbing its ionic properties at an altered pH value.

Porin aggregated by heating above the transition temperature for 5 minutes was subjected to an increase and decrease of pH values. It was observed visually that the turbid aggregated solution tends to clear up into transparent solution when the pH was increased above 12. The aggregated solution tends to become more turbid on decreasing the pH to acidic range. Analyzing the secondary structure changes in a CD spectrum, it was evident that there is a gradual opening of the aggregated mass into unordered structure when incubated at pH 12 and above. Figure 3.6.2 shows the comparison between native, aggregated and unfolded porin. Aggregated porin cannot be characterized in CD due to light scattering.

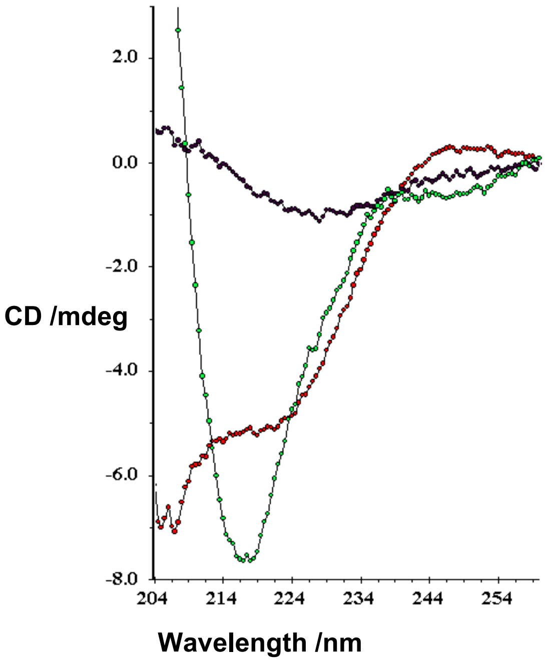

Figure 3.6.2 CD spectra of porin in native (•) aggregated (•) and unordered state (•).

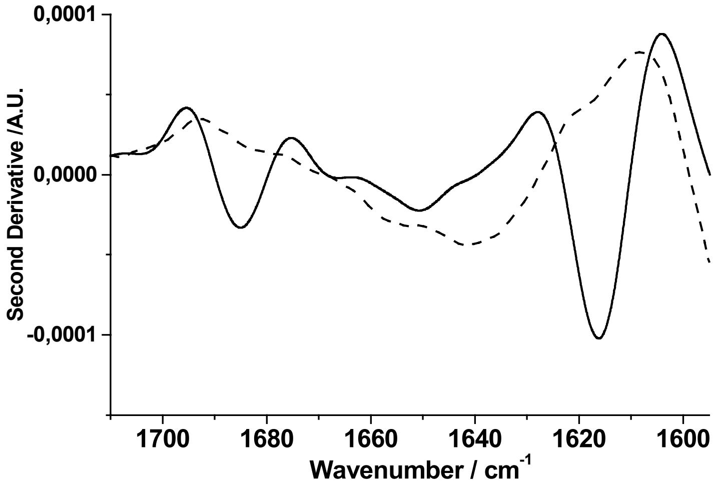

Figure 3.6.3 FTIR second derivative spectra of aggregated protein (solid line), opened up into unordered structure (dotted line).

Similar results were observed by FTIR transmission spectroscopy, too. Figure 3.6.3 depicts the second derivative spectra of aggregated porin and aggregated porin unfolded by raising pH. It is evident from the spectra that the representative bands for the aggregate are completely lost and replaced by a broad band in the 1650 cm^{-1} region, clearly showing that the protein is unfolded into a unordered structure. Hence the results from CD and FTIR spectroscopy give consistent results. Disaggregation of aggregated β-sheet amyloid A protein at pH 12 was studied by FTIR (Dubois *et al*., 1999). The band position obtained in the case of diaggregated amyloid protein was also 1650 cm^{-1}.

3.6.1.2 Unfolding of native porin at high pH

To observe the changes in the secondary structure of the natively folded protein, CD spectra were analyzed from porin incubated at various pH values. Figure 3.6.4 depicts the CD spectra of porin collected after 4-5 minutes of incubation at the respective pH values. It is evident from the spectra that porin incubated at lower pH values (pH 1 and pH 4) have similar spectra as the native one at pH 8. The spectrum of protein at pH 11 is slightly altered from the native one. At pH 12, it shows an intermediate state which in another 40 minutes unfolds into unordered structure. At pH 13 and above, it unfolds into unordered structure in a short time, which could not be resolved in this study.

The unfolding of the porin at pH 12 was measured from after 4 to 50 minutes of incubation. The time dependent unfolding of porin observed by CD spectroscopy is shown in Figure 3.6.5. The spectra at 10 and 50 minutes is compared with the native protein. After 50 minutes no change was observed in the spectra. The changes observed between 0 and 10 minutes could not be resolved in the observed time range starting from 4 minutes whereas further changes were slow and gradual, indicating that the initial denaturation of the solvent exposed region is fast compared to the β-sheet region. Wild type and one of the mutants analyzed

E81Q showed a very similar unfolding pattern. Hence it can be concluded that increasing the pH to 12 makes the protein unstable. At the same time decreasing the pH to extreme acidic range at pH 1, does not bring about any apparent change in the secondary structure. Unfolding of proteins at high pH is reported for other soluble proteins like barstar (Khurana *et al*., 1995).

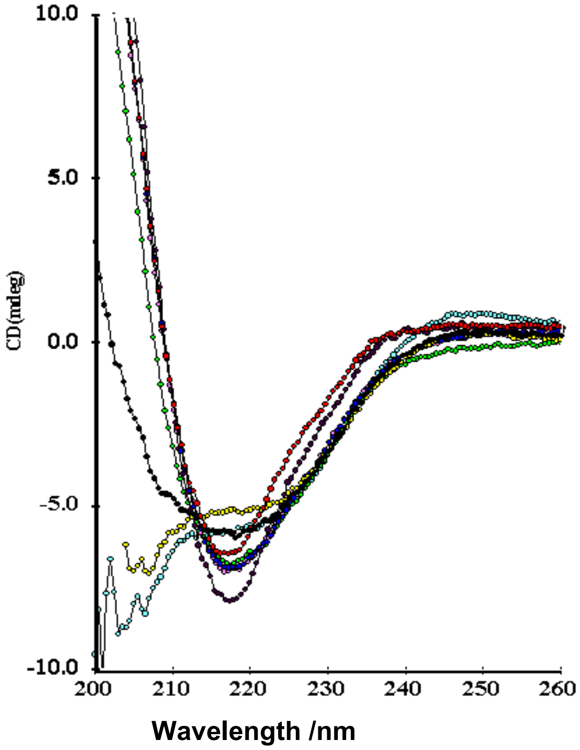

3.6.4 Secondary structure conformation at various pH values.
(●) pH 1, (●) pH 5, (●) pH8, (●) pH 10, (●) pH 11, (●) pH 12, (●) pH 13, (●) pH 13.5.

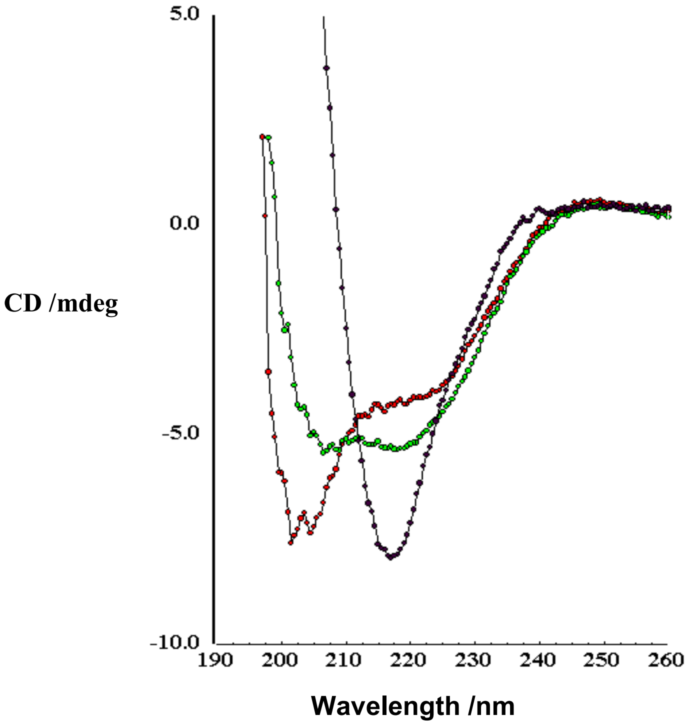

Figure 3.6.5 Time dependent unfolding of porin at pH 12.
(●) Native at pH 8, (●) native at pH 12 and after 10 minutes of incubation,
(●) native at pH 12 and after 50 minutes of incubation.

3.6.1.3 Analysis of pH dependent thermal stability

Thermal stability of protein incubated at various pH was analyzed using FTIR spectroscopy. The results are discussed separately for acidic and basic pH range respectively, in comparison to the native-one at pH 8.

Thermal stability at low pH (pH 1.5 and pH 4)

Thermal stability of porin was analyzed at pH 1.5 and pH 4. Figure 3.6.6 shows the amide I maximum as a function of temperature. The temperature profile was analyzed for the transition temperature T_M as explained in section 3.5. The T_M value for porin was found to be 78.2 °C at pH 1.5 and 82.6 °C for pH 4. Even though the T_M value observed for pH 4 is close to the T_M value for pH 8, the shape of the transition region is quite broad. This is probably due to the fact that pH 4 is very close to its calculated isoelectric pH of 4.03. Nevertheless it is evident that at pH 1.5, 4 and 8 thermal unfolding of porin results in aggregation.

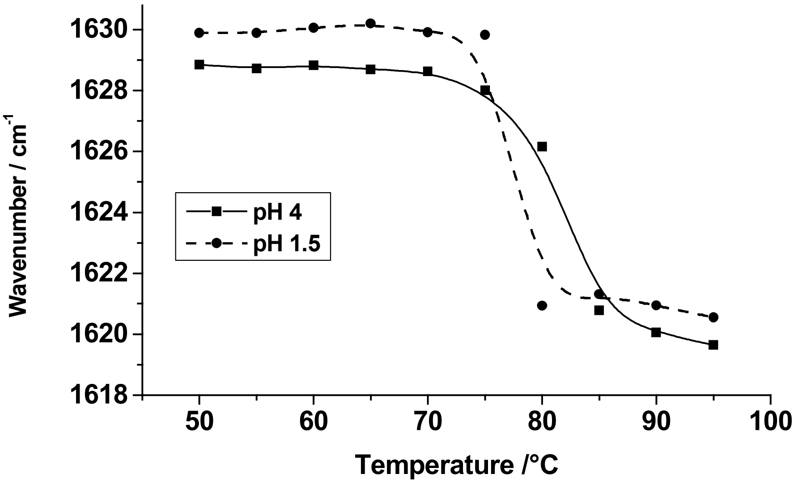

Figure 3.6.6 Temperature dependent position of amide I for porin incubated at pH 1.5 and 4.

Thermal stability at pH 10, 11.5 and 12.5

Thermal stability analysis of protein at pH 10 showed no change in transition temperature or in the pathway of unfolding as is evident from figure 3.6.7. It shows that the protein is stable up to pH 10. A notable feature of *Paracoccus* porin is that it has not only very high thermal stability but it is quite stable towards extreme alteration in ionic strengths. Thus even in the presence of cumulative effect of two denaturing conditions, the protein maintains the stability to a very large extend.

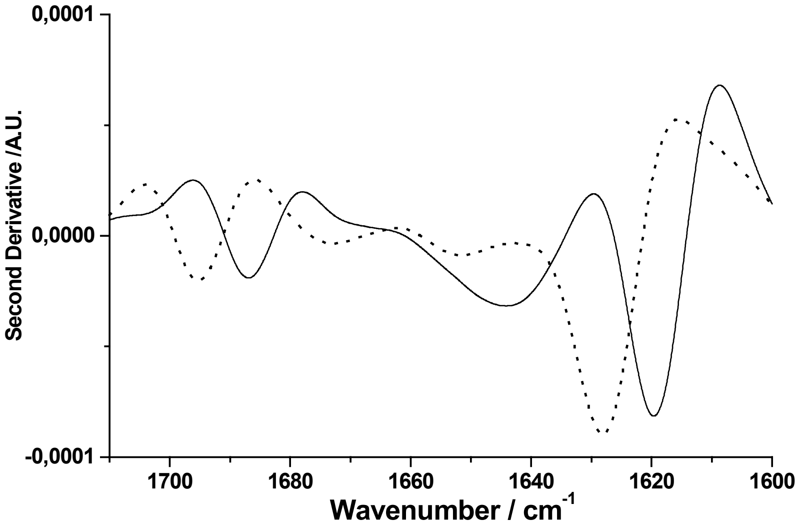

Figure 3.6.7 Second derivative spectra of protein at pH 10.
Room temperature (dotted line), 90 °C (solid line).

Figure 3.6.8 shows the spectra of porin incubated at pH 11.5 and heated from room temperature to 95 °C. It is observed that upon incubation at room temperature there is a large band characteristic for unordered protein. Upon heating further to 70 °C, the protein seems to unfold into unordered structure, as is evident from the band at 1648 cm^{-1} and from the reduction of the amplitude of the band at 1630 cm^{-1} and 1695 cm^{-1}. However, this seems to be a highly unstable state as upon further heating to 75 °C bands at 1620 cm^{-1} and 1685 cm^{-1} start to appear, which indicates aggregation of the protein. The aggregated bands become very prominent upon heating to 95 °C. There is no detectable change in the aggregate bands upon cooling. The observation here supports the fact that initial unfolding of the protein is fast and the probable regions involved are the loops and helices which are the easily accessible hydrophilic surfaces. Even though a large fraction of the protein attains unordered structure at 70 °C, a further increase causes it to aggregate. This result is crucial as it indicates that an immediate effect on the protein in the presence of denaturing condition causes it to unfold, but the thermodynamic threshold is not crossed and instead it moves into a thermodynamically stable form.

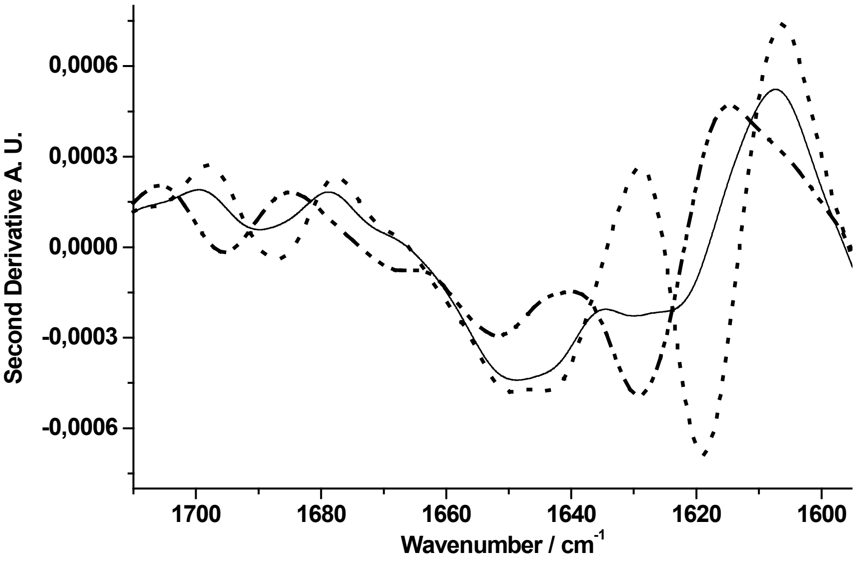

Figure 3.6.8 Second derivative spectrum of protein at pH 11.5.
At room temperature (dash dot dot), 70 °C (solid line) and 75°C (dashed line).

The protein incubated at pH 12.5 had a slight shift in the β-sheet band position; it is observed to be shifted to 1625 cm^{-1} and 1687 cm^{-1} at room temperature (Figure 3.6.9). Upon heating up to 50 °C, the 1625 cm^{-1} band shifts to 1619 cm^{-1}, but there seems to be no shift in the 1687 cm^{-1} band. As there is an increase in the area of band around 1650 cm^{-1}, it can be argued that some part of the protein unfolds, too. Upon further heating to 80 °C, it was observed that the protein unfolds into unordered structure as seen by the further increase in the 1650 cm^{-1} band area and disappearance of bands at 1619 cm^{-1} and 1687 cm^{-1}. This indicates that as the first step the protein tries to prevent itself from unfolding by forming an aggregate, but due to the presence of the destabilizing ionic environment the protein tends to unfold. It is evident that at high pH the protein tends to unfold completely into unordered structure rather than denaturing into an aggregate. The thermal stability of porin incubated at pH 11.5 and 12.5 showed an entirely different unfolding pattern when compared to the denaturation in the acidic range.

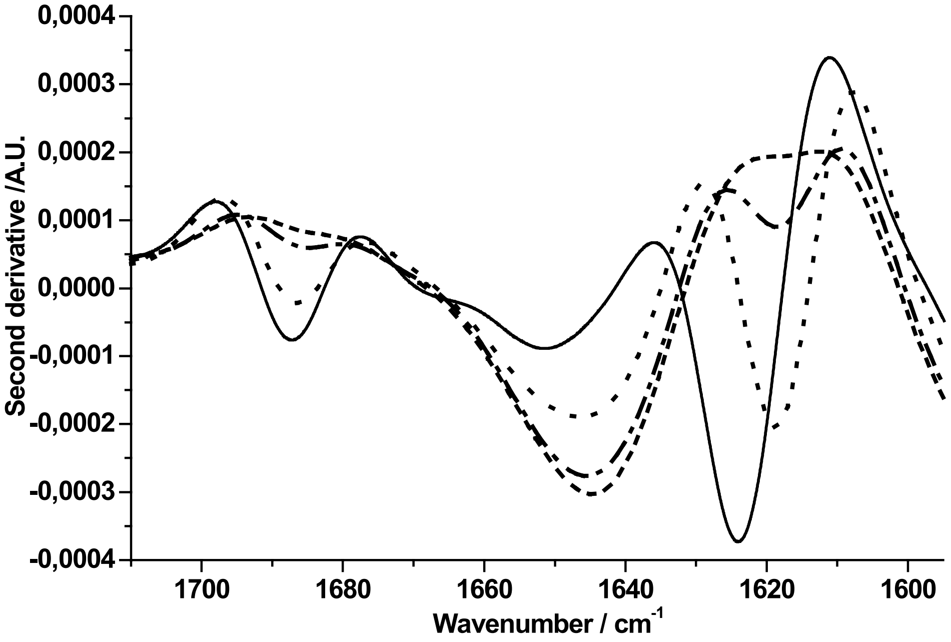

Figure 3.6.9 Second derivative of protein at pH 12.5 heated to various temperatures. Room temperature (solid line), 50 °C (dotted line), 70 °C (Dash dot), 80 °C (dashed line)

3.6.1.4 A basic mechanism of ‘opening up’ into unordered structure

Porins have the tendency to aggregate as result of instability. Aggregates are thermodynamically stable species (Kopito, 2000), they tend to become unstable due to the changes in electrostatic interactions experienced by the amino acid residues. (The change that could be detected in Tyr residues and assigned spectroscopically is discussed in section 3.6.4).

At lower pH it is observed that the change in pH induces mild instability in the β-barrel structure. At pH 11.5 it is observed that the loop and helix region are unfolded into unordered structure before heating. Upon heating the fraction of unordered structure increases, but a major portion of the protein still aggregates. This probably indicates that the thermodynamic instability caused in the protein due to electrostatic changes is not sufficient to unfold the protein completely, but only partially. This partially unfolded protein is a highly unstable species which aggregates further to protect some of its hydrophobic residues. It is further supported by the data at pH 12.5, where the immediate effect on the protein is the shift in the β-sheet bands. The protein probably tends to generate further interactions through the hydrophobic residues to protect from unfolding. On heating further the initial tendency is to aggregate at lower temperature. However, it then opens up into unordered structure, showing that the basic mechanism behind high pH unfolding is prevention of aggregation due to chemical and thermodynamical changes to the amino acid residues, which contribute to the extreme stability of porins. If these residues are unstable enough the protein unfolds.

Various interactions which are altered due to the change in pH is discussed in this section.

Hydrogen bonds

As described in the beginning of this section hydrogen bonds play a very crucial role in stabilizing the aggregate. Hydrogen bond occurs between two electronegative atoms for the same hydrogen atom, D-H----A. In protein major hydrogen bond donors are Arg with five hydrogen and lysine with three hydrogen. The strongest acceptors are Asp and Glu with 4 acceptor sites each. Upon reducing the pH of the solution the most of the acidic residues will be getting protonated. Most of these acidic residues are located in the loops which are the hydrophilic part of the protein, it is also likely that all the groups are already protonated. Thus having more H^+ around these residues may not bring a drastic change to these residues, but on the other hand it is very likely that extremely low pH would break a salt bridge interaction.

On the other hand increasing the pH would lead to the deprotonation of the basic residues Arg and Lys, which are found in the barrel wall, probably involved in many hydrogen bonds in native state. Deprotonation would disrupt the stability of many residues involved, which may lead to unfolding of the protein. In the aggregated state the hydrogen bonds are known to be formed between intramolecular species, which may be very close to each other. Hence to deprotonate any residue deep inside takes longer and heating helps in faster deprotonation. Aromatic residues Tyr and Trp are also involved in H-bond formation.

Another important feature to be noted is porins are anti parallel β-sheet structure and the stability of the sheet itself depends on the hydrogen bonds, and the peptide group by itself forms the easiest target for destabilization.

Electrostatic interactions

Salt-bridges between ionizing groups may be weakened or disrupted at extreme pH, at which one of the interacting groups is no longer ionized. The protonation of aspartic and glutamic acids at low pH, should contribute to weaken internal electrostatic interactions like salt bridges and hydrogen bonds. There is little evidence that repulsive charges on the surface of the protein are sufficiently large to cause denaturation. However they may influence the process of denaturation.

3.6.2 Refolding

Protein unfolded from aggregated and native state was folded back into detergent micelles by buffer exchange.

3.6.2.1 Refolding of protein unfolded from an aggregate

Second derivative spectra of native protein and protein refolded from aggregate unfolded porin are shown in Figure 3.6.10. It is clear from the spectra that the refolded protein has the β-sheet structural features but in comparison to the native the amide I β-sheet components are shifted to 1635 cm^{-1} and 1687 cm^{-1}. The bands representing loops and helices are not as well defined as in the native protein. It has to be considered that the helix and loop regions are unfolded upon heating up the protein as seen in section 3.5, so it cannot be ruled out that these regions are completely denatured by heat beyond repair. Hence it can be said that the proteins refold back into native-like structures which also form trimers (Figure

3.6.12), but local interactions among the amino acids are altered in the protein such that the amide I region of the protein is different, as amide I is mainly composed of C=O vibrations. Nevertheless this study shows that it is possible to refold a heat-aggregated protein to native-like structure without the presence of any chaperones. Probably with optimization of the refolding methods, proteins, which are same or close enough to be called native, can also be obtained.

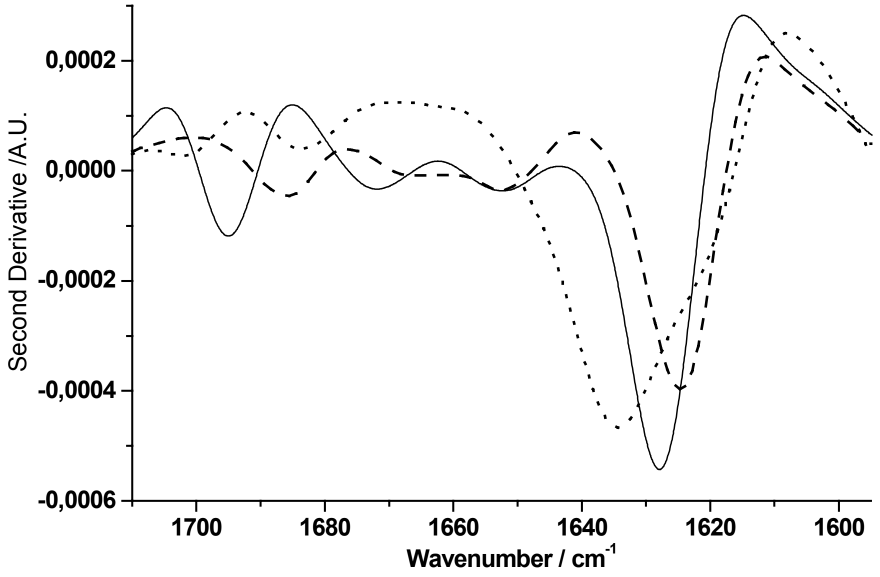

Figure 3.6.10 Second derivative spectra of aggregated refolded protein (dotted line) in comparison to native protein (solid line).

3.6.2.2 Refolding of native protein unfolded at high pH

Unfolded protein obtained from denaturation of porin at high pH was refolded by exchanging the buffer of pH 8. FTIR spectra showed that the protein has characteristic β-sheet structure evident from the peaks at 1625 cm $^{-1}$ and 1687 cm $^{-1}$. The bands representing the helix and loops were also seen at 1650 cm^{-1} and 1670 cm $^{-1}$respectively. It can thus be argued that native-like structures are formed on refolding are characterized by trimer in SDS-PAGE (Figure 3.6.11). However, some changes in local interaction among residues that lead to the shift in the amide I position of the β-sheet. The quaternary structure of the protein was analysed using SDS-PAGE gels. It was observed that unfolded protein from both aggregated and native protein folded into a trimeric structure (Figure 3.6.12).

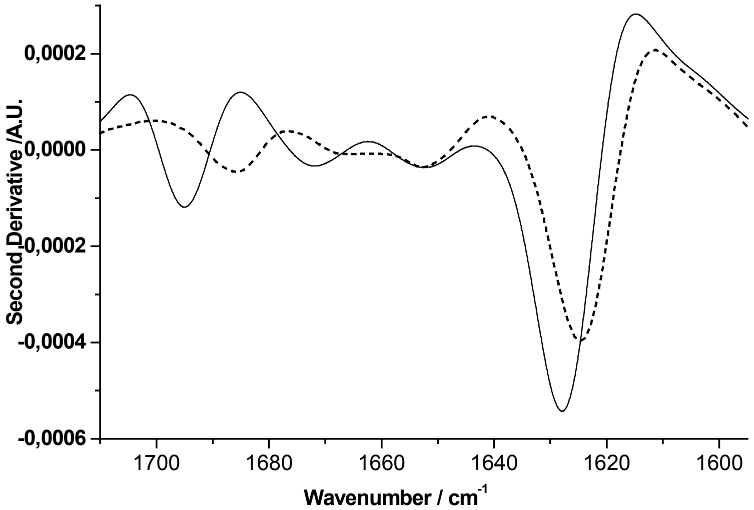

Figure 3.6.11 Second derivative of FTIR spectra of refolded protein (dashed line) and native (solid line).

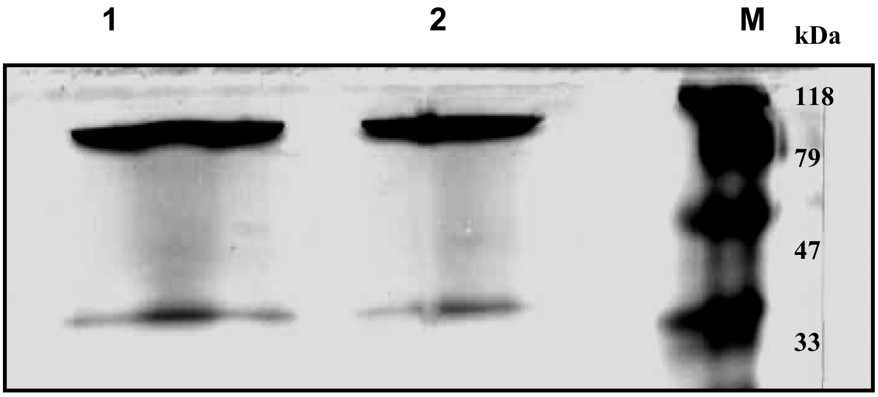

Figure 3.6.12 SDS-PAGE gel profile of refolded protein.
Lane 1 refolded aggregated porin, Lane 2 refolded native porin, M protein molecular weight marker.

3.6.3 Thermal stability of refolded protein

The thermal stability of the refolded protein was analyzed using FTIR spectroscopy.

3.6.3.1 Refolded protein, unfolded from an aggregate

Figure 3.6.13 depicts the heating and cooling spectra of refolded protein. The spectra of the refolded protein show that upon heating to 90 °C, there is a gradual shift of the band at 1634 cm^{-1} towards the 1642 cm^{-1} and on cooling the band does not shift to the original position but only to 1637 cm^{-1}. There is small shoulder at 1619 cm^{-1} in the room temperature spectra of protein which disappears on heating. Instead, a small band appears at 1615 cm^{-1} probably indicating aggregation. The small bands at 1685 cm^{-1} and 1697 cm^{-1} are not seen in the spectra of the heated protein spectra, but the band at 1685 cm^{-1} reappears on cooling. It is evident from the amide I region of the spectra that there are changes happening to the secondary structure of the protein, which are not reversible. The results also indicate that the refolded protein has an entirely different unfolding pathway when compared to the native one.

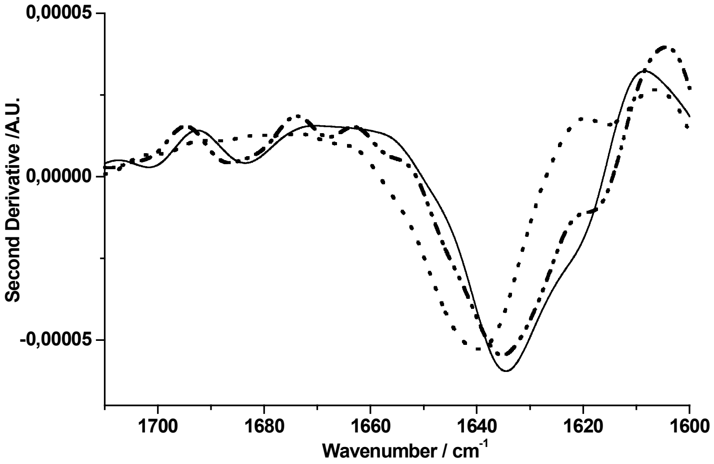

Figure 3.6.13 Second derivative spectra of thermal stability analysis of refolded porin. Room temperature (solid line), 90 °C (dotted line), 35 °C (dash dot dot).

3.6.3.2 Refolded protein unfolded from native protein at high pH

The thermal stability profile of protein refolded from native is shown in Figure 3.6.14 (a) and (b). It is evident that upon heating up to 60 °C the protein unfolds into unordered structure characterized by the appearance of a broad band centered around 1650 cm^{-1}. Cooling the protein to room temperature results in aggregation as evident from the bands at 1615 cm^{-1} and 1685 cm^{-1}. It should be noted that in the second derivative spectra at 60 °C, where the majority of the secondary structure is unordered, a small band is seen at 1615 cm^{-1}, which possibly denotes a small aggregated region. It can also be observed in the second derivative spectra that upon cooling the unordered region does not show bands denoting any ordered secondary structure. The thermal denaturation is irreversible.

It is evident from the spectra that the unfolding pattern of the refolded protein does not match the unfolding of the native protein at pH 8 or at pH 12.5. The unfolding at 12.5 shows the presence of an aggregated intermediate which opens up into random, but in this case it directly unfolds into unordered structure and maintains the unordered structure upon heating up to 90 °C. On cooling the native protein at pH 12.5 maintains the unordered structure (Figure 3.6.15) but the refolded protein aggregates. Consequently both of the proteins are different thermodynamically. The refolded protein differs from the native protein slightly in the secondary structure, but the thermal stability is entirely different.

Probably there are some key interactions which are modified, as a result of high pH induced unfolding. It is also possible that there are some interactions, which were not restored back during refolding. It is not easy to speculate on the nature of these interactions and more experimental evidences will be required to identify the changes that have occurred to the refolded protein

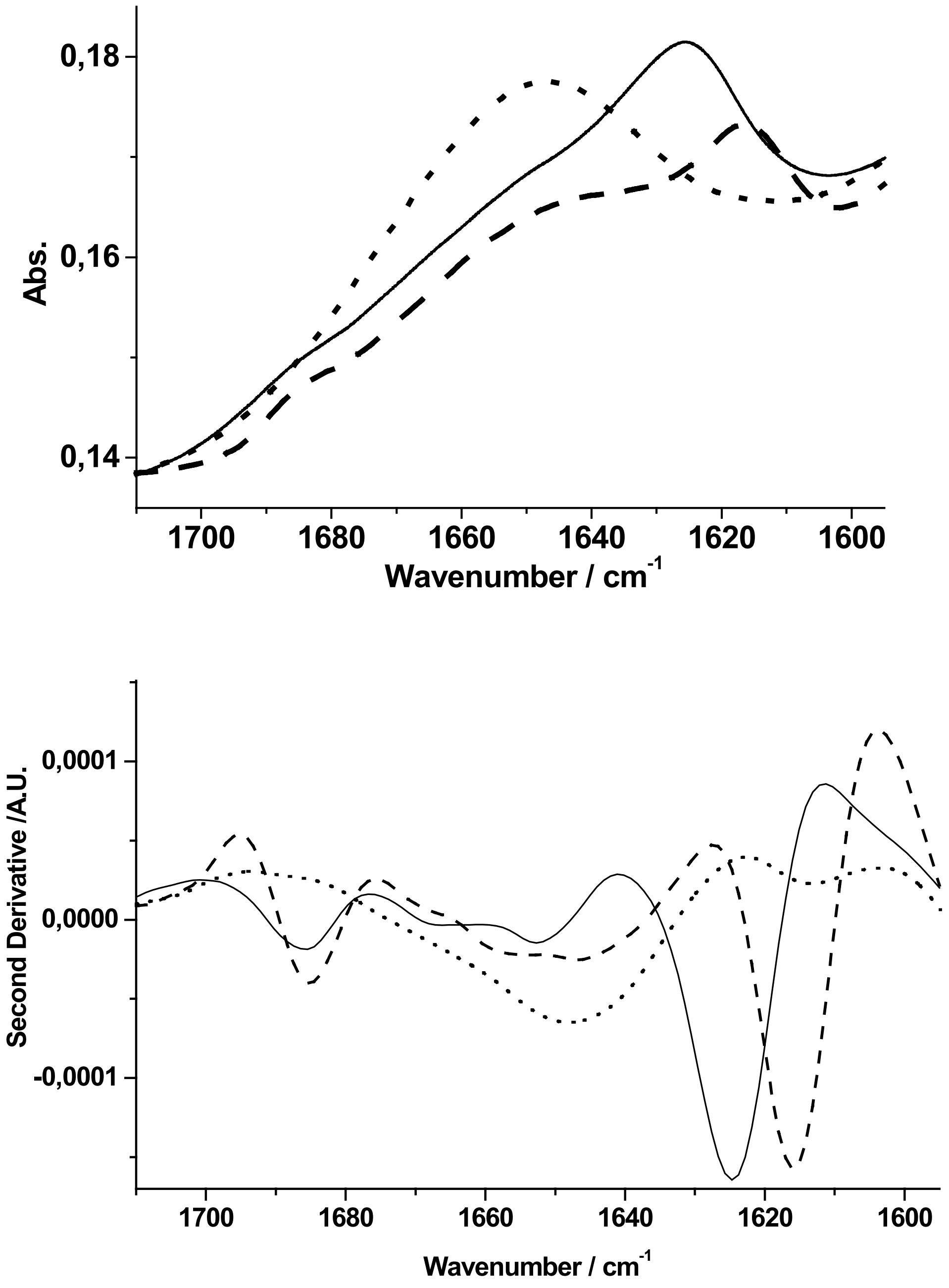

Figure 3.6.14 (a) Absorption spectra
(b) Second derivative spectra of thermal stability analysis.
Room temperature (solid line), 75 °C (dotted line), 30 °C (dashed line).

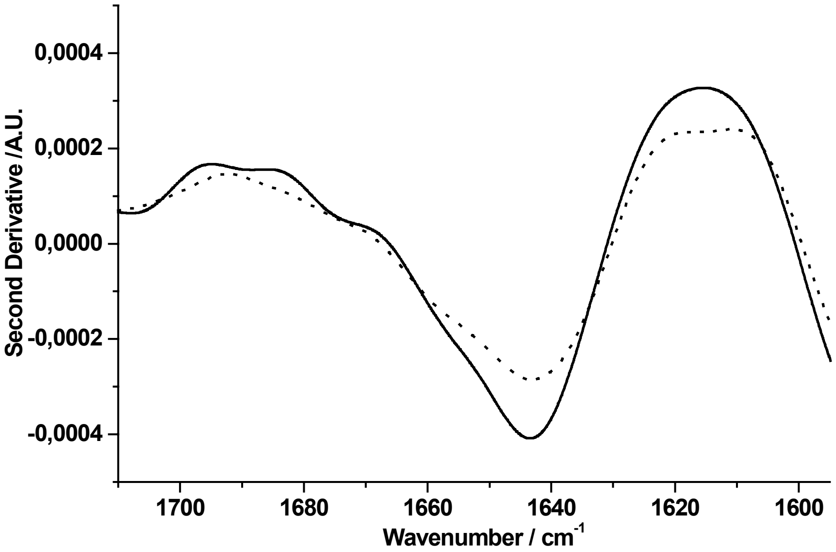

Figure 3.6.15 Second derivative spectra of thermal stability analysis at pH 12.5. 90 °C (Solid line), 30 °C (dotted line).

3.6.4 Residues probably involved in the unfolding mechanism

As discussed in this section there are many residues, which are affected by change in ionic strength of the solution. One of the modes which can be identified clearly arises from tyrosine, which is described in the next section. FTIR spectroscopy provides information about various other side chains, too.

Tyrosine deprotonation

The C-C ring mode of tyrosine can be detected in the second derivative spectra of the protein , hence providing access to observe the changes in Tyr deprotonation. It is reported for tyrosine that when protonated the band is positioned around 1515 cm^{-1}, whereas deprotonated mode shifts down to 1498 cm^{-1} (Barth, 2000; Chirgadze *et al.*, 1975). Figure 3.6.16 represents the second derivative spectra of porin at pH 12 in comparison with pH 8. The tyrosine ν(C-C) band position at pH 8 is 1515 cm^{-1} and is 1498 cm^{-1} at completely deprotonated state at pH 12.5. It is evident from the results that deprotonation of tyrosine occurs at a very high pH of 12 and above, probably due to the fact that Tyr residues are located in the hydrophobic, detergent protected girdles in porins.

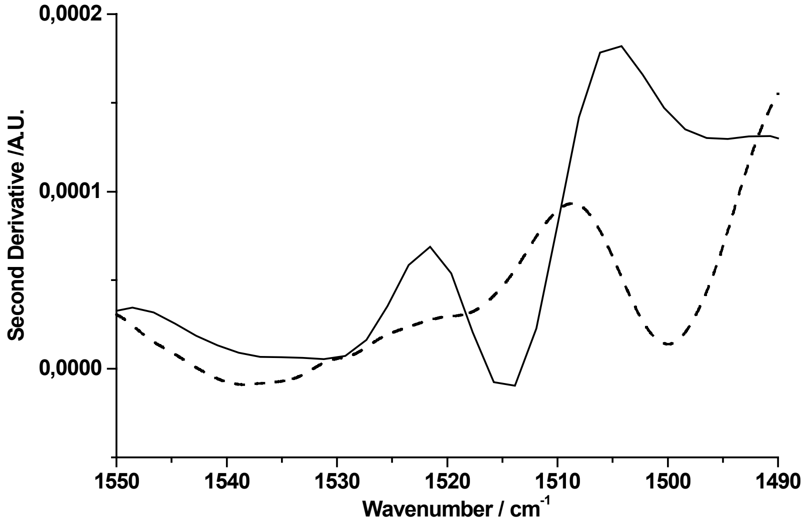

Figure 3.6.16 Second derivative spectra of tyrosine at pH 8 (solid line) and pH 12.5 (dashed line).

Tyrosine deprotonation may play a role in causing the instability to the protein in the native state, but it is the cumulative effect of the instabilities in various charged residues that the protein tends to open up. Studies have shown that tyrosines play a key role along with lysines in unfolding of spectrin from human erythrocytes (Fujita *et a*l., 1998).

In the case of aggregated proteins it can be speculated that the aggregation is the result of intramolecular interactions. It can be argued that these interactions occurs to protect the hydrophobic regions of the protein. In the barrel wall of porins the aromatic girdles with tyrosines are key players in the interactions as they are H-bond donors and acceptors. Thus a major amount of H bonds are contributed by

Tyr residues, as indicated by the down shift of the Tyr position in section 3.5. Then it can be argued that the deprotonation of the Tyr plays a key role in opening up of the aggregated proteins. However, more experimental evidences from similar membrane protein and soluble proteins may be needed for a conclusive explanation.

3.7 Chemical denaturation

Chemical denaturation of porin was studied using urea and GuHCl. Urea and GuHCl are not reported to have any role in unfolding in cells but they provide a very efficient system to study the unfolding and refolding characteristics of proteins *in vitro* (Makhatadze *et al*., 1992). CD and fluorescence spectroscopy were carried out to characterize the changes in secondary structure and Tryptophan (Trp) environment.

Urea and GuHCl increases the aqueous solubility of the protein backbone and side chains with increasing concentration. A linear relationship has been observed between the change in the unfolding free energy and the urea concentration with a proportionality constant that is related to the exposed surface area. Binding of urea and GuHCl to proteins is responsible for a significant decrease of enthalpy and entropy of the system (Makhatadze *et al*., 1992).

3.7.1 Unfolding studied by CD spectroscopy

CD spectroscopy provides information about the secondary structure of a protein. It can be used very precisely to study the changes in secondary structure of the protein even in presence of denaturants like urea and GuHCl, which is not an easy task with FTIR spectroscopy as the absorption from the denaturants in the amide I region prevents the exact evaluation of secondary structure.

3.7.1.1 GuHCl induced unfolding

GuHCl ($H_2NC(=NH)NH_2.HCl$) also called carbamidine, it is a strongly alkaline, water soluble compound.

Denaturation of porin was analyzed at various concentrations of GuHCl. Figure 3.7.1 shows the concentration dependant denaturation of porin. The CD spectra were recorded after 30 minutes of incubation with GuHCl. This indicated that at a concentration of 7.5 M GuHCl porin denatures into random structure characterized by a shift in the band towards negative CD values from 225 nm to 195, which is very typical for denatured proteins with unordered structure. Experiments were performed to analyze the effect of incubation time on denaturation. The shortest time measured was 4 minutes and the longest time was 2 hours. Furthermore, it was found that the unfolding is concentration dependent. At concentrations lower than 7.5 M spectra indicates the presence of some β-sheet, showing that at various lower concentrations partially folded structure still exists. . Similar results were obtained for the mutant E81Q and E81Q/D148N. It follows that fast unfolding kinetics represents most of the changes in the secondary structure occurs before 4 minutes, which is the shortest time measured. At concentrations lower than 7.5 M the spectra indicates the presence of some β-sheet, showing that at various lower concentrations a partially folded structure exists. The mechanism involved in unfolding of protein by guanidinium hydrochloride is discussed along with unfolding by urea in section 3.7.4.

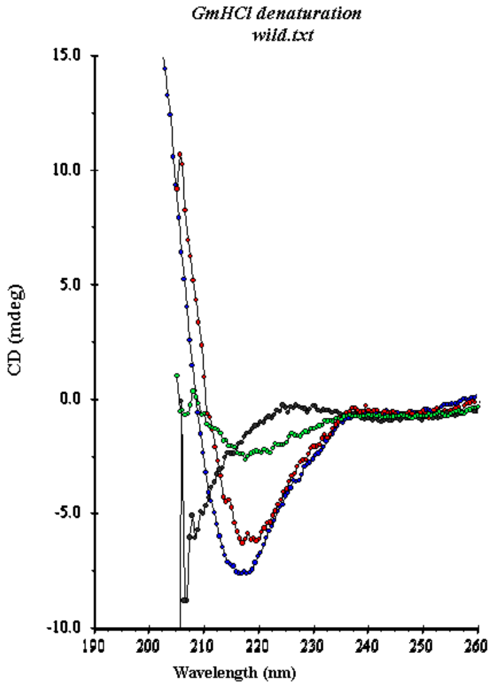

Figure 3.7.1 Denaturation of porin at various concentrations of GuHCl. (•) 0 M GuHCl, (•) 2 M GuHCl, (•) 6 M GuHCl, (•) 7.5 M GuHCl.

3.7.1.2 Urea-induced unfolding

Figure 3.7.2 shows the unfolding of wild type porin at various concentrations of urea. It was observed that at 7.5 M and 8M urea with 1mg/mL protein the sample solution turned turbid, probably indicating that some part of protein gets aggregated. This also reflects in the spectra. The spectra of protein denatured with urea are shifted from the baseline, thus indicating light scattering. The reduction in the CD value at 217 nm indicates that the protein was unfolded at increasing concentration of urea. Figure 3.7.3 depicts the spectra recorded of porin at 6 M urea after 4 minutes, 30 minutes and 2 hours, which indicates that not much change occurs to the protein even if incubated for longer period, showing that the unfolding of porins in urea is concentration dependent. Similar results were observed for GuHCl. Due to the problem of light scattering at high concentration of urea detailed experiments of porin denaturation with urea were carried out using fluorescence spectroscopy.

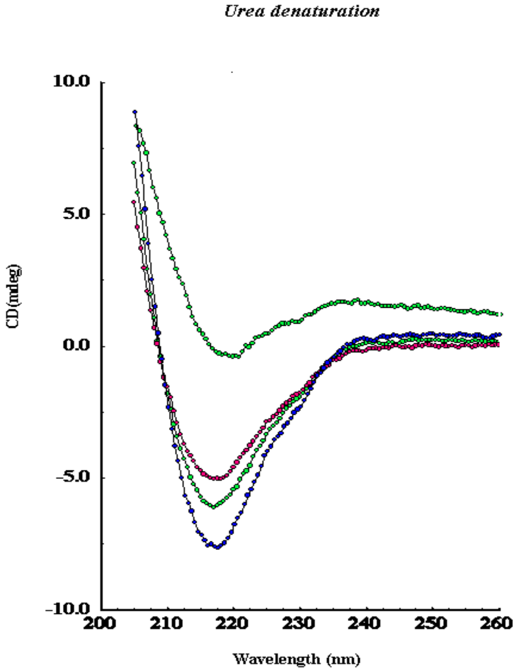

Figure 3.7.2 Unfolding of porin at various concentration of urea.
(●) 0 M urea, (●) 4 M urea, (●) 6 M urea (●) 7.75 M urea.

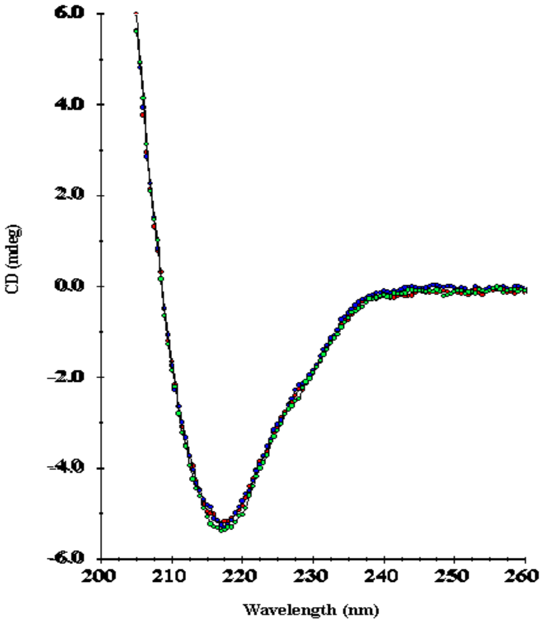

Figure 3.7.3 Time dependant denaturation of porin at 6M Urea.
(●) 4 min, (●) 30 min, (●) 2 hour.

3.7.2 Results from Fluorescence spectroscopy

Intrinsic fluorescence of a protein is contributed by Trp, Tyr and Phe side chains. Trp is the most efficient fluorophore with a sensitivity of ε_{max} = 1100 M^{-1} cm^{-1} and a fluorescence quantum yield of φ = 0.2. Trp fluorescence is studied in this work, as it is very sensitive to the polarity of the environment.

3.7.2.1 GuHCl induced unfolding

Denaturation of porin at various concentrations of GuHCl was analyzed using fluorescence spectroscopy. Figure 3.7.4 depicts the spectra of porin at 0 M and 7.5 M GuHCl. It is evident from the spectra that in the absence of any denaturant the intensity of Trp fluorescence is high and the emission maximum is at 340 nm. Upon denaturation, there is reduction in intensity and shift of the emission maxima to 352 nm, clearly indicating that due to the presence of denaturants the Trp vicinity has changed. The basic theory behind this peak shift is explained at the end of section 3.7.2.

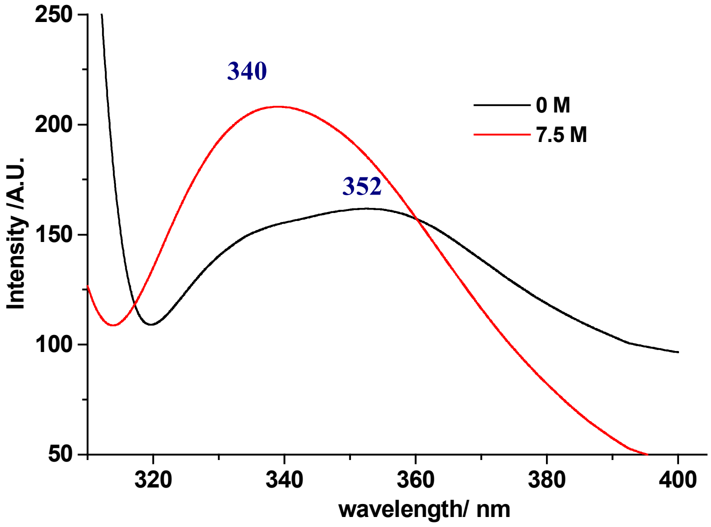

Figure 3.7.4 Denaturation of porin at 7.5 M GuHCl observed by Trp fluorescence intensity.

3.7.2.2 Urea induced unfolding

Porin denaturation in the presence of urea was analyzed using fluorescence spectroscopy. Figure 3.7.5 shows the spectra of porin with 0 M urea and at 7.75 M urea. It is evident from the spectra that the peak shifts from 340 nm to 354 nm, clearly indicating that the tryptophan environment is changed. A detailed concentration dependant denaturation was carried out for the wild type and the mutants E81Q, W74C and ED (Figure 3.7.6 (a) to (d)). The shift in emission maxima at various concentration of denaturant showed a linear pattern, showing that the transition value should approximately be 4 M.

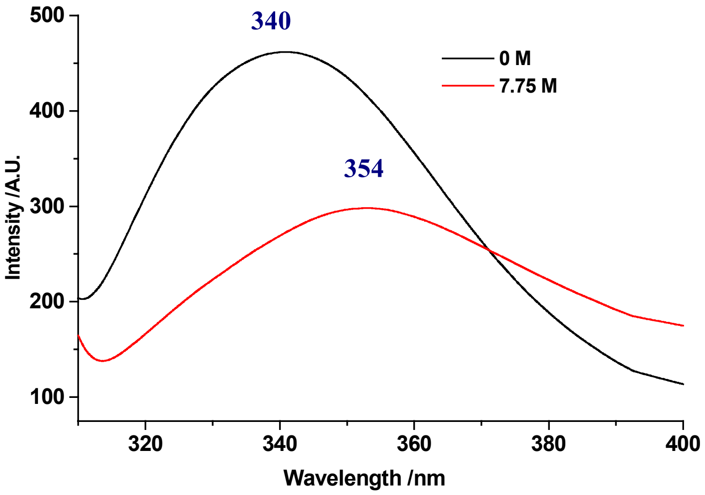

Figure 3.7.5 Denaturation in the presence of 7.75 M urea observed by Trp fluorescence intensity.

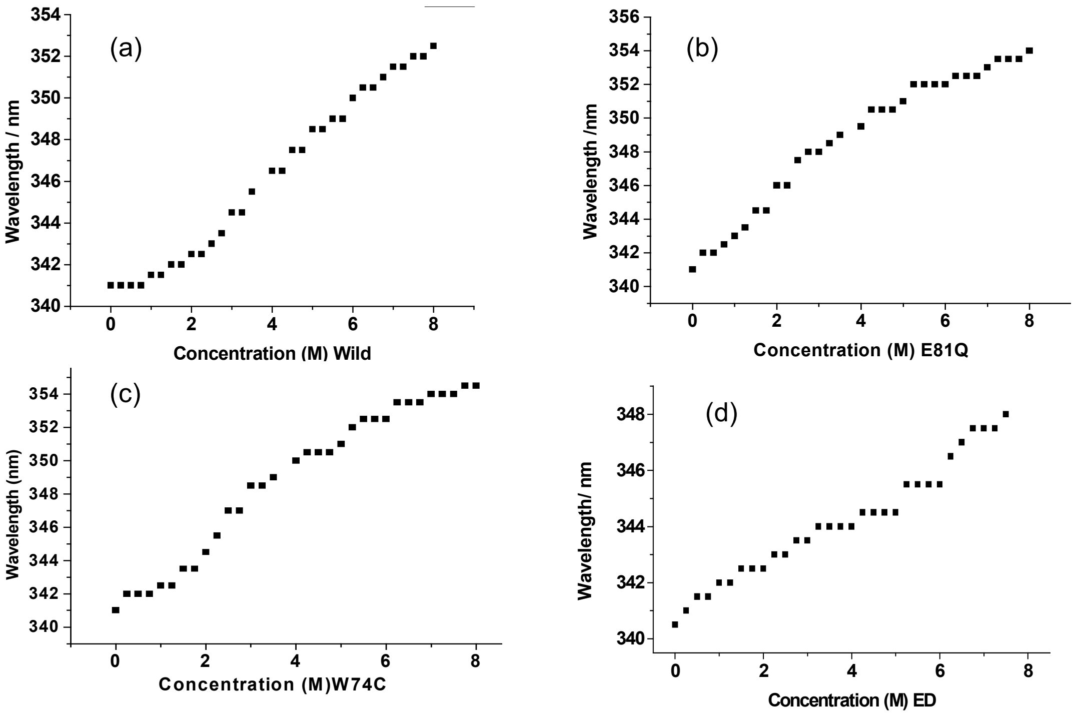

Figure 3.7.5 Concentration dependant denaturation of porin.
(a) Wild type (b) E81Q (c) W74C (d) ED.

3.7.2.3 Change in tryptophan environment

In *Paracoccus* porin the tryptophans (Trp) are located in the aromatic girdles of the porin β-barrel (Figure 3.7.6). Trp74 and Trp191 are located in the trimer interface region. Trp90 is located in the bilayer-exposed side. As suggested earlier, Trp fluorescence is highly sensitive to the environment. The emission maximum depends on the environment : it is around 355 nm for highly exposed residues and 320 nm for highly shielded residues (Cantor and Schimmel, 1980). For porin each monomer has 3 residues the emission maxima is obtained at 340 nm in absence of denaturant and close to 354 nm in the presence of denaturant. The peak observed at 340 nm is probably due to the fact that some contribution may arise from tyrosines, too, as there are 18 tyrosines in each monomer.

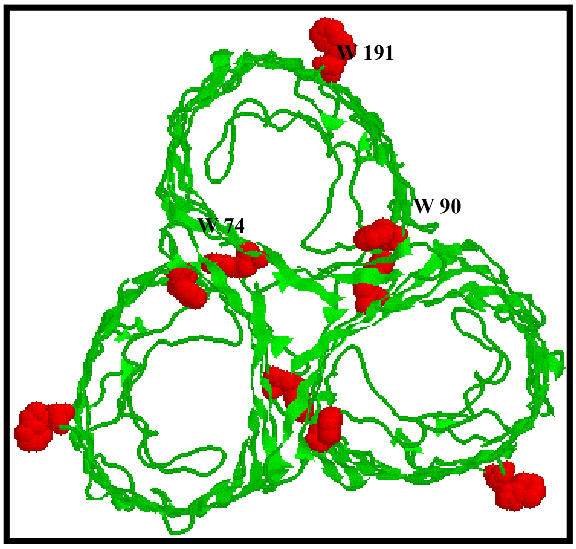

Figure 3.7.6 *Paracoccus* porin trimer with 9 Trp residues highlighted in red.

3.7.4 Unfolding analyzed by Sodium Dodecyl Sulfate Polyacrylamide Gel Electrophoresis (SDS-PAGE)

Changes in the quaternary structure of the protein were analyzed using SDS-PAGE. Figure 3.7.7 shows the SDS-PAGE profile of porin denatured in various concentrations of urea. It is evident that there are problems in running a gel with high concentration of urea but nevertheless it is obvious from the gel that at concentrations above 6 M urea the protein completely monomerises. Similar results were obtained for the denaturation studies with GuHCl (Figure 3.7.8).

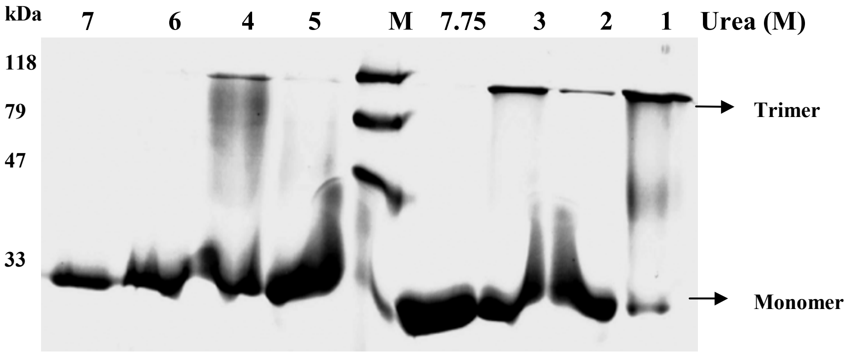

Figure 3.7.7 SDS-PAGE profile of denaturation of porin with urea Concentration are indicated in mol/L. M is the protein marker.

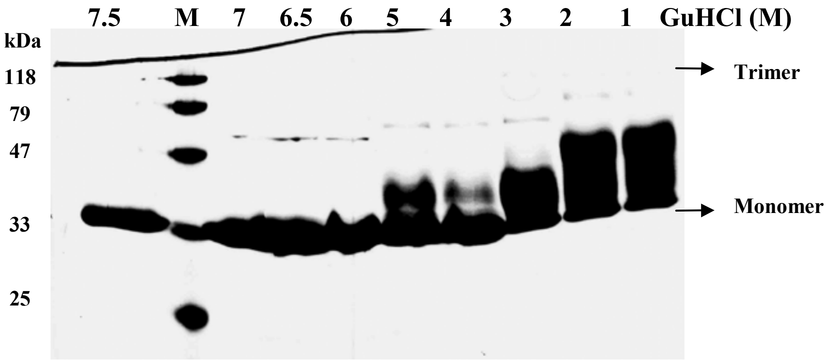

Figure 3.7.8 SDS-PAGE profile of denaturation of porin with GuHCl. Concentrations are indicated as mol/L. M is the protein marker.

3.7.4 Unfolding mechanism of urea and GuHCl

Even though urea and GuHCl are commonly used in unfolding studies of proteins the exact mechanism by which these chemicals cause the denaturation is not yet clear. Basically there are two models for the denaturation of proteins.

The first model suggests that the dominant effect of urea and GuHCl arises from the fact that these interact more strongly with the polar groups of the protein than water does and thus bring about a change in electrostatic forces and hydrogen bonding. High resolution X-ray structure of lysozyme crystals grown in presence of 0.7, 2, 3, 4, and 5 M urea as well as crystals soaked in 9 M urea have shown that the urea molecules interact via multiple hydrogen bonds, mainly to the peptide group but also with polar sidechains, while the conformation of the enzyme is practically unchanged (Thayer *et al.*,1993; Pike *et al.*, 1994).

In a second model aqueous solutions of urea is presumed to stabilize hydrophobic groups of the protein in water by forming partial clathrates around them with less perturbation of the water structure than that involved in corresponding clathrates formed by water molecules. It was found by Whitney *et al.,* 1962, that aqueous urea solutions can stabilize hydrophobic amino acids better than pure water. Molecular dynamic simulation has shown that urea and GuHCl molecules are found to interact with both polar and non polar groups on the surface of proteins. The presence of urea improves the capability of water molecules to participate in hydrogen bonds with hydrophilic groups of proteins.

Both the models are now shown to be true by molecular simulation dynamics on small soluble proteins and peptides (Caflisch *et al.,* 1998). Energetic analysis have shown that in an aqueous solution both the hydrophilic and hydrophobic regions of the protein chain are solvated more favorably than in a pure water. Monera *et al*. (1994) have shown that Gdn^+ and Cl^- ions mask electrostatic interactions (attractive and repulsive ionic interaction), thereby resulting in an instability of the protein which is not the same for urea. Even though both denaturants more or less affect the proteins in similar way, there are a few subtle differences, too, in their mode of action.

Generally it can be explained that protein unfolding occurs when the balance of forces between the proteins interaction with itself and the proteins interaction with its environment is disrupted (Schiffer *et al.*, 1996). The basic principles of unfolding should be the same for membrane proteins when compared to soluble ones. But as explained in previous sections membrane proteins shield their hydrophobic residues with detergent micelles or lipids. Therefore should be noted that the concentration needed to denature such proteins may be very high and it is of importance to understand the mechanism by which these chemical denaturants interact with detergents or lipids and how they get into the vicinity of the various residues.

Another notable point is that porins are water filled channels hence the regions exposed to water is very high compared to other membrane proteins but still it takes a very high concentration of denaturants to unfold these molecules completely as seen in the results here.

From the results obtained on porins it can be concluded that there is change a in secondary structure and also in exposure of hydrophobic residues to the aqueous environment as seen by the changes in the Trp environment model. There is change in secondary structure even at lower concentrations suggesting that a threshold concentration is required to completely attach enough urea molecules to the protein, so that the urea or GuHCl is able to directly interact with the backbone of the protein. The changes in the Trp environment suggest that the hydrophobic residues are exposed to the aqueous solvent.

3.8 Refolding

3.8.1 Refolding of porin into detergent micelles

Protein unfolded in the presence of 7.75 M urea was diluted to 0.05 M urea concentration and analyzed for Trp fluorescence immediately (dead time 3 minutes) after dilution (Figure 3.8.1). It was observed that the Trp fluorescence was almost the same as that for native with an emission maximum at 340 nm. This shows that the molecular environment of Trp again changed back to native, indicating that the unfolding of porin in presence of urea is reversible.

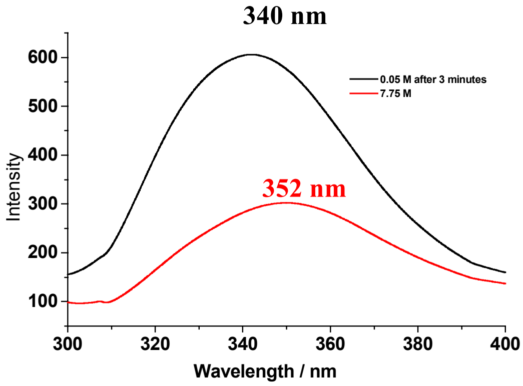

Figure 3.8.1 Trp emission at 7.75 M and 0.05 M urea concentration.

The SDS-PAGE profile showed that trimerization was also a fast process when refolded back into detergent micelles (Figure 3.8.2). It is evident from the gel that there are trimers existing after 3 minutes. However there is detectable amount of monomers, too.

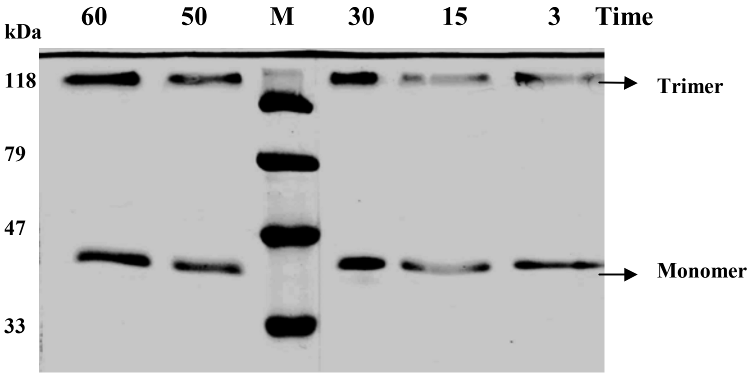

Figure 3.8.2 SDS-PAGE profile of refolding back into LDAO micelles. Time is indicated in minutes. M is the protein marker.

3.8.2 Refolding of porin into Liposomes

After the protein was unfolded with 7.75 M urea it was refolded back into liposomes. Formation of the secondary structure was analyzed using CD spectroscopy. Figure 3.8.3 shows the spectra from the urea-denatured porin and from porin diluted with preformed liposomes. The formation of β-sheet structure is fast within the mixing time and no increase in the β-sheet content was observed with respect to time. The results from SDS-PAGE show an intermediate band at 66 kDa, similar to the intermediate stage observed in OmpF (Surrey *et al.,* 1996). No trimer band can be observed until 15 minutes of incubation; detectable trimers appear only after about 30 minutes. There is a decrease in intensity of the band at 66 kDa. These results need to be analyzed further to clearly identify a trimer formation rate, since it is highly possible that the trimers are undetectable at lower concentrations. Another factor that has to be taken into account while observing the trimers is that it was seen through out the study that trimers appear as very faint band compared to same concentration of monomers, which is also indicated in some other studies (Heinz *et al*., 2003).

The band at 66 kDa can be denoted as a dimer in comparison to the studies with OmpF, where the band is identified as a dimer. The kinetic model reported on OmpF (Surrey *et al*., 1996) suggests that upon dilution of OmpF unfolded by urea, a fast transition from the unfolded state U_W to a misfolded intermediate P_W takes place. Upon association with membranes, Pw undergoes a moderately slow transition to a partially folded, membrane bound monomeric intermediate $P1_M$, the analogue of the molten globule state of the soluble proteins from which it proceeds in a slow transition to the folded, membrane inserted state $F2_M$ followed by trimerization $F3_M$.

$$U_W \rightarrow P_W \rightarrow P1_M \rightarrow F2_M \rightarrow F3_M$$

It is reported in the case of OmpF that the dimeric and trimeric state is protected from trypsin digestion. The trimerization of OmpF into DMPC vesicles devoid of detergent was slower by several orders of magnitude than in the bacterium. The fastest trimerization of OmpF in mixed membranes of DMPC and DM does not approach the rate of trimerization *in vivo*. The rate of assembly of a OmpF porin trimer *in vivo* is found to be 25-40 seconds (Reid *et al*., 1988) and LamB is reported to be 30 seconds (Misra *et al*., 1991). OmpF inserts into membranes with a lower yield than OmpA does (Surrey *et al*., 1996; Kleinschmidt *et al*., 1996). The difference is attributed to oligomerization of OmpF. The yield of insertion of the two proteins depends on various parameters such as pH, concentration of lipid and the presence of detergent.

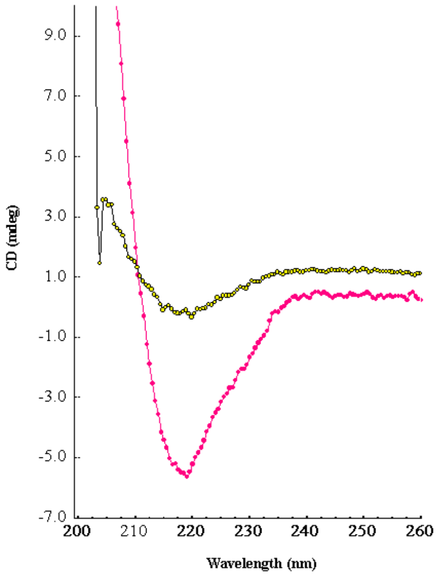

Figure 3.8.3 Refolding of porin into liposomes.
(●) unfolded protein diluted with liposomes, (●) porin unfolded with urea.

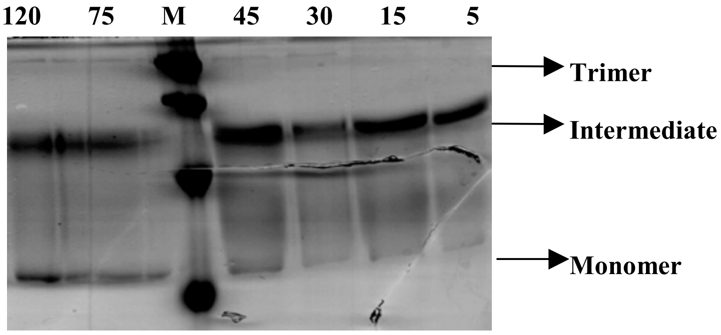

Figure 3.8.4 SDS-PAGE profile of refolding into liposomes.
Time is indicated in minutes, M is the protein marker.

The results in this study supports the model suggested by Surrey *et al.* (1996) and Klienschmidt *et al*. (2003) but it has to be considered that the refolding in presence of liposomes is very slow. It shows that these *in vitro* conditions created are not close enough to mimic the natural periplasmic space, where this folding occurs in seconds. In order to fully achieve the *in vivo* conditions, changes of the experimental parameters as the absence of all denaturants and of detergnts as well as the exact physiological pH and temperature would have to be performed.

3.7.4 Thermal stability of the refolded protein

The protein refolded into detergent micelles and liposomes were subjected to a thermal stability analysis. For the protein refolded into detergent micelles, it was necessary to remove the last traces of urea and the excess of detergent. It was achieved by reloading the refolded protein into a pre-equilibrated Q sepharose column. The refolded protein showed similar unfolding pattern as the natively folded wild type. For the protein which was refolded into liposomes bio-beads were added and incubated for 30 minutes to remove the impurities. This was followed by centrifugation, which resulted in the trimeric fraction of the protein showing the same stability as the natively folded protein. Therefore the unfolding is completely reversible.

Conclusions

Membrane protein stability, unfolding and refolding is addressed in this study using the outer membrane protein porin from *Paracoccus denitrificans*. Gene manipulations are carried out to generate the mutants. Fourier transform infrared (FTIR), circular dichroism (CD) and fluorescence spectroscopy are used to study the changes in secondary structure and tryptophan environment of the protein.

Construction of mutants and protein purification

Protein from wild type and mutants E81Q, W74C, E81Q/D148N, E81Q/D148N/W74C are characterized for structure and function. The site-directed mutants are constructed based on conserved residues and details from previous studies with OmpF.

Secondary structure and functional activity analysis

Secondary structure analysis of wild type and mutant porins by FTIR and CD spectroscopy are in line with the fact that the porins are predominantly β-sheet structure. The results from this study support the X-ray crystal structure data. The functional activity studies by black lipid bilayer technique shows that the wild type porin and the mutants W74C, E81Q/D148N, E81Q/D148N/W74C have a conductance of 3,25 nS. The result observed is in line with the conductance values reported for porin from *Paracoccus denitrificans* and other non-specific porins. For the mutant E81Q, a conductance of 1.25 nS is predominant over 3.25 nS. The activity of the mutants is observed to be far less than the wild type. Relative activity profile indicates that the mutants E81Q and W74C has only 20 % activity in comparison to the wild type. For E81Q/D148N the activity is only 10 %. The probable reason for the reduction in activity is due to the presence of porin not only in the stable trimeric form, but also as monomers and dimers. This shows that structural similarity does not mean similar functional activity.

Thermal stability analysis of porin in detergent micelles and reconstituted into liposomes

Thermal stability analysis of wild type and mutants shows that these proteins are highly stable. The unfolding of protein at high temperature causes aggregation in detergent micelles with a transition temperature (T_M) of 86.2 °C for the wild type and 84.2 °C, 80.3 °C, 80.2 ° C for E81Q, W74C, and ED, respectively. It is observed that the major part of the protein, probably the β-sheet region, is involved in the formation of aggregates. The disappearance of bands indicating loop and helix regions and appearance of a band at unordered region indicates that some region of the protein unfolds into unordered structure, too. The SDS-PAGE gel shift assays shows that the protein monomerises at a temperature close to 90 °C, hence indicating that heating up the protein to its transition temperature brings about changes in secondary and quaternary structure. Functional activity assays at high temperatures reveals that the protein looses its activity on heating. This shows that structural stability does not mean functionality in the case of porins.

Thermal stability analysis of porin reconstituted into liposomes showed that there is no change in the secondary and quaternary structure of the protein up to 100 °C, revealing that the protein becomes more thermostable when it is reconstituted into liposomes.

The difference in the thermal stability of porin in detergent micelles and liposomes can be proved by the change in environment of the residues, especially of tyrosine, which can be probed by analysing the ring C-C mode around 1515 cm^{-1}. From the analysis of this Tyr mode in detergent micelles and in liposomes, it can be concluded that there is a downshift of this mode in the case of porin in detergent micelles whereas the band position of Tyr remains more or less constant up to 80 °C in liposomes. Above this temperature, a loss of water molecules by evaporation cannot be prevented which brings about the change in Tyr environment and hence the shift of the band position.

Refolding of aggregated porin

Aggregation is generally considered the final stage in protein denaturation and it can be termed completely irreversible. However this study shows that disaggregation of β-sheet membrane protein porin is possible by changing its environment. An increase of the solution pH to 12 or above, results in opening up of the aggregated protein into unordered structure, as observed by FTIR and CD spectroscopy. This unordered structure could be refolded into a native-like structure forming trimers. The native-like structure thus formed shows characteristic β-sheet structure, but the position of the amide I mode is slightly different from the native one. Nevertheless this study shows that aggregated proteins can be refolded back without any chaperones and only by changing the chemical and thermodynamic parameters.

The thermal stability of refolded native-like protein is entirely different from the native one. These proteins unfold into unordered structure on reheating rather than forming aggregates. Furthermore, it maintains the unordered structure even on cooling. This shows that the unfolding is irreversible.

pH dependent unfolding of porin

Thermal stability of porin at different pH values shows that the protein tends to be stable in a pH range of 1-11. The protein irreversibly unfolds into aggregated structures in this pH range. Even though there is a decrease in the transition temperature if the protein is incubated at acidic pH of 1.5 and 4. The transition temperature is only few degrees lower than that of the protein at pH 8. At pH 12 and above, the protein unfolds into unordered structure instead of aggregating. This indicates that the stability of the protein changes at higher pH.

It was also seen that incubating the protein at pH 12 results in unordered structure, the reaction being slow and takes approximately 1 hour for completion. The high pH unfolding of porin is a reversible process. On refolding native-like structures are formed which is verified spectroscopically and by formation of trimers in SDS- PAGE gels. The refolded protein is called “native-like protein” because its amide I mode shows a β-sheet pattern in FTIR spectra, but with frequency positions at 1625 cm^{-1} and 1687 cm^{-1}. The thermal stability of the refolded native-like porin is entirely different from the native protein as upon heating it unfolds into unordered structure rather than into an aggregated form and on cooling it aggregates. This shows that even though the unfolding of porin at high pH is reversible, certain local interactions between the amino acids change resulting in a difference in stability. It will be of interest to understand how the different interactions deviate from the native structure.

Unfolding in the presence of urea and guanidinium hydrochloride

Denaturation of porin in the presence of chemical denaturants like urea and GuHCl shows that porins unfold into unordered structure. The unfolding is almost linear with respect to concentration. The unfolding is a reversible process. Unfolded protein is refolded into detergent micelles and liposomes. Spectroscopically the β-sheet formation is rapid and observed within 4 minutes in both the cases. Refolding into detergent micelles is faster when compared to liposomes as seen by kinetic gel shift assays. There is no intermediate observed in the gel when refolding back into detergent micelles. In the case of liposomes, intermediates were observed in the gel, which is similar to the intermediates observed in the case of OmpF.

This study shows the difference in thermal stability of the outer membrane protein porin from *Paracoccus denitrificans* in detergent micelles and native-like liposomes. It suggests various unfolding pathways, which can be further investigated for unfolding and refolding kinetics. This report also suggests that it is possible to refold a heat-aggregated porin.

Zusammenfassung

In der vorliegenden Arbeit werden die Stabilität, das Entfalten und Rückfalten des Außenmembranproteins Porin von *Paracoccus denitrificans* untersucht. Durch Mutagenese wurden Proteinmutanten hergestellt und mit Hilfe der Fourier Transform Infrarot (FTIR)-, Zirkulardichroismus (CD)- und Fluoreszenz-Spektroskopie Änderungen in der Sekundärstruktur und in Tryptophan-Regionen des Proteins verfolgt.

Konstruktion der Mutanten und Proteinreinigung

Das Protein des Wildtyps und der Mutanten E81Q, W74C, E81Q/D148N, E81Q/D148N/W74C wurde bezüglich Struktur und Funktion charakterisiert. Die Auswahl der ortsgerichteten Mutationen basieret auf konservierten Aminosäuren und auf vorangegangenen Studien mit OmpF.

Analyse der Sekundärstruktur und der funktionellen Aktivität

Die Sekundärstrukturanalyse des Wildtyps und der Porinmutanten sind in Übereinstimmung mit dem Befund, dass Porine vorwiegend β-Faltblattstruktur besitzen. Die Daten aus der Röntgenstrukturanalyse werden durch die Ergebnisse dieser Arbeit unterstützt. Untersuchungen über die funktionelle Aktivität mit Hilfe von Lipiddoppelschichten zeigen, dass der Wildtyp und die Mutanten W74C, E81Q/D148N und E81Q/D148N/W74C eine Leitfähigkeit von 3,25 nS, bezogen auf das einzelne Protein besitzen. Das beobachtete Ergebnis steht in Einklang mit den Leitfähigkeitsmessungen, die für Porin von *Paracoccus denitrificans* und andere nicht spezifische Porine berichtet werden. Die Leitfähigkeit der Mutante E81Q beträgt 1,25 nS und ist damit auffällig niedrig. Die Aktivität der Mutanten ist um einiges geringer als die vom Wildtyp. Messungen der relativen Aktivität zeigen, dass die Mutanten E81Q und W74C nur 20% der Aktivität des Wildtyps besitzen. Für E81Q/D148N beträgt die Aktivität nur 10%. Der Grund für die reduzierte

Aktivität liegt wahrscheinlich darin, dass das Porin nicht nur in der stabilen Trimerform, sondern auch als Monomere und Dimere vorliegt. Dies zeigt, dass eine strukturelle Ähnlichkeit nicht unbedingt eine vergleichbare funktionelle Aktivität bedeutet.

Analyse der thermischen Stabilität von Porin in Detergensmizellen und in Liposomen

Die Analyse der thermischen Stabilität des Wildtyps und der Mutanten zeigt, dass diese Proteine sehr stabil sind. Entfalten des Proteins bei hohen Temperaturen führt zur Aggregation in Detergensmizellen mit einer Übergangstemperatur (T_M) von 86,2 °C für den Wildtyp bzw. 84,2 °C, 80,3 °C und 80,2 °C für die Mutanten E81Q, W74C und E81Q/D148N. Obwohl der Hauptteil des Proteins, wahrscheinlich der β-Faltblatt-Bereich, an der Aggregatbildung beteiligt ist, gibt es Hinweise darauf, dass einige Proteinbereiche auch in ungeordnete Struktur entfalten, da Banden verschwinden, die charakteristisch für Loop- und Helix-Bereiche sind und zusätzlich eine Bande erscheint, die eine ungeordnete Struktur kennzeichnet. Die Analyse mit SDS-PAGE zeigt, dass das Protein bei Temperaturen nahe 90 °C monomerisiert, was somit bedeutet, dass das Erwärmen des Proteins bis zu seiner Übergangstemperatur Veränderungen in seiner Sekundär- und Quartärstruktur erzeugt. Funktionelle Aktivitätsbestimmungen bei hohen Temperaturen machen deutlich, dass das Protein dazu tendiert, beim Erwärmen seine Aktivität zu verlieren. Dies bedeutet, dass im Fall von Porinen eine strukturelle Stabilität nicht gleichbedeutend mit einer funktionellen ist.

Die Analyse der thermischen Stabilität von Porin, das in Liposomen rekonstituiert wurde, zeigt, dass bis zu 100°C keine Veränderung in der Sekundär- oder

Quartärstruktur des Proteins stattfindet, was deutlich macht, dass das Protein durch die Rekonstitution in Liposomen noch weiter stabilisiert wird.

Der Unterschied der thermischen Stabilität von Porin in Detergensmizellen und Liposomen kann durch Änderungen in der Umgebung von Residuen belegt werden, insbesondere die von Tyrosinen, was durch die Analyse der Ring C-C Streckschwingung bei 1515 cm^{-1} untersucht werden kann. Aus der Analyse dieser Tyrosinschwingung in Detergensmizellen und in Liposomen kann gefolgert werden, dass bei Porin in Detergensmizellen eine Verschiebung dieser Mode zu kleineren Wellenzahlen erfolgt, wohingegen die Bandenposition in Liposomen bis 80 °C annähernd konstant bleibt. Oberhalb dieser Temperatur konnte aufgrund von Verdampfen ein Verlust von Wassermolekülen nicht vermieden werden, was eine unspezifische Veränderung der Umgebung der Tyrosinreste und damit auch der Bandenposition zu Folge hat.

Rückfalten des aggregierten Porins

Aggregation wird im Allgemeinen als der Endzustand des Proteins beim Denaturieren angenommen und kann als vollständig irreversibel bezeichnet werden. Diese Studie zeigt jedoch, dass die Desaggregation des β-Faltblatt Membranproteins Porin durch die Veränderung seiner Umgebung möglich ist. Eine Erhöhung des pH-Wertes des Lösungsmittels auf 12 oder höher resultiert in einem Öffnen des aggregierten Proteins in eine ungeordnete Struktur, was durch FTIR und CD Spektroskopie dokumentiert wird. Diese ungeordnete Struktur kann in eine nativ-ähnliche Struktur zurückgefaltet werden, welche Trimere bildet. Diese so gebildete nahezu native Struktur zeigt charakteristisches β-Faltblatt, allerdings weicht die Position der Amid I Bande leicht von der der nativen Struktur ab. Trotzdem wird durch diese Untersuchung gezeigt, dass aggregiertes Protein ohne jegliche Chaperone, sondern allein durch das Verändern chemischer und thermodynamischer Parameter rückgefaltet werden kann.

Die thermische Stabilität des zurückgefalteten nativ-ähnlichen Porins ist vollkommen unterschiedlich. Beim erneuten Erwärmen entfalten diese Proteine in ungeordnete Struktur und nicht in Aggregate. Desweiteren bleibt die ungeordnete Struktur sogar beim Abkühlen erhalten, das heißt, dass von nun an das Entfalten irreversibel ist.

pH abhängiges Entfalten des Porins

Die Untersuchung der thermischen Stabilität von Porin bei unterschiedlichen pH-Werten zeigt, dass sich das Protein in einem pH-Bereich zwischen 1 und 11 ähnlich verhält. In diesem pH- Bereich entfaltet das Protein irreversibel in Aggregate. Obwohl die Übergangstemperatur bei saurem pH von 1,5 und 4 abnimmt, ist sie nur ein paar Grad niedriger als bei pH 8. Bei pH 12 entfaltet das Protein in ungeordnete Struktur, anstatt zu aggregieren. Dies bedeutet, dass sich die Stabilität des Proteins bei höherem pH-Wert ändert. Auch das Entfalten oberhalb eines pH-Wertes von 12 resultiert in ungeordneter Struktur, die Reaktion ist aber langsam und braucht zur Vervollständigung ungefähr eine Stunde.

Das Entfalten des Porin bei hohem pH ist ein reversibler Prozess. Beim Rückfalten werden nativ-ähnliche Strukturen gebildet, was spektroskopisch und durch das Entstehen von Trimeren in SDS-PAGE Gelen überprüft wurde. Das zurückgefaltete Protein wird nativ-ähnlich genannt, weil in den FTIR Spektren die Amid I Banden für β-Faltblatt zwar auftreten, jedoch die Bandenpositionen bei 1625 cm^{-1} und 1687 cm^{-1} leicht von denen der nativen Form abweichen. Die thermische Stabilität des zurückgefalteten nativ-ähnlichen Porins ist vollkommen anders als beim nativen Protein, da es beim Erwärmen zunächst in eine ungeordnete und nicht in eine aggregierte Struktur entfaltet und erst beim erneuten Abkühlen aggregiert. Obwohl das Entfalten von Porin bei hohem pH reversibel ist, wird deutlich, dass sich lokale Wechselwirkungen zwischen Aminosäuren verändern, was in einer unterschiedlichen Stabilität resultiert. Hier wäre es wichtig, zu verstehen, wie diese unterschiedlichen Wechselwirkungen von denen der nativen Struktur abweichen.

Entfalten durch Harnstoff und Guanidiniumhydrochlorid

Die Denaturierung von Porin mit Hilfe von chemischen Denaturierungsmittel wie Harnstoff und Guandiniumhydrochlorid entfaltet dass Porin in eine ungeordnete Struktur. Das Entfalten hängt fast linear von der Konzentration ab und ist ein reversibler Prozess. Entfaltetes Protein wurde sowohl in Detergensmizellen als auch in Liposomen zurückgefaltet. Die spektroskopische Aufnahme der Bildung von β-Faltblatt Struktur zeigt in beiden Fällen Faltungszeiten unter 4 Minuten. Das Rückfalten in Detergensmizellen ist verglichen mit dem Rückfalten in Liposomen schneller, was durch eine SDS-PAGE Analyse beobachtet wurde. Im Gel werden beim Rückfalten in Detergensmizellen keine Intermediate beobachtet, wohingegen für Liposomen Intermediate auftreten, ähnlich wie sie für OmpF beobachtet werden.

Diese Arbeit zeigt Unterschiede in der thermischen Stabilität des Außenmembranproteins Porin von *Paraccocus denitrificans* in Detergensmizellen und nativ-ähnlichen Liposomen auf. Mehrere Entfaltungswege werden vorgeschlagen, die bezüglich Entfaltungs- und Rückfaltungskinetiken weiter untersucht werden können. Desweiteren konnte gezeigt werden, dass es möglich ist, ein durch Erwärmen aggregiertes Protein in eine nativ-ähnliche Proteinstruktur zurückzufalten.

References

Anfinsen, C. B. (1973) Principles that govern the folding of protein chains. Science 181, 223-230.

Arrondo, J. L.R., Young, N.M., Mantsch, H.H. (1988) The solution structure of concanavalin A probed by FT-R spectroscopy. Biochim. Biophys. Acta 952,261-268.

Arrondo, J.L.R., Castresana, J., Valpuesta, J.M., Goni, F.M. (1994) Structure and thermal denaturation of crystalline and noncrystalline cytochrome oxidase as studied by infrared spectroscopy. Biochemistry 33,11650-11655.

Arora, A., Tamm, L.K. (2001) Biophysical approaches to membrane protein structure determination. Curr. Opin. Struct. Biol. 11, 540-547.

Bainbridge, G., Mobasheri, H., Armstrong, G.A., Lea, E.J., Lakey, H. (1998) Voltage-gating of *E. coli* porin: A cysteine scanning mutagenesis study of loop 3. J. Mol. Biol. 275, 171-176.

Barth, A., Zscherp, C. (2002) What vibrations tell us about proteins. Q. Rev. Biophys. 35, 369-430.

Barth, A. 2000.The infrared absorption of amino acid side chains. Prog. Biophys. Mol. Biol. 74, 141-173.

Benz, R., Janko, K., Boos, W., Läuger, P. (1978) Formation of large, ion-permeable membrane channels by the matrix protein (porin) of *Escherichia coli*. Biochim. Biophys. Acta 511, 395-319.

Benz, R., Janko, K., Boos, W., Läuger, P. (1973) J. Membrane Biol. 14, 339-364.

Brockwell, D.J., Smith, D.A., Radford, S.E. (2000) Protein folding mechanisms: new methods and emerging ideas. Curr. Opin. Struct. Biol. 10,16-25.

Butler, J.S., Loh, S.N. (2003) Structure, function, and aggregation of the zinc-free form of the p53 DNA binding domain Biochemistry 42, 2396-2403.

Byler, D.M., Susi, H. (1986) Examination of the secondary structure of proteins by deconvoluted FTIR sprectra. Biopolymers 25, 469-487.

Caflisch, A., Karplus, M. (1998) Structural details of urea binding to barnase: a molecular dynamic analysis. Structure 7, 477-488.

Cantor, C.R., Schimmel, P.R. (1980) Biophysical Chemistry, part **I**, chapter 5, W H Freeman.

Capaldi, A.P., Radford, S.E. (1998) Kinetics of β-sheet protein folding. Curr. Opin Struct. Biol. 8, 86-92.

Carlsson, U., Jonsson B-H. (1995) Folding of β –sheet proteins. Curr. Opin. Struct. Biol. 5, 482-487.

Chen, R., Henning, U. (1996) A periplasmic protein (Skp) of Escherichia coli selectively binds a class of outer membrane proteins. Mol. Microbiology. 19, 1287-1294.

Chou, P.Y., Fasman, G.D. (1974) Conformational parameters for amino acids in helical, beta-sheet, and random coil regions calculated from proteins. Biochemistry 13, 211-222.

Chirgadze, Y.N., Fedorov, O.V., Trushina, N.P. (1975) Estimation of amino acid residue side chain absorption in the infrared spectra of protein solutions in heavy water, Biopolymers 14, 679-694.

Conlan, S., Zhang, Y., Cheley, S., Bayley, H. (2000) Biochemical and biophysical characterisation of OmpG: A monomeric porin. Biochemistry 39, 11845-11854.

Delcour, A. H. (1997) Function and modulation of bacterial porins: insights from electrophysiology. FEMS Microbiol. Letts. 151, 115-123.

Deléage, G., Geourjon, C.(1993) An interactive graphic program for calculating the secondary structures content of proteins from circular dichroism spectrum. Comp. Appl. Biosc. 9, 197-199

Dobson, C.M., Karplus, M. (1999) The fundamentals of protein folding: bringing together theory and experiment. Curr. Opin. Struct. Biol. 9, 92-101.

Dobson, C. M. (2004) Principles of protein folding, misfolding and aggregation. Semin Cell. Dev. Biol. 15, 3-16.

Dubois, J., Ismail, A.A., Chan, S.L., Ali-Khan, Z. (1999) Fourier Transform Infrared spectroscopic investigation of temperature and pressure induced disaggregation of amyloid A. Scand. J. Immunol. 49, 376-380.

Ellis, R.J., Minton, A.P. (2003) Join the crowd. Nature. 425, 27-8.

Ellis, R.J., Pinheiro, T.J.T. (2002) Danger-misfolding proteins. Nature. 416, 483-484.

Elliot, A., Ambrose, E. J. (1950) Structure of synthetic polypeptides. Nature 165, 921-922.

Engel, A., Lyubchenko, Y., Muller, D. (1999) Atomic force microscopy : a powerful tool to observe biomolecules at work. Trends Cell Biol. 9, 77-80.

Fabian, H., Mäntele. W. (2002) Infrared spectroscopy of proteins, in: J.M. Calmers, P.R. Griffiths, (Eds.), Handbook of vibrational spectroscopy, John Wiley & Sons Ldt., Chichester, 5, 3399-3426.

Fabian, H., Schultz, C., Naumann, D., Landt, D.O., Hahn, U., Saenger, W. (1993). Secondary structure and temperature-induced unfolding and refolding of ribonuclease T1 in aqueous solution, J. Mol. Biol. 232, 967-981.

Fabian, H., Falber, K., Gast, K., Reinstädler, D., Rogov, V.V., Naumann, D., Zamyatkin, F., Filimonov, V.V. (1999) Secondary structure and oligomerization behavior of equilibrium unfolding intermediates of the Cro repressor. Biochemistry, 38: 5633-5642.

Fabian, H., Schultz, C., Backmann, J., Hahn, U., Saenger, W., Mantsch, H.H., Naumann, D. (1994) Impact of point mutations on the structure and thermal stability of ribonuclease T1 in aqueous solution probed by Fourier transform infrared spectroscopy. Biochemistry 33, 10725-10730.

Faller, M., Niederweis, M., Schulz, G.E. (2004) The Structure of a Mycobacterial Outer-Membrane Channel . Science 303, 1189-1192.

Ferguson, N., Fersht, A.R. (2003) Early events in protein folding. Curr. Opin Struct Biol, 13, 75-81.

Fish, W.W., Danielsson, A., Nordling, K., Miller, S.H., Lam, C.F., Bjork, I. (1985) Denaturation behavior of antithrombin in guanidinium chloride. Irreversibility of unfolding caused by aggregation. Biochemistry 24, 1510-1517.

Frankish, H. (2002) Researchers uncover a shared mechanism for protein aggregation disorders. The Lancet. 359, 1214.

From, N.B., Bowler, B.E. (1998) Urea denaturation of staphylococcal nuclease monitored by Fourier transform infrared spectroscopy. Biochemistry 37, 1623-31.

Fujita, T., Ralston, G.B., Morris, M.B. (1998) Biophysical properties of human erythrocyte spectrin at alkaline pH: implications for spectrin structure, function, and association. Biochemistry 37, 264-271.

Galziskaya, O.V., Ivankov, D.N., and Finkelstein, A.V. (2001) Folding nuclei in proteins. FEBS lett. 489, 113-118.

Garriga, P., Manyosa. J. (2002) The eye photoreceptor protein rhodopsin. Structural implications for retinal disease. *FEBS Lett.* 528, 17-22.

Gokce, I., Bainbridge, J., Lakey, J.H. (1997) Stabilising and destabilising modifications of cysteines in the *E. coli* outer membrane protein OmpC. FEBS Lett. 411, 201-205.

Goormaghtigh, E., Cabiaux, V., Ruysschaert, J-M. (1994) Physicochemical methods in the study of biomembranes, edited by Hilderson H.J, Ralston. G.B. Subcellular Biochemistry 23, 329-403.

Goto, Y., Takahashi, N., Fink, A.L. (1990) Mechanism of acid induced folding of proteins. Biochemistry 29, 3480-3488.

Haltia, T., Freire. E. (1995) Forces and factors that contribute to the structural stability of membrane proteins. Biochim. Biophys. Acta 1241, 295-322.

Haltia, T., Semo, N., Arrondo, J. L. R., Goni, F., Freire, E. (1994) Thermodynamic and structural stability of cytochrome c oxidase *from Paracoccus denitrificans*. Biochemistry 33, 9731-9740.

Hanahan, D. (1983) Studies on transformation of Escherichia coli with plasmids. J. Mol. Biol. 166, 557.

Hirch, A., Breed, J., Saxena, K., Richter, O-M.H., Ludwig, B., Diederichs, K., Welte, W. (1997) The structure of porin from *Paracoccus denitrificans* at 3.1 Å resolution. FEBS Letts. 404, 208-210.

Hsu, Y-R., Arakawa, T. (1985) Structural studies on acid unfolding and refolding of recombinant human interferon. Biochemistry 24, 7959-7963

Jackson, M., Mantsch, H.H. (1995) The use and misuse of FTIR spectroscopy in the determination of protein structure. Crit. Rev. Biochem. Mol. Biol. 30, 95-120.

Kelly, S.M., Price, N.C. (2000) The use of circular dichroism in the investigation of protein structure and function. Curr. Protein Pept. Sci. 1, 349-84

Khurana, R., Hate, A.T., Nath, U., Udgaonkar, J.B. (1995) pH dependence of the stability of barstar to chemical and thermal denaturation. Prot Sci. 4,1133-1144.

Kleffel, B., Garavito, R.M., Baumeister, W., Rosenbusch, J.P.(1985) Secondary structure of a channel-forming protein: porin from *E. coli* outer membranes. EMBO. J. 4, 1589-1592.

Kleinschmidt, J.H., Tamm, L.K. (1996) Folding Intermediates of a β-barrel membrane protein. Kinetic evidence for a multi step membrane insertion mechanism. Biochemistry 35, 12993-13000.

Koebnik, R., Locher, K.P., Van Gelder, P. (2000) Structure and function of bacterial outer membrane proteins: barrels in a nutshell. Mol. Microbiol. 37, 239-253.

Kopito, R.R. (2000) Aggresomes, inclusion bodies and protein aggregation. Trends Cell Biol. 10, 524-530.

Landt, D.O., Hahn, U., Saenger, W. (1993) J. Mol. Biol. 232, 967-981.

Lazar, S., Kalter, R. (1996) SurA assists the folding of Escherichia coli outer membrane proteins. *J. Bacteriol.* 178,1170-1773.

Lee, A.G. (2003) Lipid-protein interaction in biological membranes. A structural prespective. Biochim. Biophys. Acta 1612, 1-40.

Liu, J., Rost, B. (2001) Comparing function and structure between entire proteomes. *Protein Sci.* 10, 1970-1979.

Maiti, N.C., Aperti, M.M., Zargorski, M.G., Carey, P.R., Anderson, V.E. (2004) Raman spectroscopic characterization of secondary structure in natively unfolded proteins: alpha-synuclein. J. Am. Chem. Soc. 126, 2399-2408.

Makhatadze, G.I. Privalov, P.L. (1992) Protein interaction with urea and guanidinium chloride. J. Mol. Biol. 226, 491-505.

Manavalan, P., Johnson, W.C. (1987) Variable Selection Method improves the Prediction of Protein Secondary Structure from CD. Anal. Biochem. 167, 76-85.

Meersman, F., Heremans. K. (2003) Temperature-induced dissociation of protein aggregates: Accessing the denatured state. Biochemistry 42, 14234-14241.

Misra, R., Peterson, A., Ferenci, T., Silhavy, T.J. (1991) A genetic approach for analyzing the pathway of LamB assembly into the outer membrane of *Escherichia coli*. J. Biol. Chem. 266, 1392-13597.

Muller, D.J., Kessler, M., Oesterhelt, F., Moller, C., Oesterhelt, D., Gaub, H. (2002) Stability of bacteriorhodopsin helices and loops analysed by single molecule force spectroscopy. Biophys. J. 83, 3578-3588.

Myers, J.K., Oas, T.G. (2002) Mechanism of fast protein folding. Annu. Rev. Biochem. 71,783-815.

Nabedryk, E., Garavito, R.M., Breton, J. (1988) The orientation of β-sheets in porin. A polarized Fourier transform infrared spectroscopic investigation. Biophys. J. 53, 671-676.

Nazarova, T., Zscherp, C., Mäntele, W. (2003) Temperature dependent behaviour of the amide I band- an indicator for protein stability. 10th ECSBM, Szeged, Hungary, 33.

Pautsch, A., Schulz, G.E. (2000)High-resolution structure of the OmpA membrane domain. J Mol. Biol. 298, 273-282.

Perozo, E., Cortes, D.M., Cuello, L.G. (1999) Structural rearrangements underlying K^+ channel activation gating. Science 285, 73-78.

Phale, P.S., Philippsen, A., Widmer, C., Phale, V.P., Rosenbusch, J.P., Schirmer, T. (2001) Role of charged residues at the OmpF porin channel constriction probed by mutagenesis and simulation. Biochemistry 40, 6319-6325.

Phale, P.S., Philippsen, A., Kiefhaber, T., Koebnik, R., Phale, V.P., Schirmer, T., Rosenbusch, J.P.(1998) Stability of trimeric OmpF porin: the contributions of latching loop L2. Biochemistry 37, 15563-15670.

Pike, A.C.W., Acharya, K.R. (1994) A structural basis for the interaction of urea with lysozyme. Protein Sci. 3, 706-710.

Pollack, L., Tate, M.W., Darnton, N.C., Knight, J.B., Gruner, S.M., Eaton, W.A. (1999) Compactness of the denatured state of a fast folding protein measured by sub millisecond small angle X-ray scattering. Proc. Natl. Acad. Sci. 96, 10115-10117.

Popot, J.L., Engelman, D.M. (2000) Helical membrane protein folding, stability, and evolution. *Annu. Rev. Biochem.* 69, 881-922.

Popot, J.L., Gerchman, S.E., Engelman, D.M. (1987). Refolding of bacteriorhodopsin in lipid bilayers. A thermodynamically controlled two-stage process. J. Mol. Biol. 198, 655-676.

Radionova, N.A., Tatulian, S.A., Surrey, T., Tamm, L.K. (1995) Characterization of two membrane bound forms of OmpA. Biochemistry 34, 1921-1929.

Reid, J., Fung, H., Gehring, K., Klebba, P.E., Nikaido, H. (1988) Targeting of porin to the outer membrane of *Escherichia coli.* J. Biol. Chem. 263, 7753-7759.

Rief, M., Gautel, M., Schemmel, A., Gaub, H.E. (1998) The mechanical stability of immunoglobulin and fibronectin III domains in the muscle protein titin measured by atomic force microscopy. Biophys. J. 75, 3008-3014.

Saier, M.H. jr. (2000) Families of proteins forming transmembrane channels. J. Membrane Biol. 175, 165-180.

Saint, N., Lou, K.L., Widmer, C., Luckey, M., Schirmer, T., Rosenbusch, J.P. (1996) Structural and functional characterization of OmpF porin mutants selected for larger pore size. J. Biol. Chem. 271, 20676-20680.

Saxena, K., Richter, O-M.H., Ludwig, B., Benz, R. (1997) Molecular cloning and functional characterization of the *Paracoccus denitrificans* porin. Eur. J. Biochem. 245, 300-306

Saxena, K., Drosou, V., Maier, E., Benz, R., Ludwig, B. (1999) Ion selectivity reversal and induction of voltage-gating by site-directed mutations in the *Paracoccus denitrificans* porin. Biochemistry 38, 2206-2212.

Schiffer, C.A., Dotsch, V. (1996) The role of protein-solvent interaction in protein unfolding. Curr. Opin. Biotechnol. 74, 428-432.

Schulz, G.E. (2000) Barrel membrane proteins. Curr. Opin. Struct. Biol. 10, 443-447

Schirmer, T. (1998) General and specific porins from bacterial outer membranes. J. Struct. Biol. 121, 101-109.

Seshadri, K., Garemyr, R., Wallin, E., Von Heijne, G., Elofsson, A. (1998) Architecture of beta barrel membrane proteins: analysis of trimeric porins. Prot.Sci. 7, 2026-2032.

Srikumar, R., Dahan, D., Francis, F.A., Tawa, P., Diederichs, K., Coulton, J.W. (1997) Porins of *Haemophilus influenzae* type b mutated in loop 3 and loop 4. J. Biol. Chem. 272, 13614-13621.

Surrey, T., Jähnig, F. (1992) Refolding and oriented insertion of a membrane protein into a lipid bilayer. Proc. Natl. Acad. Sci. 89, 7457-7461.

Surrey, T., Schmid, A.., Jähnig, F. (1996) Folding and membrane insertion of the trimeric β-barrel protein OmpF. Biochemistry 35, 2283-2288.

Surrey, T. Jähnig, F. (1995) Kinetics of Folding and Membrane Insertion of a β -Barrel Membrane Protein. J. Biol. Chem. 270, 28199-28203.

Takeshita, K., Imamoto, Y., Mihara, K., Tokunaga, F., Terayima, M. (2002) Structural change of site-directed mutants of PYP: new dynamics during pR state. Biophys. J. 83, 1567-1577.

Tamm, L. K., Arora, A., Kleinschmidt, J.H. (2001) Structure and assembly of β-barrel membrane proteins. J. Biol. Chem. 276, 32399-32402.

Taneva, S.G., Caaveiro, J.M.M., Muga, A., Goni, F.M. (1995) A pathway for the thermal destabilization of bacteriorhodopsin. FEBS Lett. 367, 297-300.

Thayer, M.M., Haltiwagner, R.C., Allured, V.S., Gill, S.C., Gill, S.J. (1993) Peptide–urea interaction as observed in diketopiperazine-urea cocrystal. Biophys. Chem. 46, 165-169.

Tobi, D., Elber, R., Thirumalai, D. (2003) The dominant interaction between peptide and urea is electrostatic in nature: A molecular dynamics simulation study. Biopolymers 68, 359-369.

Trifonov, E. D., Berezovsky, I. N. (2003) Evolutionary aspects of protein structure and folding. Curr. Opin. Struct. Biol. 13, 110-114.

Urversky, V.N. (2003) Protein folding revisited. A polypeptide chain at the folding-misfolding – nonfolding cross-roads: which way to go? Cell. Mol. Life.Sci. 60, 1852-1871.

Varley, P., Gronenborn, A.M., Christensen, H., Wingfield, P.T., Pain, R.H., Clore, G.M. (1993) Kinetics of folding of all β sheet protein interleukin-1β. Science 260, 1110-1113.

Vogel, R., Siebert, F. (2002a) Conformation and stability of α-helical membrane proteins. 1. Influence of salts on conformational equilibria between active and inactive states of rhodopsin. Biochemistry 41, 3529-3535.

Vogel, R., Siebert, F. (2002b) Conformation and stability of α-helical membrane proteins. 2. Influence of pH and salts on stability and unfolding of rhodopsin. Biochemistry 41, 3536-3545.

Vu, D.M., Peterson, E.S., Dyer, R.B. (2004) Experimental resolution of early steps in protein folding: testing molecular dynamics simulations. J. Am. Chem. Soc. 21, 6546-6547.

Weiss, S. (2000) Measuring Conformational Dynamics of Biomolecules by Single Molecule Fluorescence Spectroscopy. Nat. Struct. Biol. 7, 724-729.

White, S.H. (2003) Translocons, thermodynamics and the folding of membrane proteins. FEBS Lett. 555, 116-121.

Whitney, P.L., Tanford, C. (1962) Solubility of amino acids in aqueous urea solutions and its implication for denaturation of protein by urea. J. Biol. Chem. 237, PC1735-PC 1737.

White, S. H., Wimley, W.C. (1999) Membrane protein folding and stability: physical principles. Annu. Rev. Biophys. Biomol. Struct. 28,319-365.

Wolf, E., Zahr, M., Benz, R., Imhoff, J.F., Lustig, A., Schiltz, E., Stahl-Zeng, J., Weckesser, J. (1996) The porins from the halophilic species *Ectothiorhodospira shaposhnikovii* and *Ectothiorhodospira vacuolata.* Arch. Microbiol. 166,169-175.

Xu, Z., Ozola, R., Gai, F. (2003) Infrared studies of the stability and folding kinetics of 15-residue beta-hairpin. J. Am. Chem. Soc. 125, 15388-94.

Zscherp, C., Aygün, H., Engels, J.W., Mäntele, W. (2003) Effect of proline to alanine mutation on the thermal stability of the all β-sheet protein tendamistat. Biochim. Biophys. Acta 1651, 139-45.

Abbreviations

Ag	Silver
AgCl	Silver chloride
A U	Arbitrary unit
Amp	Ampicillin
ATR	Attenuated total reflection
CaF_2	Calcium Fluoride
CD	Circular dichroism
DM	Dodecyl Maltoside
D_2O	Deuterium oxide
E. Coli	*Escherichia Coli*
EDTA	Ehylene diamine tetraacetic acid
EPR	Electron paramagnetic resonance
FTIR	Fourier transform infra-red
GuHCl	Guanidinium Hydrochloride
IPTG	Iso propyl thio galactoside
KCl	Potassium chloride
kDa	Kilo Daltons
LDAO	Lauryl dimethyl-N-amine oxide
NaCl	Sodium Chloride
NMR	Nuclear magnetic resonance
OD	Optical Density
OG	Octyl Glucoside
Omp	Outer membrane protein
PAGE	Poly acrylamide gel electrophoresis
PC	Phosphatidyl choline
Phe	Phenylalanine
PCR	Polymerase Chain Reaction
RPM	Rotations per minute
RT	Room temperature
SDS	Sodium dodecyl sulphate
TEN	Tris EDTA Sodium chloride
T_m	Temperature of melting
Trp	Tryptophan
Tyr	Tyrosine

8. Appendix

8.1 List of cell stock

Name	Cell	Plasmid	Resistance
SS1	DH5α	pJC40_porG$_{WT}$	Amp
SS2	DH5α	pJC40_porG$_{(E81Q)}$	Amp
SS3	DH5α	pJC40_porG$_{(W74C)}$	Amp
SS4	DH5α	pJC40_porG$_{(D148N)}$	Amp
SS5	DH5α	pJC40_porG$_{(D61N)}$	Amp
SS6	DH5α	pJC40_porG$_{(E81Q/D148N)}$	Amp
SS7	DH5α	pJC40_porG$_{(E81Q/W74C/D148N)}$	Amp
SS8	DH5α	pJC40_porG$_{(W74C/W90C/W191C)}$	Amp
SS9	DH5α	pJC40_porG$_{(\Delta\ 86\text{-}116)}$	Amp
SS10	DH5α	pJC40_porG$_{(\Delta 1\text{-}5)}$	Amp
SS11	BL21(DE3)	pJC40_porG$_{WT}$	Amp
SS12	BL21(DE3)	pJC40_porG$_{(E81Q)}$	Amp
SS13	BL21(DE3)	pJC40_porG$_{(W74C)}$	Amp
SS14	BL21(DE3)	pJC40_porG$_{(D148N)}$	Amp
SS15	BL21(DE3)	pJC40_porG$_{(D61N)}$	Amp
SS16	BL21(DE3)	pJC40_porG$_{(E81Q/D148N)}$	Amp
SS17	BL21(DE3)	pJC40_porG$_{(E81Q/W74C/D148N)}$	Amp
SS18	BL21(DE3)	pJC40_porG$_{(W74C/W90C/W191C)}$	Amp
SS19	BL21(DE3)	pJC40_porG$_{(\Delta\ 86\text{-}116)}$	Amp
SS20	BL21(DE3)	pJC40_porG$_{(\Delta 1\text{-}5)}$	Amp

8.2 Optimisation of PCR based site-directed mutagenesis

A PCR based site-directed mutagenesis was carried out to obtain site-directed mutants. The list of primers designed for this study is shown in Table 8.2.1. During the course of experimentation a few steps were studied in detail so as to optimize the mutagenesis protocol to obtain 100 % mutants with no background wild type. It was found that PCR optimization and *Dpn* I digestion was the most crucial steps to achieve this target which is discussed in the following sections.

Table 8.2.1 List of primers designed

Name/ Mutation	**Primer used**	**Restriction Site modified**
E81Q	5'-GGG ACC AAG GGG AAG AGG GTC AAG CCC AGA CCA ACG CTG GC-3' 5'GCC AGC GTT GGT CTG GGC TTG ACC CTC TTC CCC TTG GTC CC-3'	*Hph* I
D61N	5'-GCC TCG TCC TCG ACC AAT TCG GGC GTC GAC TTC GG-3' 5'-CCG AAG TCG ACG CCC GAA TTG GTC GAG GAC GAG GC-3'	*Sal* I
D148N	5'-GGC ATT GAC GAA GTG AAT CGC GTC GGG ATC CGC GCG-3 5'-CGC GCG GAT CCC GAC GCG ATT CAC TTC GTG AAT GCC –3"	*Pst* I
W74C	**5'-CGC TTC CGT CTT CAG TGC GAC CAA GGG GAA GAG GG –3'** **5'-CCC TCT TCC CCT TGG TCG CAC TGA AGA CGG AAG CG-3'**	*Bam*H I
E81Q/ D148N	Combination of E81Q and D148N	*Hph* I , *Pst* I
W74C/D148N	Combination of W74C and D148N	*Bam*H I, *Pst* I

E81Q/D148N/ W74C	Combination of E81Q, D148N and W74C	*Hph* I, *Bam*H I *Pst*I
Del I	5`-GGC GCC TTC TTC GCC TAT GAA TTC AAT GGT TAT GGC-3` 5`-GTA GAT CAG GCC GTT GAA TTC GAA GGC GGT GTC-3`	*Eco*R I
Del II	5'- AAA ATC TCG GCC ATG GGC CGG ACC GGT GTG-3' 5'-CCG GGA TCC TCA GAA CTC GAA GCG GCC-3'	*Nco* I *Bam* HI
Del III	5'-GAC GCC TCG TCC ATG GAT TCG GGC GTT-3' 5'-CCG GGA TCC TCA GAA CTC GAA GCG GCC-3'	*Nco* I *Bam* HI
W90C	5'- GGC AAACTC TGC GTC AGC GCC CAA GGC-3' 5'- GCC TTG GGC GCT GAC GCA GAG TTT GCC-3'	Nil
W191C	5'-GGC TTC TCG GTC GAA TAC ACT TGC AAC GAG-3' 5'-CTC GTT GCA AGT GTA TTC GAC CGA GAA GCC-3'	Nil
W74C/W90C/ W191C	Combination of W74C, W90C, W191C	*Pst* I

The underlined bases represent the codon for the altered amino acid.

Sequencing primers

Primer 1	5'- TCG ACG CCT CGT CCT CGA CCG ATT CGG –3'
Primer 2	5'- GCG ATC CAC TTC GTG AAT GCC ATA ACC -3'

8.2.1 PCR optimization

For a given set of primers PCR was carried out for 35 cycles as a test and the amplification checked on 1 % agarose gel. Figure 8.2.1 shows the PCR amplified product using 3 different concentration of template. Only when a good amplification was seen on the gel, the number of cycles in the PCR was reduced to 20 for the mutagenic PCR.

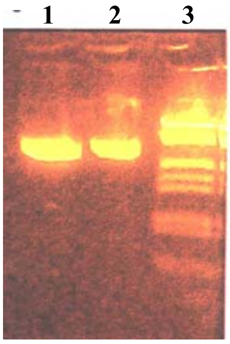

Figure 8.2.1 Optimization of PCR conditions.
Lane 1 with 5 ng template DNA,
Lane 2 with 10 ng template DNA,
Lane 3 DNA Marker**.**

8.2.1 Dpn I Digestion

It was observed that to maximize the digestion of all the wild type template the digestion was set with only 5 µl of the amplified product diluted to 30 µl of the reaction. The reaction mix was directly used for transforming *E. coli* DH5α cells.

8.2.2 Screening for site-directed mutants

During primer design wherever possible a restriction site was introduced to the mutagenic primer to allow easy screening of the clones. DNA of the clones were screened for the presence of the newly introduced restriction site. Figure 8.2.2 (b) indicates that the digestion of the mutant D148N with *Bam* HI. The wild type has only

1 *Bam* HI site while the mutants should have two. It is clearly evident from the restriction analysis profile of D148N that while the wild type linearises on digestion with *Bam* HI, the mutants show a 600 bp (base pair) product along with the linearised DNA. Similar restriction analysis were carried out for all other mutants with the respective enzyme. And it was found that all the clones screened were positive. It indicates that such a cloning approach for the construction of site-directed mutants can prevent any wild type background, making the cloning efficiency 100 %.

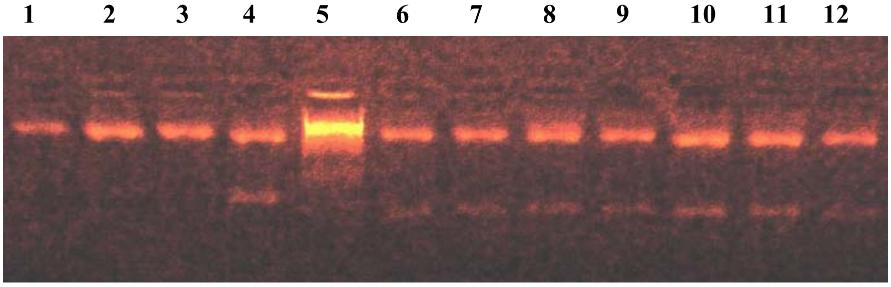

Figure 8.2.2 Screening of D148N mutant.
Lane 1-3 Wild type DNA digested with *Bam*HI,
Lane 4, 6-12 D148N mutant DNA digested with *Bam* HI, Lane 5 Marker**.**

Acknowledgement

I would like to express my sincere gratitude to **Prof. Dr. W. Mäntele**, Institute for Biophysik, Frankfurt am Main, Germany for accepting me as a Ph.D student. Thank you for introducing me to the world of FTIR spectroscopy and for providing such a wonderful topic to work with. You have been a wonderful and enthusiastic mentor to me. Danke schon !

I would like to express my sincere gratitude to **International Max Planck Research School** for giving me an opportunity to study here, and for the generous funding throughout.

My sincere gratitude to **Prof. Dr. B. Ludwig** and **Dr. K. Saxena**, Institute for Biochemie, Frankfurt am Main for giving the porin wild type gene to work and for allowing me to do experiments in the laboratory. I would like to thank all members of the group too.

My sincere gratitude to **Prof. Dr. R. Benz**, Lehrstuhl fuer Biotechnologie, Universitaet Wuerzburg for allowing me to work in his laboratory. **Mrs. Elke Maier** and all the members of the group are sincerely thanked for their help throughout my stay there and also for showing me the lovely city of Wuerzburg and for making my stay there a beautiful experience.

I would like to thank **Dr. Karin Hauser** for her constant help and support, throughout my work. Thank you very much for the German conclusions of this work.

I would like to thank **Dr. Christian Zscherp**, for guiding through this work.

I would like to thank **Dr. T.A. Link and Dr. Vitali Vogel** for teaching me to work with CD spectroscopy and Fluorescence spectroscopy.

I would like to thank **Dr. Ute Pfitzner**, **Dr. Petra Hellwig** for all the laboratory guidance and help.

I would like to thank **Mrs Elizabeth Uloth,** Max Planck Institute for Biophysik, Frankfurt am Main for DNA sequencing.

I would like to thank all the members of **Institute for Biophysik**, Frankfurt am Main for all their help and support.

9. Acknowledgements

I express my sincere gratitude to **Ms Nana Shimosako,** Frankfurt International School for helping me with my experiments.

My special gratitude to **Mrs Evelyne Maneg** for all the encouragement and support. You made my stay in Frankfurt such a memorable experience. Thank you!

My gratitude to my **daddy** and **mummy**. Your words ”It will work, don’t worry, we are here for you “ drives me forward every time. Thank you for being there for me always. I express my sincere gratitude to **ambaji** and **achan** for all their love and prayers. My sincere gratitude to **achan** and **amma**. I am indebted to you for all the love and encouragement you have showered on me.

My sincere thanks to all my friends in Frankfurt and around the globe for being so supportive. My sincere thanks to **Sreeja** and **Saji** for being there for me. Special thanks to **Ankita**, ever ready to discuss science over telephone.

My gratitude to you is beyond words. Thank you **Chanju, Unnu, Miki**, **Sonu, Bitu,** names can be many more, but it all means you, Thank you for being there for me always.

Suja Sukumaran

Address

101, Henriette Furth Strasse 2

Frankfurt am Main 60529

Germany

Email: suja_sanjeev@yahoo.com

Personal Details

Date of Birth	17-09-1976
Marital status	Married
Nationality	Indian

Academic Qualification

Degree	Board/University	Year of passing
M.sc (Biotechnology)	Cochin University, Kerala, India	2000
Bsc (Botany)	Kerala University, Kerala, India	1997
Pre-Degree	Kerala University, Kerala, India	1994
High School	Madhyamik Siksha Mandal, Bhopal, India	1992

University Ranks

1st rank in M.Sc (Biotechnology) Cochin University

2nd rank in B.Sc (Botany) Kerala University

Awards and Scholarships

- National Merit Scholarship (1992)
- Cochin University Scholarship (1997-1999)
- Terry Adams Award in Biotechnology (1999)
- Summer Research Fellowship (JNCASR) (1998 and 1999)
- Rajiv Gandhi Science Talent Research Scholarship (2000)
- CSIR-UGC (NET) Fellowship valid from Jan (2000).
- **International Max Planck Research School Fellowship, Germany** (Jan 2002 till date).

Publications

Suja Sukumaran, Christian Zscherp, Werner Mäntele (2004) Investigation of the thermal stability of porin from *Paracoccus denitrificans* by site-directed mutagenesis and FTIR-spectroscopy. **Biospectroscopy.** 74, 82-86**.**

Publications in preparation

Suja Sukumaran, Karin Hauser, Christian Zscherp, Werner Mäntele. Spectroscopic investigations of pH dependent stability, unfolding and refolding of porin.

Suja Sukumaran, Karin Hauser, Christian Zscherp, Werner Mäntele. Stability of Outer Membrane Protein Porin from *Paracoccus denitrificans* : The role of Tyrosines.

Poster Presentations in Conferences

1. Suja Sukumaran, Karin Hauser, Christian Zscherp, Werner Mäntele (2004) Jahrestagung der Deutschen Gesellschaft für Biophysik, Sept 12th-15th, Freiburg, Germany.

2. Suja Sukumaran, Karin Hauser, Christian Zscherp, Werner Mäntele (2004) Keystone meeting, Frontiers in structural biology, April 13th to 18th , Snowbird, Utah, USA.

3. Suja Sukumaran, Karin Hauser, Christian Zscherp, Werner Mäntele (2004) Optical Spectroscopy of biomolecular dynamics. Minerva Gentner symposium, March 21st to 25th, Kloster Banz, Germany.

4. Suja Sukumaran, Christian Zscherp, Werner Mäntele (2003) 10th ECSBM August 30-4th September, Szeged, Hungary.

Previous Research Experience

- **Molecular mechanisms involved in directed evolution of organisms** (2001). A review written under the guidance of Prof. P.J. Bhat, Dept. of Biotechnology, Indian Institute of Technology, Bombay for the partial fulfilment of PhD course work.

- **Engineering Cytochrome P450s for Bioremediation** (2000) A Research work carried out under the guidance of Dr. R. Shanker, at National Environmental Engineering Research Institute, Nagpur, India.
  (S Sukumaran,, W M Atkins, R Shanker (2002) **Applied Biochemistry and Biotechnology** 103, 291-302.)

- ***In vitro* evolution of human Hypoxanthine Guanine Phosphoribosyl transferase : Generation of enzymes with altered substrate specificity.** (1999). A masters thesis work carried out under the guidance of Dr. H. Balaram, JNCASR, Bangalore, India, submitted to Cochin University for partial fulfilment of Master of Science Degree.

- **Protein Engineering of human and *Plasmodium falciparum* HGXPRT.** (1998). A research work carried out under the guidance of Dr. H. Balaram, JNCASR, Bangalore, India.
  (INS Subbaya, S Sukumaran, K Shivshanker and H Balaram.(2000). **Biochemical and Biophysical Research Communication** 272, 596-602.)